THE ABILITY TO GENERATE DIFFERENTIATED AND SENECESENT PROGENY IS A MAJOR DETERMINANT OF BREAST CANCER HETEROGENEITY

A THESIS SUBMITTED TO
THE DEPARTMENT OF MOLECULAR BIOLOGY AND GENETICS
AND THE INSTITUTE OF ENGINEERING AND SCIENCE OF
BILKENT UNIVERSITY
IN PARTIAL FULFILLMENT OF THE REQUIREMENTS FOR
THE DEGREE OF DOCTOR OF PHILOSOPHY

BY
MİNE MUMCUOĞLU
AUGUST 2009

I certify that I have read this thesis and that in my opinion it is fully adequate, in scope and in quality, as a thesis for the degree of Doctor of Philosophy.

Prof. Mehmet Öztürk

I certify that I have read this thesis and that in my opinion it is fully adequate, in scope and in quality, as a thesis for the degree of Doctor of Philosophy.

Prof. Dr. Ediz Demirpence

I certify that I have read this thesis and that in my opinion it is fully adequate, in scope and in quality, as a thesis for the degree of Doctor of Philosophy.

Assoc. Prof. Işik Yuluğ

I certify that I have read this thesis and that in my opinion it is fully adequate, in scope and in quality, as a thesis for the degree of Doctor of Philosophy.

Assoc. Prof. Rengül Çetin-Atalay

I certify that I have read this thesis and that in my opinion it is fully adequate, in scope and in quality, as a thesis for the degree of Doctor of Philosophy.

Assoc. Prof. Esra Erdal

Approved for the Institute of Engineering and Science

Director of Institute of Engineering and Science
Prof. Mehmet Baray

ABSTRACT

THE ABILITY TO GENERATE DIFFERENTIATED AND SENECESENT PROGENY IS A MAJOR DETERMINANT OF BREAST CANCER HETEROGENEITY

Mine Mumcuoğlu
Ph.D. in Molecular Biology and Genetics
Supervisor: Dr. Mehmet Öztürk
August 2009, 124 Pages

Breast cancer displays distinct subtypes, such as luminal A, luminal B, and basal-like. The prognosis and therapeutic response of each subtype is different. The mechanisms involved in the generation of these tumor types are poorly understood. Our aim was to test whether the ability to generate senescent progeny contributes to breast cancer heterogeneity. A panel of 12 breast cancer cell lines, 31 isogenic clones, and 12 breast tumors were used. We classified breast cancer cell lines into senescent cell progenitor (SCP) and immortal cell progenitor (ICP) subtypes. All ER+ cell lines tested and some ER-positive (ER+) breast tumors displayed senescence. Acute loss and tamoxifen-mediated inactivation of ER triggered a robust senescence response in SCP type T47D cell line. In contrast, ER-overexpression, estrogen treatment and $p21^{Cip1}$ knockdown inhibited senescence. Neutralization of reactive oxygen species also abolished senescence. Breast cancer cell subtypes displayed divergent ability to produce differentiated progeny. The SCP subtype cells produced CD24+ or ER+ luminal-like and ASMA+ myoepithelial-like progeny, in addition to CD44+ stem/progenitor-like cells. In contrast, ICP cell lines acted as differentiation-defective stem/progenitor cells. Some cell lines generated only CD44+/CD24-/ ER-/ASMA- progenitor/stem-like cells, and others only CD24+/ER- luminal-like, but not ASMA+ myoepithelial-like cells. SCP cell lines were less tumorigenic, and they clustered with luminal A/normal like tumors. In contrast, ICP subtypes were more tumorigenic, and they clustered together with basal/luminal B tumors. Our results show that breast cancer cell lines clustering with luminal A/normal-like and basal/luminal B tumors respectively, differ from each other by the ability to generate differentiated and senescence-arrested progeny.

ÖZET

FARKLILAŞMIŞ VE SENESANT PROJENİTÖR OLUŞTURMA POTANSİYELİ MEME KANSERİNİN HETEROJEN YAPISININ BAŞLICA BELİRLEYİCİLERİNDENDİR

Mine Mumcuoğlu
Moleküler Biyoloji ve Genetik Doktorasi
Tez Yöneticisi: Dr. Mehmet Öztürk
Agostos 2009, 124 Sayfa

Meme kanseri luminal A, lüminal B ve basal-benzeri gibi farklı alttürlerden oluşmaktadır. Her alt türün prognozu ve tedaviye yanıtı farklıdır. Söz konusu alt türlerin oluşumunde yer alan mekanizmalar iyi bilinmemektedir. Bu çalışmanın amacı, hücre yaşlanması ya da senesansın meme kanerinin heterojen yapısına herhangi bir katkıda bulunup bulunmadığını araştırmaktı. Bu amaçla 12 meme kanseri hücre hattı, 31 izogenik hücre klonu ve 12 meme tümörü incelendi. Meme kanseri hücre hatlarını senesant hücre (SCP) ve ölümsüz hücre (ICP) projenitörleri olarak iki türde sınıflandırdık. Test edilen tüm östrojen almaç-pozitif (ER+) hücre hatları ve bazı ER+ meme tümörleri senesans gösterdi. Estrojen almacının akut kaybı ve tamoksifenle etkisizleştirilmesi SCP türü T47D hücre hattında güçlü bir senesans yanıtına yol açtı. Buna karşılık, östrojenle muamele, estrojen almacının aşırı ifadesi ve $p21^{Cip1}$ geninin "knock-down" yöntemi ile etkisizleştirilmesi senesensı baskıladı. Ayrıca, reaktif oksijen türlerinin N-asetil sistein ile nötralize edilmesi de senesens yanıtını engelledi. Meme kanseri alt türleri farklılaşmış projeni oluşturma potansiyeli açısından farklılık gösterdi. SCP alttürü hücreler, CD44+ kök/projenitör hücrelere ek olarak, CD24+ veya ER+ lüminal-benzeri, ve ASMA+ miyoepitel-benzeri hücreler ürettiler. Buna karşılk, ICP hücre hatları farklılaşmada kusurlu olan kök/projenitör hücreler olarak davrandılar. Bazı hücre hatları sadece CD44+/CD24-/ ER-/ASMA- projenitör/kök-benzeri hücreler üretirken, diğerleri CD24+/ER- lüminal-benzeri hücreler ürettiler. Ancak ASMA+ miyoepitel-benzeri hücre üretemediler. SCP hücre hatları daha az tümörijenik olup luminal A/normal-benzeri tümörlerle kümeleştiler. Buna karşılık ICP alttürü hücreler daha fazla tümörijenik olup bazal/lüminal B tümörlerle kümeleştiler. Sonuçlarımız lüminal A/normal-benzeri ve bazal/lüminal B tümörlerle kümeleşen meme kanseri hücre hatlarının farklılaşma ve senesensa girebilme özellikleri açısından birbirlerinden ayrıldıklarını göstermiştir.

TO MY FAMILY…

ACKNOWLEDGEMENTS

First and foremost, I would like to express my sincere gratitude to my supervisor, Prof. Dr. Mehmet Öztürk, who has always been helpful, understanding and patient, and has offered guidance generously throughout my Ph.D. studies. It is a great honor having a chance to work with him. He has always been my best teacher and mentor in helping me gaining skills in every aspect of scientific research. I will always treasure them.

Thanks to all MBG faculties and especially Assoc. Prof. Rengül Çetin-Atalay, Assoc. Prof. Işik Yuluğ, Assist. Prof. Can Akçali and Assist. Prof. Özlen Konu for their valuable advice, helps and supports during my PhD study.

I am very thankful to Dr. Hani Alotaibi, Sevgi Bağışlar and Haluk Yüzügüllü for their contributions to the critical experiments related with my thesis.

My special thanks go to group members: Ayça Arslan-Ergül, Şerif Şentürk, Nilgün Taşdemir, Sevgi Bağışlar, Haluk Yüzügüllü, Pelin Gülay and Dr. Hani Alotaibi for their friendship and experimental support during my most desperate times. We also shared many good memories together. In addition, I will never forget our former group members, Dr. Esra Erdal and Dr. Nuri Öztürk, for patiently teaching me lab techniques and helping me to pick up speed in my early years.

Special thanks to all my graduate friends, especially Ceyhan Ceran for their friendship and moral support.

I am thankful to all MBG family, especially Sevim Baran, Füsun Elvan, Abdullah Ünnü, Tülay Arayıcı, Bilge Özbayoğlu and Bilge Kılıç for willingly running for help whenever I needed, even during weekends.

The last but not the least, I want to thank to my family. Without their support and patience, this study would have never been finished.

TABLE OF CONTENTS

LIST OF TABLES

LIST OF FIGURES

ABBREVIATIONS

APS	Ammonium Persulfate
ASMA	Alpha smooth muscle actin
bp	Base pair
BrdU	5-bromo-2-deoxyuridine
cDNA	Complementary DNA
Ct	Cycle threshold
Ck	Cytokeratin
DCFH-DA	2'-7' dichloro dihydro fluorescein diacetate
DCIS	Ductal carcinoma in situ
ddH_2O	Double distilled water
DES	Diethyl stilbesterol
DEPC	Diethlypyro carbonate
DMEM	Dulbecco's Modified Eagle's Medium
DMSO	Dimethyl sulfoxide
ER	Estrogen receptor
E2	17-β-estradiol
4-OHT	4 hydroxy tamoxifen

FCS	Fetal calf serum
HCC	Hepatocellular carcinoma
ICP	Immortal cell progenitor
µg	Microgram
mg	Miligram
min	Minute
µl	Microliter
ml	Mililiter
µM	Micromolar
mM	Milimolar
mRNA	Messenger RNA
nM	Nanomolar
NAC	N-acetyl-L-cystein
NBT	Nitroblue tetrazolium
nM	nanomolar
Nox	NADPH oxidases
NP-40	Nonidet P-40
pmol	picomol
PBS	Phosphate Buffered Saline
PCR	Polymerase chain reaction

PR	Progesterone receptor
RA	Retinoic Acid
RT-PCR	Reverse transcription PCR
TAE	Tris-Acetate-EDTA Buffer
TBS-T	TBS tween
tRA	All-*trans*-retinoic acid
Temed	Tetramethyl ethylene diamide
TERT	Telomerase reverse transcriptase
Tm	Melting temperature

CHAPTER 1. INTRODUCTION

1.1 Breast Cancer

Development of breast starts during embryonic period. Ductal morphogenesis begins by a bud-like structure with branching, and then continues with elongation and canalization. Both smooth muscle actin and cytokeratin expressing basal cells appear at the end of the second trimester. Adult breast is composed of two types of cells: Myoepithelial cells and secretory luminal cells. It is possible to categorize different steps clinically and histopathologically during progression to malignancy. Ductal hyperplasia is accepted as a very early step of the malignancy. In this stage, cells are cytologically benign. Transformation from hyperplasia to atypical hyperplasia presents increased risk for breast cancer. The following step is ductal or lobular carcinoma in situ. Cells in this step show cytological characteristics of malignancy, but without stromal invasion across the basement membrane. Tumor becomes invasive when the cells detach from basement and invade the stroma. When the cells reach the blood and lymph vessels, it can easily metastasize distant organs and locoregional lymph nodes (Kenemans *et al.*, 2004).

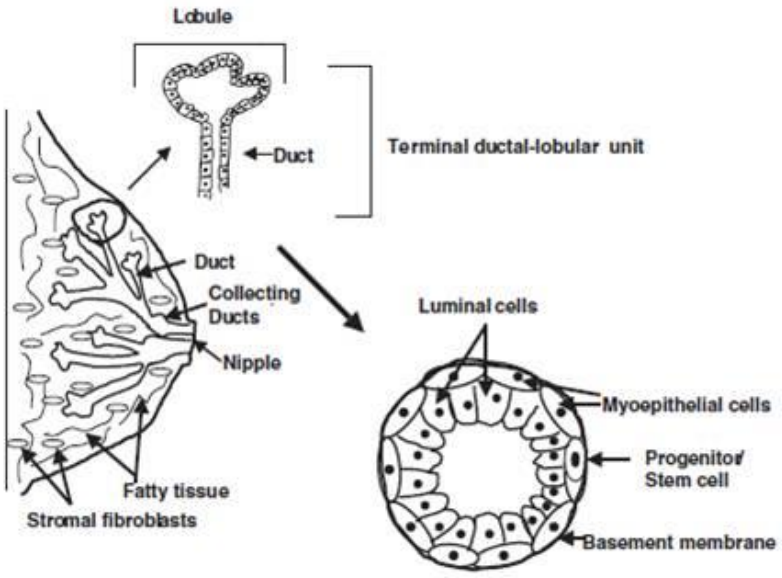

Figure 1: Mammary gland, terminal ductal-lobular unit. (Dimri et al., 2005)

Breast cancer appears as multistep process where accumulation of various genetic alterations can cause transformation of normal cells via steps of hyperplasia, premalignant change and in situ carcinoma (Beckmann *et al*, 1997). In recent years, it has been suggested that besides intrinsic malignant properties of tumor epithelial cells, other factors such as microenvironmental changes may play role in tumorigenesis (Hu and Polyak, 2008)

1.1.1 Epidemiology

Breast cancer is the most common malignancy and the second leading cause of cancer deaths in women (after lung cancer). Breast cancer comprises 15% of all female cancers. During 2009, over 190,000 new cases of invasive breast cancer are expected to occur among women in the US; about 1,900 for men. (Source: American cancer society).

Age is one of the most important risk factors for breast cancer, beside gender. Breast cancer incidence increases with age. Until menopause, disease incidence doubles every 10 years then slows down significantly.

Geographical variations also affect incidence and mortality. The difference between Western and Far East countries is fivefold, but it is declining.
Reproductive history could affect the incidence such as long menstrual history (early menarche and/or late menopause), recent use of oral contraceptives, nulliparity or having a first child after age 30.

In Western countries, 10% of breast cancer is due to genetic predisposition. Breast cancer susceptibility genes, BRCA1 and BRCA2, have been identified as a substantial proportion of high-risk families. In some populations, certain mutations occur at high frequency. For example, 2% of Ashkenazi Jewish women carry either BRCA1 185 del AG (deletion of two base pairs at position 185), BRCA1 5382 ins C (insertion of an extra base pair at position 5382) or BRCA 6174 del T (deletion of a single base pair at position 6174), while BRCA2 999 del 5 (deletion of five base pairs at position 999) accounts for about half of all familial breast cancer in Iceland. Li-Fraumeni and Cowden's syndromes, associated with inherited mutations in p53 and PTEN respectively, carry high risk of breast cancer but both are rare (McPherson *et al*., 2000).

Other risk factors of breast cancer include high-dose radiation to the chest, being overweight or obese after menopause, use of hormone replacement therapy (especially combined estrogen and progestin therapy), physical inactivity, and consumption of one or more alcoholic beverages per day.

1.1.2 Molecular pathogenesis

Hereditary breast cancer is characterized by an inherited susceptibility to breast cancer on the basis of an identified germline mutation in one allele of a high penetrance susceptibility gene (such as BRCA1, BRCA2, CHEK2, TP53 or PTEN). Inactivation of the second allele of these tumor suppressor genes would be an early event in this oncogenic pathway (Knudson's "two-hit" model).

Sporadic breast cancers result from a serial stepwise accumulation of acquired and uncorrected mutations in somatic genes, without any germline mutation playing a

role. Mutational activation of oncogenes, often coupled with non-mutational inactivation of tumor suppressor genes, is probably an early event in sporadic tumors, followed by more, independent mutations in at least four or five other genes (the chronological order is not important). Oncogenes that have been reported to play an early role in sporadic breast cancer are MYC, CCND1 (Cyclin D1) and ERBB2 (HER2/neu). In sporadic breast cancer, mutational inactivation of BRCA1/2 is rare, as inactivation requires both gene copies to be mutated or totally be deleted. However, non-mutational functional suppression could result from various mechanisms, such as hypermethylation of the BRCA1 promoter or binding of BRCA2 by EMSY (Kenemans *et al*., 2004).

Until recently, breast cancer tumorigenesis has been described by a multi-step progression model. One or more distinct mutations in regulatory genes are associated with each of these steps (Beckmann *et al*, 1997). But recently, Melchor and Benítez proposed integrative hypothesis about origin and development of hereditary and sporadic breast cancer subtypes. In their approach they try to explain breast cancer tumorigenesis by combination of the cancer stem cell hypothesis (for the carcinogenesis processes) and the clonal selection model (in terms of tumor development). (Melchor and Benitez, 2008)

ER and breast cancer:

Estrogens are steroid hormones that play significant role in mammary gland development and physiology. They are produced mainly by developing follicles in the ovary which are operative only during menstrual life in women. Other endogenous source of estrogen is peripheral conversion of adrenal derived-androgens to estrogen in fat cells**.** Estrogen can also be supplied by exogenous sources such as oral contraceptives during reproductive years or hormone replacement therapies. Until 1970's the use of DES (Diethyl Stilbestrol) during pregnancy was another exogenous source for estradiol. Later, it was shown that women who use DES have an increasing risk for development of breast cancer (Henderson *et al*., 1988).

Despite its role in normal mammary gland physiology, estrogen is implicated in development and progression of breast cancer based on the data both from clinical and animal studies (Henderson and Feigelson, 2000). Estrogen mediates its proliferative effect through an intracellular receptor, the estrogen receptor (ER). Steroid hormones are lipophilic and they enter the cell by diffusing through the plasma and nuclear membranes. Once estrogen enters the nucleus, it binds to ER. Estrogen binding to ER transforms the receptor to an active transcription factor, allowing it to bind estrogen response element (ERE) regulatory sequences in target genes, and regulate the transcription of target genes in the nucleus.

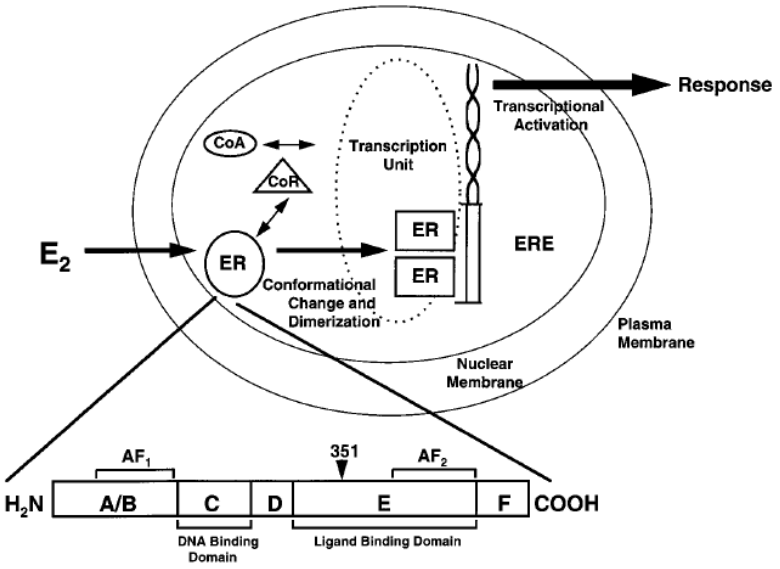

Figure 2: A subcellular model of estradiol (E2) action in target tissue. (Morrow and Jordan, 1999)

There are two receptors for estradiol, ERα and ERβ, which have distinct tissue expression patterns (Couse JF *et al*., 1999). Both ER receptors are members of the steroid/thyroid hormone nuclear receptor superfamily and are homologous in their DNA-binding and steroid binding domains. But ERβ gene is smaller, encoding a smaller protein and is located in a different chromosomal location. (Kumar V *et al*., 1987; Enmark E *et al*., 1997)

Since ER mediates estrogen activity, researchers have heavily studied the role of ER in breast cancer. Increased ER expression is probably one of the earliest changes occurring during breast cancer tumorigenesis. Increased ER expression has been shown in benign breast epithelium of women diagnosed to have breast cancer (Khan SA *et al*., 1994) and in the very early stages of ductal hyperplasia (Allred DC *et al.*, 2001, Shoker BS *et al*., 1999). Another study also showed that breast tissue of Japanese women from a population with high risk of breast cancer expresses higher percentage of ERα compared to those who have a low risk of the disease (Lawson JS *et al*., 1999). These and many other studies have indicated that ER receptor status is a very important factor for evaluation of breast cancer patients. For example ER– (ER negative) breast tumor patients have early recurrence and poor survival compared to ER+ (ER positive) breast tumor patients. In addition, ER+ patients confer good response to endocrine therapy compared to ER- counterparts.

In clinics, several estrogen antagonists have been successfully used in breast cancer therapy. They target estrogen mediated proliferation pathways but their effectiveness change in different patients and their mechanism of action is not fully understood. There are two groups of antiestrogens: Steroidal and nonsteroidal. Antiestrogens such as ICI 164.384 and ICI 182.780 are steroidal compounds which have only antagonistic activities. Nonsteroidal antiestrogen agents such as tamoxifen and raloxifen have mixed agonist/antagonist action depending on the cell type. The antitumor effects of tamoxifen are thought to be mediated by competitive inhibition of estrogen due to its binding to estrogen receptors. As a result, tamoxifen inhibits the expression of estrogen-regulated genes. But recent data suggests that tamoxifen can cause conformational changes in the ER, change its interaction with specific accessory proteins and lead to its recruitment to the transcriptional machinery.

Epidermal Growth Factor (EGF) family of proteins:

Besides estrogen, other hormones perform essential roles in mammary gland development and also progression of mammary tumorigenesis. It has been shown that estrogen affects mammary epithelial cells both directly and indirectly by

modulating the expression of growth factors and their receptors. EGF-family of peptides is also involved in mammary gland regulation. EGF, Transforming growth factor-α (TGFα) and Heregulin are implicated in breast cancer development. 83% of human breast tumors express EGF mRNA. 15-30% invasive tumors express EGF protein. EGF can promote anchorage dependent growth in mouse and human mammary gland. EGF mRNA level is found to be very high in estrogen receptor positive breast cancer cell line, T47D (Bowcock AM, 1999).

Transforming Growth Factor-β (TGFβ):

Most cells produce Transforming growth factor-β (TGFβ) and its growth receptor proteins. TGFβ signaling acts as a regulator in many cellular processes such as cell-growth regulation, development, morphogenesis, chemotaxis, connective tissue and extracellular matrix protein production. TGFβ is also a very important growth regulator for mammary gland development and this powerful growth inhibitory signal barrier is generally destroyed in cancer cells. Due to its pleiotropic and context-dependent effect, animal studies that target TGFβ signaling components gave different results about its action on breast cancer development. It is now mostly clear that elevated TGFβ plays tumor suppressive function at early stages of breast development, whereas it induces a malignant conversion and progression of cancer at later stages (Barcellos-Hoff and Akhurst, 2009).

Insulin-like Growth Factor (IGF):

It is shown that, there is an association between serum concentrations of insulin-like growth factor 1 (IGF1), IGF-binding protein 3 (IGFBP3), and increased risks of breast, prostate, colorectal, and lung cancers (Fürstenberger and Senn, 2002). Despite some controversies, meta-analysis results suggest correlation between circulating IGF1 level and cancer risk in pre-menopausel breast (Werner and Bruchim, 2009). IGFs and their binding proteins play role on cell proliferation, differentiation, and apoptosis. IGF1R signal transduction causes activation of several intracellular signaling pathways, including the Ras/Raf/MAP kinase and the phosphoinositide-3 kinase pathways. Moreover interaction between IGF receptors

and other cell surface receptors such as the estrogen, integrin, and cytokine receptors is important.

Oncogenes

Oncogene amplification is frequently found in breast cancer, but only a few of these amplified genes are important in breast cancer development, i.e. MYC, Int2, EMS1, BCL2, CCND1 and ERBB2. Oncogene amplification is not a very early event, but it can be found during DCIS (Ductal carcinoma *In Situ*) stage (Beckmann *et al*, 1997).

Tumor suppressor genes

The BRCA1 gene is located on chromosome 17q12-21 and participates in many transcriptional processes. It interacts with more than 15 different proteins that are involved in transcriptional activation or transcriptional repression. It also functions as a tumor suppressor and plays a role in apoptosis, DNA recognition and repair. Germline mutations in BRCA1 impose high risk to breast and ovarian cancer. In sporadic breast cancer, BRCA1 mutation is less frequently seen (Kenemans *et al*., 2004).

The BRCA2 gene which is located on chromosome 13q12-13, codes for a protein that play role in DNA repair, cell cycle control and transcription. It is also implicated in terminal differentiation of breast epithelial cells. BRCA1 and BRCA2 are high penetrance genes for breast cancer. Germ-line mutations of BRCA1 and BRCA2 are associated with 40-70% of familial breast cancers, including the hereditary breast and/or ovarian cancer sendrome (Beckmann *et al*, 1997).

p53 (TP53) is one of the most frequently mutated genes in sporadic human cancer, which is located on chromosome 17p13.1. Generally these mutations are point mutations that effect sequence-specific DNA binding and activation of p53-responsive genes. In sporadic breast carcinomas, TP53 mutation is a late event. Constitutional mutation of p53 is found in Li-Fraumeni sendrome but it is rare (Kenemans *et al*., 2004).

Other tumor supressors like Rb, PTEN, CHEK2 are also involved in breast cancer pathogenesis.

1.1.3 Molecular subtypes

Human breast tumors are very heterogenous in terms of their pathological and molecular profiles, and their clinical response to the therapy. In breast tumors, we could not observe one dominant pathway on the formation of tumorigenesis unlike colon cancer or pancreatic cancer. Also histological presentation of breast cancer is very diverse. Human breast tumors can be classified histologically into 18 subtypes at the time of diagnosis. Although this tumor classification helps physicians for prognostic evaluation of the patients, there is still quite variation in response to therapy (Stingl and Caldas, 2007).

Human breast tumors have been classified in terms of their gene expression profiling by microarray analysis (Perou *et al*., 2000). According to their gene expression patterns, breast tumors could be categorized into five molecular subtypes: Luminal A, Luminal B, ERBB2 (HER2), basal, and normal-like. These subtypes reflect the gene-expression patterns of the two principal epithelial-cell types in the normal adult breast: the luminal epithelial cells and myoepithelial cells. Luminal tumors are ER+ positive tumors. They express ER responsive genes and other genes that encode characteristic proteins of luminal epithelial cells like PR, GATA3, BCL-2, and the luminal cytokeratins CK8 and CK18. The HER2+, normal breast-like and basal-like subtypes are predominantly ER-negative. A subset of ER-positive and HER2-positive tumors cluster with the luminal B subtype. HER2+ tumors express high levels of genes located in the HER2 amplicon on chromosome 17q21, including HER2 and growth factor receptor-bound protein 7 (GRB7). Normal breast-like tumors express non-epithelial genes and genes in the basal cluster. Basal-like tumors are largely ER-, PR- and HER2-negative (triple negative) and express genes characteristic of basal epithelial cells and normal breast myoepithelial cells, including the basal cytokeratins CK5 and CK17. Importantly, later studies associated these breast-cancer subtypes with distinct clinical outcomes (Sorlie T *et al*., 2001; Sotiriou C *et al*., 2003). In Sorlie's study, they found significant difference in overall and relapse- free survival between tumor subtypes. While ER+ Luminal A subtype has most favorable prognosis, ER-, HER2+ and basal-like subtypes are associated

with shortest and relapse-free survival. Sotiriou's result provided supporting evidence for the previous studies. Moreover they found that ER status is a better discriminatory factor for tumor subtypes instead of other clinical features and tumor grade. These findings suggest that ER biology plays pivotal role in breast tumorigenesis and final configuration of breast cancer.

1.1.4 Breast cancer stem cells

Unlike other organs, human mammary gland undergoes many structural changes throughout adult life. In humans, before birth mammary fat pad is already invaded by branching network of ducts. Ducts are mainly composed of myoepitelial cells and specialized luminal layer of epithelial cells. During puberty, with hormonal stimulation ductal side branching occurs. Extensive proliferation and terminal differentiation is achieved during pregnancy and lactation by formation of lobulo-aciner structures which contain milk-secreting alveolar cells. After cessation of lactation, apoptosis and tissue remodeling convert mammary gland to pre-pregnancy state. In order to achieve this kind of great plasticity, mammary gland must contain stem cells or early progenitor cells that have ability to differentiate and proliferate. It has been proposed that stem cells may be potential targets for malignant transformation (Reya *et al*., 2001). It is hypothesized that normal stem cells and cancer cells share many similar characteristics like self renewal capacity and differentiation ability. When mutations are accumulated in cancer stem cells their functions could be distrupt and ultimately resulting with self-renewal deregulation, tumorigenesis and aberrant differentiation which generates cellular heterogeneity found in tumors. Cancer stem cells were first demonstrated in hematological malignancies (Bonnet and Dick, 1997) and later, in solid tumors of breast, brain, lung, colon, pancreas, prostate (Al-Hajj *et al*, 2003; Prince *et al*., 2007; Eramo *et al*., 2008; Dalerba *et al*., 2007; Li *et al*., 2007; Ceder *et al*., 2008). Al-Hajj and colleagues identified that a small population of breast cancer cells had ability to form tumor in NOD/SCID mice. These cells were identified by surface markers ($CD44^{+}/CD24^{-/low}Lineage^{-}$). They also noticed that tumors formed in mice share same phenotypical heterogeneity with the initial tumor. Therefore $CD44^{+}CD24^{-/low}$

lin^- population shows cancer stem cell characteristics like self renewal, differentiation and tumorigenic potential. It appers that CD44 is a shared stem cell marker and common to different organs and pathologies. But probably $CD44^+CD24^{-/low}Lin^-$ phenotype is tissue-restricted. For example, in pancreatic tumors, a stem cell population with the $CD44^+CD24^{-/low}$ Lin^+ phenotype was isolated.

Human mammary tumor-initiating cells isolated from patients express $EpCAM^+CD44^+CD24^{-/low}$ phenotype. CD24 is expressed only by human luminal epithelial cells, like MUC1. No expression of CD24 in tumor initiating cells indicate that these cells are located in basal epithelium (Stingl *et al*., 2007)

1.1.5 Experimental creation of breast cancer

To understand molecular pathways involved in breast cancer development mouse models have been used in many studies. In early studies chemical carcinogens were used in these models to induce breast cancer. Different genes expressed under either the MMTV (mouse mammary tumor virus) or the WAP (whey acidic protein) promoter was preferred in later studies for the same purpose. These are viral proteins, such as SV40 large T, polyoma virus T antigen or cellular proteins such as c-Myc, ErbB2/neu, cyclin D1, cyclin E, ERs, mutant p53, c-Ha-ras, and Wnt-1. Current studies generally examine function of cell cycle proteins or tumor suppressors by knockout model. Recent findings indicate important role of cyclin D1 overexpression in a subset of human breast cancers. Altogether some oncogenes and pathways are described in mammary gland tumorigenesis, including p53, pRb, BRCA1/2, cyclins, CDKs, ErbB2, c-Myc, Wnt-1, ER, and progesterone receptor. Another important finding is that these proteins or pathways seem to target different cell types or progenitors during tumorigenesis. It has been reported that expression of Wnt1 proto-oncogene in transgenic mice generated tumor and this tumor expresses progenitor cell markers and contains both luminal and myoepithelial cells. On the other hand, mammary tumors from transgenic mice expressing Neu, H-Ras, or polyoma T antigen are lacking progenitor cell marker expression and contain only myoepithelial cells (Li *et al*., 2003; Dimri *et al*., 2005).

1.2 Cellular senescence

1.2.1 Replicative senescence

Most of the primary cells undergo a limited number of cell division and then they are arrested indefinitely in G1 phase of cell cycle. This state is known as replicative senescence. It was first demonstrated by Hayflick and Moorhead more than fifty years ago. They revealed that normal embryo fibroblasts have limited number of cell divisions and then they cease proliferation (Hayflick and Moorhead, 1961). Senescence is described as a defense program leading to irreversible cell cycle arrest that protects cell when it is exposed to internal and external stress signals (Schmitt *et al*., 2007). Because of this characteristic of senescence, it is also described as a tumor-suppressive mechanism or anti-carcinogenic program (Collado *et al*., 2007; Shay and Roninson, 2004). We now know that replicative senescence is due to three main reasons: erosion of telomeres in every round of cell division, accumulation of unrepaired DNA and activation of tumor-suppressive pathways, P53 and Rb (Harley *et al*., 1990; Serrano and Blasco, 2007; Ben-Porath and Weinberg, 2004).

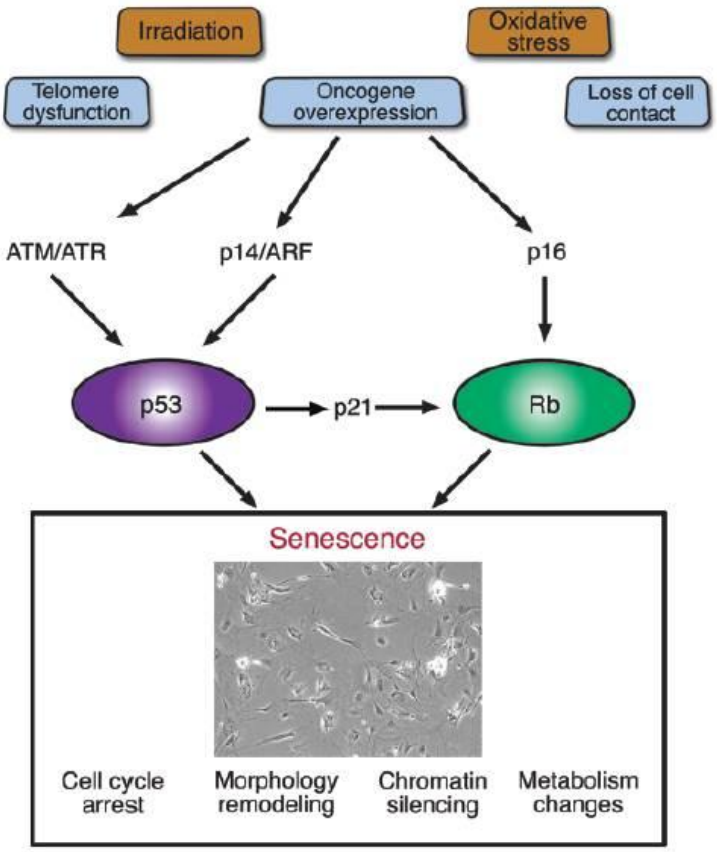

Figure 3: A variety of intrinsic and extrinsic signals lead to the onset of senescence (Ben-Porath and Weinberg, 2004).

Telomers are composed of stretches of repetitive DNA (tandem hexameric repeat units-5′-TTAGGG-3′ in vertebrates) and associated proteins that cap the ends of linear chromosomes. Telomeric cap protects chromosome from degradation or fusion by DNA-repair processes (d'Adda di Fagagna F, 2004). Telomeres are thought to end in a large circular structure, called T‑loop. During every S-phase, cells lose 50–200 base pairs of telomeric DNA because DNA polymerase cannot totally replicate DNA ends, called end-replication problem. Human telomeres range from a few kb to 10–15 kb in length. So it is possible for cells to generate many cell divisions before their telomeres are shortened critically to trigger senescence. Cells do not proliferate indefinitely mainly because of end-replication problem.

Dysfunctional telomere is recognized as a double strand break that activates DNA damage response (DDR). DDR activation causes cell-cycle arrest (senescence). DNA-damage foci can be detected in senescent cells. These foci contain many DDR proteins, such as γ-H2AX, 53BP 1, MDC1, NBS1, MRE11 and RAD17. Also senescent cells express activated protein kinases, ATM, ATR and their downstream targets CHK1, CHK2 which propagate damage signal to effector molecules such as p53 (Herbig U *et al.*,2004; d'Adda di Fagagna, F. *et al*. 2003). Telomerase which consists of a catalytic protein component (telomerase reverse transcriptase; TERT) and a template RNA component can prevent end-replication problem by adding DNA repeats to chromosome ends. Normal cells do not express TERT whereas germ-line cells and many cancer cells do. In human cells, ectopic TERT expression hinder senescence and telomere shortening (Bodnar *et al*., 1998). But senescence triggered by non-telomeric DNA damage or other inducers cannot be prevented by telomerase (Chen QM *et al*., 2001).

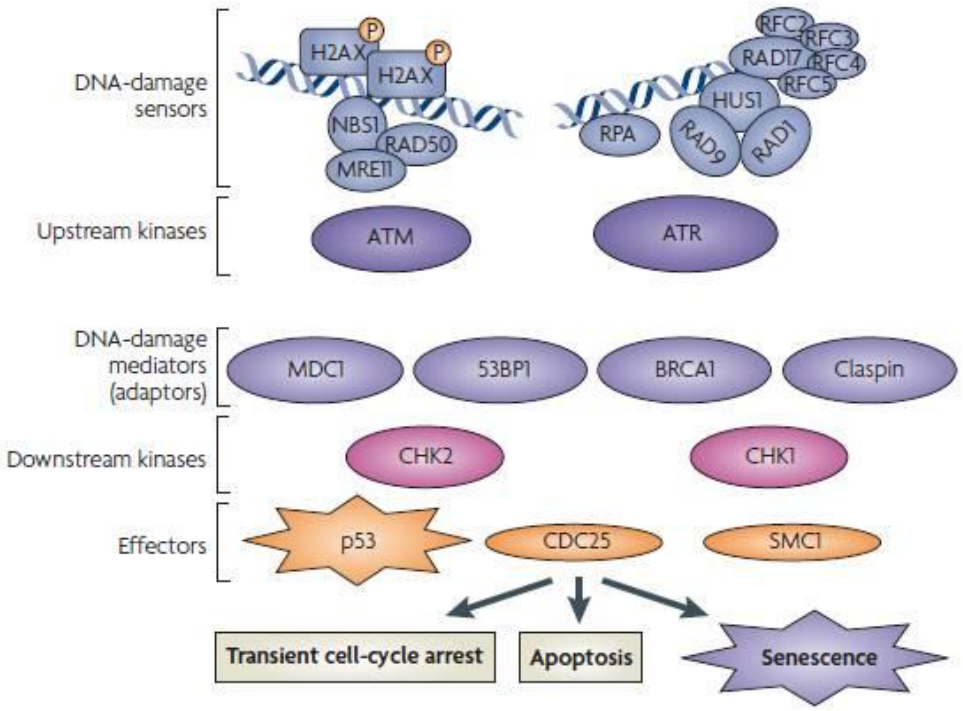

Figure 4: The DNA-damage response (Campisi and d'Adda di Fagagna, 2007).

1.2.2 Oncogene-induced senescence

Besides telomere dysfunction, senescence can be induced by different types of stresses such as oncogene activation. It has been shown that normal cells in culture enter senescence in response to the overexpression of the RAS oncogene (Serrano *et al*., 1997) or down-stream effectors RAF, activated MAP kinase and the PML oncoprotein (Zhu *et al*., 1998; Pearson *et al*., 2000). Oncogene-induced senescence has been suggested as a tumor-suppressive mechanism of cells to prevent them from uncontrolled proliferation triggered by abnormal activation of proliferation-driving oncogenes (Weinberg and Ben-Porath, 2005). Recently Courtois-Cox et al. propose that oncogene-induced senescence might not be the result of hypermitogenic signaling, and instead of hyperactivation of RAS pathway, inactivation of it causes senescence (Courtois-Cox *et al*., 2006).

Some recent studies presented evidences that DDR might also contribute oncogene-induced senescence. It is shown that some oncogenes, such as RAS, CDC6, cyclin E, and STAT5, induce both senescence and DDR which is triggered by DNA hyper-replication (Di Micco *et al*., 2006; Malette *et al*., 2007).

Nevi, which are benign type of melanocytic tumors, carry activating mutation in the BRAF protein kinase. Michaloglou and collaborators showed that human nevi present all the characteristics of oncogene-induced senescence, like carrying an activated oncogene product ($BRAF^{E600}$), expressing elevated levels of $p16^{INK4a}$ and SABG (Senescence associated β-Gal) activity. Additionally, they do not show telomere erosion. This and other evidences suggest that oncogene induced senescence in nevi present barrier to malignant transformation (Michaloglou *et al*., 2005).

In mouse, RAS activation induces senescence through $p19^{ARF}$-p53-p21-Rb pathway but in human, mainly through $p16^{ink4a}$-Rb pathway (Serrano *et a*l., 1997). But recently Collado and colleagues presented new senescence markers related with oncogene-induced senescence by using mouse model (RASV12 knock-in mice) in lung adenoma. These are $p15^{INK4b}$, Dec1 and DcR2 (Collado *et al*., 2005).

1.2.3-Oxidative stress and senescence

Reactive oxygen species (ROS) have shown to be connected with the process of senescence and organismal aging (Chen and Ames, 1994; Lee AC, 1999; Lundberg and Weinberg, 2000).

ROS are produced by different sources such as mitochondria and membrane bound enzymes, NADPH-oxidases. ROS play important physiological roles during cellular processes, and their level is strictly regulated by redox homeostasis. At high concentrations, ROS are known as toxic by-products of metabolism, and they causes damage to lipids, proteins and DNA. Oxidative stress has been connected with

several diseases such as cancer, atherosclerosis, pulmonary fibrosis and neurodegenerative diseases (Thannical VJ, 2000). On the other hand, at moderate concentrations, reactive oxygen species act as signaling molecules in different important physiological processes. For example, superoxide and other ROS types have been implicated in control of ventilation, erythropoietin production, smooth muscle relaxation, as well as involvement in signal transduction and gene expression (Droge *et al*., 2002). Superoxide anion is produced by the reduction of molecular oxygen. NADPH oxidase, xanthine oxidase or mitochondrial electron transport chains are mainly responsible from superoxide generation. These highly unstable superoxides immediately alter to hydrogen peroxide and then to water by catalase or glutathione peroxidase. When transition metal ions (ferrous and cuprous ions) interact with superoxide and hydrogen peroxide, they modify them to highly reactive hydroxyl radical (·OH).

After the mitochondria, NADPH family of oxidases is the second important generator of ROS in mammalian cell. Neutrophils and macrophages produce high amounts of ROS by phagocyte NADPH oxidase (Phox) to combat microbial pathogens. Phagocyte NADPH oxidase consists of gp91phox and the regulatory subunits p22phox, p47phox, p40phox and p67phox. However, non-phagocytic cells contain different types of Nox enzymes, which are homologous to gp91phox and generate low level of ROS. NADPH family of oxidases, comprising of five different Nox enzymes (Nox1, Nox2, Nox3, Nox4 and Nox5) and two Duox (Duox1 and Duox2). These enzymes are localized in the membrane. They all share an amino-terminal hydrophobic domain, composed of six transmembrane α-helices: the third and fifth helices, each containing two histidine residues which accommodate two heme binding sites. Carboxyl part of the enzyme holds binding sites for either flavin adenine dinucleotide (FAD) and NADPH, which are located in the cytoplasm. Alternatively, Nox5 enzymes carry gp91phox core structure and additionally amino-terminal calcium binding domain (Lambeth *et al*., 2004).

ROS and senescence association has been studied heavily in different organisms and cell types. It has been demonstrated that senescent cells have higher amount of ROS

than normal cells (Hagen *et al*., 1997). Similarly, treatment of primary fibroblasts with non-lethal dose of H_2O_2 causes senescence-like growth arrest (Chen and Ames, 1994). In Drosophila, overexpression of catalase or superoxide dismutase is result in organismal life-span increase (Parkes *et al*., 1998; Orr and Sohal, 1994). Moreover, Nox4 overexpression in NIH3T3 cells results in cellular senescence (Shiose *et al.*, 2001; Geiszt *et al*., 2000).

1.2.4 Mechanisms of senescence as a DNA damage response

Many cell types can undergo senescence after DNA damage, which is generated by irradiation or treatment with DNA damaging agents. Like telomere-initiated senescence, DNA-damage induced senescence depends on p53-p21 pathway (DiLeonardo *et al*., 1994). Stabilization of p53 after DNA damage probably is maintained by ARF (Khan *et al*., 2004). On the other hand, in many cells, p16 plays important role to induce senescence after DNA damage and dysfunctional telomeres. It is suggested that DNA damage first inducs p53 and p21 for initial response and then p16 which supplies maintenance for senescence state (Ben-Porath and Weinberg, 2005).

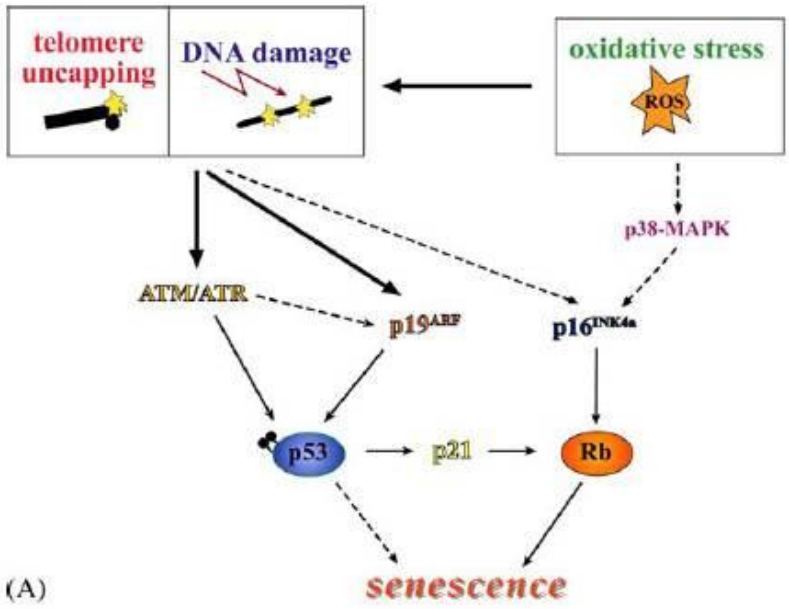

Figure 5: Activation of the senescence program (Ben-Porath and Weinberg, 2005).

Many chemotherapeutic drugs can induce senescence-like arrest especially the ones that affect DNA structure. Such drugs trigger senescence in some tumor cells in addition to normal cells and they cause severe DNA damage. Chang et al. showed that moderate doses of doxorubicin initiate senescence-like phenotype in tumor cell lines (Chang *et al*., 1999a). In another study, they also observed that drug-induced senescence in HCT116 and HT1080 cell lines is declined several fold but not totally abolished after inhibition or knockout of p53 or p21 (Chang *et al*., 1999b). Drug-induced senescence is observed in tumor cells in vivo as well (Shay and Roninson, 2004)

1.3 Senescence and immortality in breast epithelial cells

1.3.1 In vitro senescence mechanisms

Senescence in normal cells is a very powerful barrier to protect cells from tumor development. Human fibroblast and human epithelial cells present some differences when they are entering senescence state. Romanov *et al*. analyzed proliferation barriers in human mammary fibroblasts (HMF) and human mammary epithelial cells (HMEC) in vitro. They showed that human fibroblast undergo one phase of

proliferation before entering senescence whereas HMECs exhibit two phases of proliferation and plateau. They showed that, both HMFs and HMECs go through a limited number of divisions before reaching the plateau. In human fibroblast, this plateau (phase b) is also termed as Hayflick limit, replicative senescence or M1. In HMECs they called M0 or selection. Characteristics of this stage; enlarged size and flattened shape, SABG positive staining, low incorporation of BrdU (5-bromo-2-deoxyuridine) (indication of low proliferation), minimal presence of MCM2 protein, 2N/4N is >4 and low Annexin-V staining (indication of low death). Compared to fibroblast HMEC can overcome from this stage and continue to proliferate ~20-70 PD (population doublings) before entering second plateau. HMECs that survive from first plateau lose expression of p16 protein. In second stage of growth plateau (called M1 or agonescence), HMECs show characteristics of crisis instead of senescence. They are heterogeneous in size and morphology, incorporate with BrdU, express high levels of MCM2 and 2N/4N is ~1. Also they present high staining with Annexin-V, indicating that high proliferation goes with high cell death. Chromosomal abnormalities in HMECs are also observed in phase c. When the telomere status is analyzed, HMFs and HMECs showed low telomerase activity and telomere erosion in similar level. Telomere shortening continued in post-selection HMECs at the range of ~3.5kb (55% decrease). Examination of senescence mediator proteins showed minimal changes in p53 and p21 protein expression and increase in p16 protein level during first growth plateau in HMECs. They observed p53 increase during emergence from senescence instead of induction of senescence (phase b) or second plateau (phase d). Increase in p14ARF, p21 and decrease in p16 is also seen during p53 up-regulation (Figure 7) (Romanov *et al*., 2001).

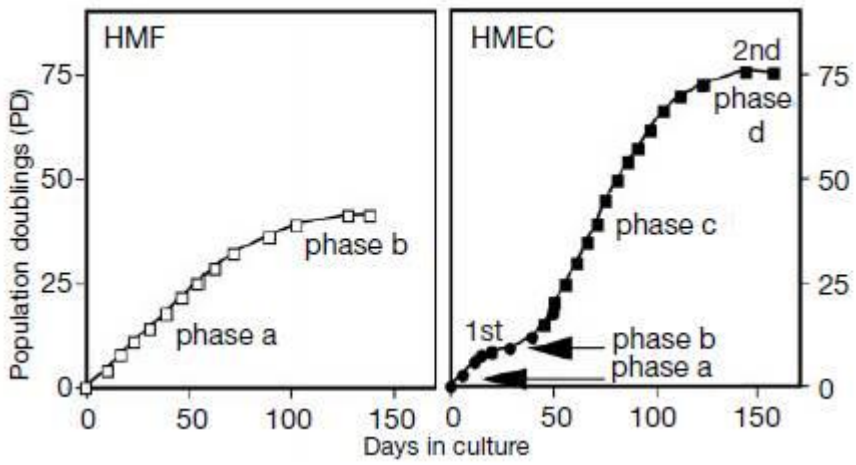

Figure 6: HMF (human mammary fibroblast) and HMEC (human mammary epithelial cells) growth curves (Romanov *et al*., 2001).

In another study, Stampfer and Yaswen, proposed that first barrier to immortalization is driven by Rb pathway respond to accumulated stress in vitro and in vivo. Rb inactivation is prevented by increased expression of CKIs. In HMEC, first growth arrest is related with elevated levels of $p16^{INK4A}$ and telomere independent. HMECs that overcome from fist barrier faces with telomere erosion and genomic instability, which leads to telomere-dependent proliferation barrier. If p53 function is absent, cell death occurs (termed as crisis). If p53 is functional, viable arrest is observed (termed agonescence). They also suggest that to derepress telomerase activity in p16-HMEC and to overcome stasis c-myc and ZNF217 amplifications are necessary. Conversion to immortalization is achieved after expression of telomerase in HMECs. Interestingly they detect telomerase activity just after loss of p53 function (Stampfer and Yaswen, 2003).

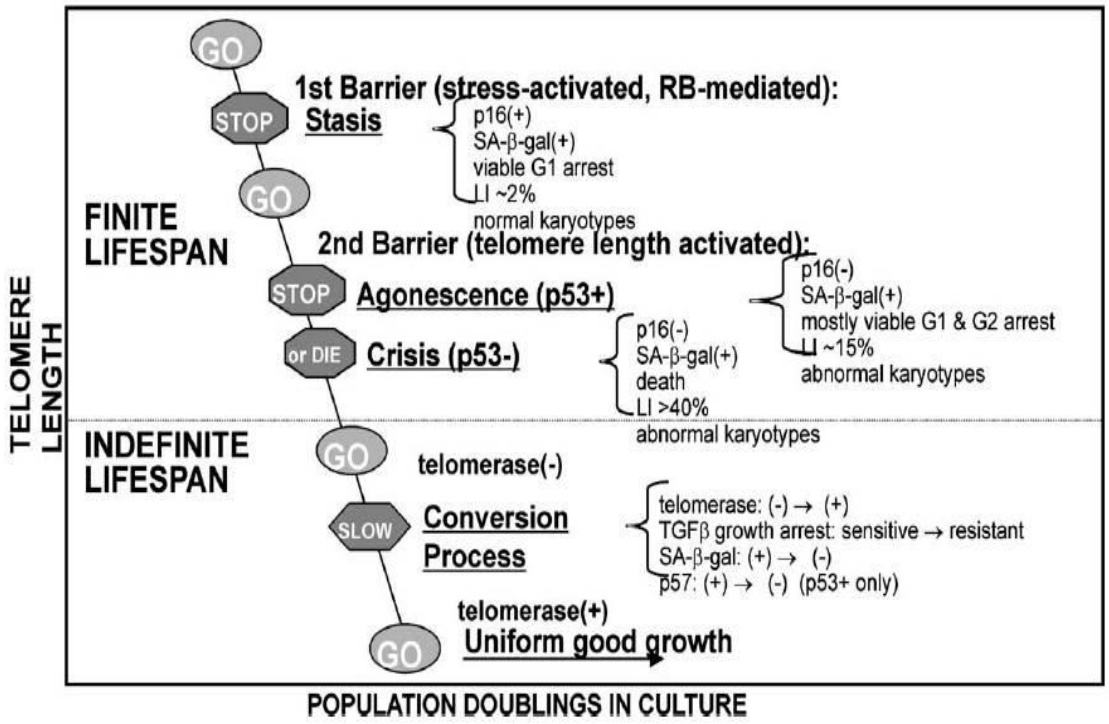

Figure 7: Model for steps in immortalization of cultured HMEC. (Stampfer and Yaswen, 2003).

1.3.2 Experimental creation of breast cancer cells

Great percentage of human breast cancer emerges from epithelial cells and they carry combination of mutations that control cell proliferation and survival. To understand the nature of biochemical alterations that leads to transformation of normal cells to tumor cells researchers tried to create carcinoma cells from immortalized HMEC by introducing cancer-associated genes. Recently Weinberg and colleagues established a multistep model for conversion of primary HMEC into tumorigenic state (Figure 8) as reviewed in Dimri et al., 2005. They serially introduced three genes, SV40 large-T antigen, hTERT and H-Ras oncoprotein into primary HMECs, which already bypassed initial M0 growth arrest. Tumorigenicity was determined by ability of tumor formation in nude mice by injecting cells subcutaneously and by anchorage-

independent growth in soft agar by forming colonies. It was shown that introduction of the large T antigen, which inactivates p53 and pRb to abolish senescence, activates hTERT to promote immortalization and oncogenic H-ras to provide constitutive mitogenic signaling. They also associated HMEC transformation with amplification of c-myc and ras oncogene expression level. By this method, when injected into nude mice, transformed HMEC generates poorly differentiated carcinoma (Elenbaas *et al*., 2006). Also it is shown that SV40 small t, which inhibits protein phosphatase 2A, has an important role in transformation of HMEC (Hahn WC *et al*., 2002). Other studies, which analyze role of small-t, showed that small-t activates PI3K pathway and active version of Akt1 and Rac1, which are downstream targets of PI3K, can substitute small-t function during transformation process (Zhao *et al*., 2003). Raf and Ral-GEF pathways are also implicated in epithelial transformation process in a cell type-specific manner (Dimri *et al*., 2005). Another recent study showed the importance of Bmi1. They achieved tumorigenic transformation of MCF10A, non-transformed, immortalized cell line, by co-overexpresion of Bmi1 and H-Ras (Datta S *et al*., 2007). All these studies show that interruption of several cellular pathways could cause tumorigenic transformation in human cells.

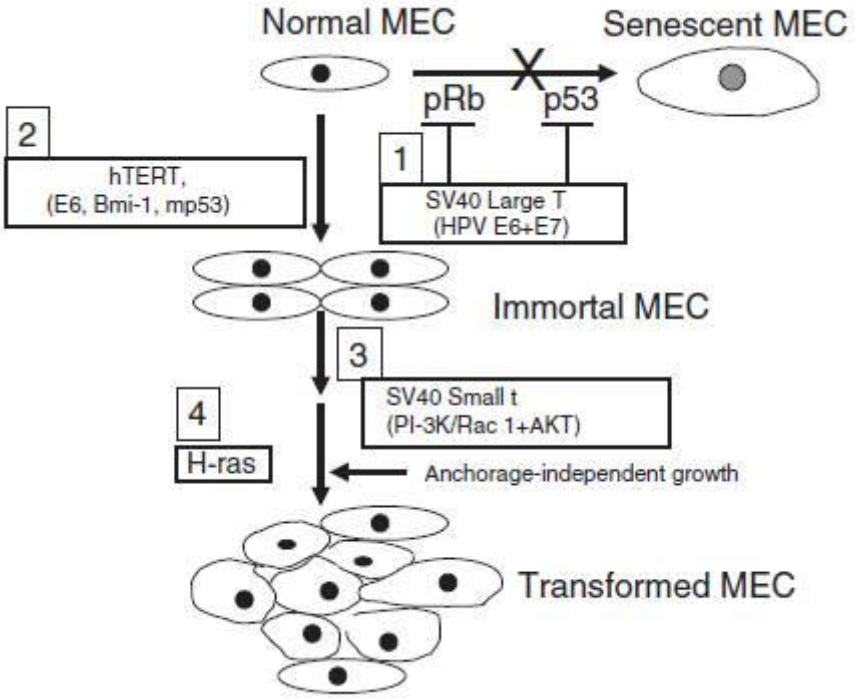

Figure 8: Transformation of HMEC (Dimri *et al*., 2005).

CHAPTER 2. OBJECTIVES AND RATIONALE

Breast cancer is the most common malignancy and despite the improvements of diagnosis and therapies still second leading cause of death among women.
Breast cancer is a heterogeneous disease in terms of histopathological and molecular features. Human breast tumors can be classified histologically into 18 subtypes at the time of diagnosis. Moreover, clinical response of patients to breast cancer therapies varies among the patients (Stingl and Caldas, 2007). Therefore, there is a great need for better understanding of molecular nature and tumorigenesis of disease.

Normal mammalian somatic cells have finite replicative potential in culture (Hayflick and Moorhead, 1961). After certain number of doublings, they cease to proliferate and undergo some biochemical and morphological changes which is referred as senescence. On the other hand, cancer cells have limitless replicative potential (Hanahan-Weinberg, 2000). In contrast to this general concept, our group observed that some of the Hepatocellular carcinoma-derived and breast cancer-derived cell lines enter senescence spontaneously (Ozturk N *et al.*, 2006). Senescence has been suggested as a barrier against tumorigenesis and proposed as a potent anticarcinogenic program (Reddel, 2000). For these reasons, we believed that characterization of this observed senescence phenotype and clarification of the mechanism serve great importance for generation of possible therapies related with induction of senescence in breast cancer.

In the beginning of our studies, a panel of breast cancer cell lines was screened by using low-density clonogenic assay and SABG (senescence associated β-gal) methods. We found that only 5 out of 12 breast cancer cell lines showed senescence phenotype in different percentage. More interestingly, breast cancer cell lines, which display senescence, produce heterogeneously positive SABG colonies. These results lead us to hypothesize that generation of senescent progeny that we observed in a group of breast cancer cell lines could be the result of their stem cell capacity and differentiation ability.

Therefore our aims in this study were:

To characterize senescence phenotype and its relationship with their stem cell and differentiation capacity; and to characterize the mechanism underlying this phenomenon

CHAPTER 3. MATERIALS AND METHODS

3.1. MATERIALS

3.1.1. Reagents

All laboratory chemicals were biotechnology grade from Sigma (St. Louis, MO, U.S.A), Farmitalia Carlo Erba (Milano, Italy), Merck (Schucdarf, Germany) and Amresco (Ohio, USA). Agarose was obtained from Prona (EU).

3.1.2. Oligonucleotides

Oligonucleotides used in polymerase chain reaction (PCR) were synthesized by IONTEK (Istanbul, Turkey).

3.1.3. Primary antibodies

The following antibodies were used: anti-CD44 (559046; BD Pharmingen), anti-CD24 (sc53660; Santa Cruz,), anti-ASMA (ab7817; Abcam), anti-CK19 (sc6278; Santa Cruz,), anti-$p21^{Cip1}$ (OP64; Calbiochem), anti-$p16^{Ink4a}$ (NA29, Calbiochem), and anti-ERα (sc8002; Santa Cruz).

3.1.4. Antibiotics

Geneticin-(G418 Sulfate) 500 mg/ml solution in double-distilled water. Sterilized by filtration and stored at -20°C (stock solution). 500 µg/ml (working solution for stable cell line selection), and 250 µg/ml (working solution for maintenance of stable cell lines).

3.1.5. Oxidative Stress Detection Reagents

2′-7′-dichlorodihydrofluorescein diacetate (DCFH-DA) was from Sigma, Taufkircher, Germany.

3.1.6. Preparation of charcoal treated FCS:

100 ml FCS (Fetal calf serum) was heat inactivated at 56C for 30 min. Then 20mg/ml charcoal were added FCS and incubated overnight at cold room with stirring. After incubation FCS was centrifuged in Beckman ultrasantrifuj at 20,000 rpm for 20 min. Charcoal incubation was repeated for 8 hours and then santrifuj again in the same conditions. Later FCS was filtered twice. Before using in cell culture filtration was repeated under the hood.

3.2. SOLUTIONS AND MEDIA

3.2.1. General Solutions

50X Tris-acetic acid-EDTA (TAE):	2M Tris-acetate, 50mM EDTA pH 8.5. Diluted to 1x for working solution
Ethidium bromide:	10 mg/ml in water (stock solution), 30 ng/ml (working solution)
1X Gel loading buffer:	0.25% bromophenol blue, 0.25% xylene cyanol, 50% glycerol, 1mM EDTA
Bradford Stock Solution	4.75 ml of 95 % ethanol, 10 ml of 85% phosphoric acid , 17.5 mg Coomassie Brilliant Blue. Stored in dark at 4°C.

Bradford Working Solution	21.25 ml double distilled water, 0.75 ml of 95% ethanol, 1.5 ml of 85% phosphoric acid 1.5 ml of Bradford stock solution. Filtered through Whatman No.1 paper and prepared freshly.

3.2.2. Tissue culture solutions

DMEM/RPMI working medium	10% FBS, 1% penicillin/streptomycin, 1% Non-Essential Amino Acid were added and stored at 4oC.
10X Phosphate-buffered saline (PBS)	*Per liter:* 80 g NaCl, 2 g KCl, 14.4 g Na2HPO4, 2.4 g KH2PO4, pH 7.4

3.2.3. SDS-PAGE Solutions

30% Acrylamide mix (1:29)	*Per 100 ml*: 29 g acrylamide, 1 g bisacrylamide in double-distilled water, filtered, degassed, and stored at 4°C (stock solution).
5X SDS gel-loading buffer:	3.8 ml double-distilled water, 1 ml of 0.5 M Tris-HCl, 0.8 ml glycerol, 1.6 ml of 10% SDS, o.4 ml of 0.05% bromophenol-blue. Before use, β-mercaptoethanol was added to final concentration of 5% to reach 1% when mixed with protein samples.
5X SDS-electrophoresis buffer	*Per liter:* 15.1 g Tris base, 95 g Glycine, 5 g SDS. Diluted to 1X for working solution. Store up to 1 month at 4°C.
10% Ammonium persulfate (APS)	0.1 g/ml solution in double distilled water. **(**Prepared freshly).
1.5 M Tris-HCl, pH 8.8 :	54.45 g Tris base (18.15 g/100 ml) ~150 ml distilled water Adjust to pH 8.8 with 1N HCl. Completed to 300 ml with distelled water and stored at 4° C.

1 M Tris-HCl, pH 6.8:	12.14 g Tris base ~ 60 ml distilled water Adjust to pH 6.8 with 1 N HCl. Completed to 100 ml with distilled water and store at 4° C.

3.2.4. Immunoblotting solutions

Semi-dry transfer buffer	*Per liter*: 48 mM Tris-base, 39 mM glycine, 0.037% SDS, 20% methanol.
310X Tris-buffer saline (TBS)	*Per liter:* 100 mM Tris-base, 1.5 M NaCl, pH 7.6 in double distilled water.
TBS-Tween (TBS-T)	0.1-0.5% Tween-20 solution in TBS. (Prepared freshly)
Blocking solution	3-5% (w/v) non-fat milk, 0.1-0.5% Tween-20 in TBS. (Prepared freshly).

3.2.5. RNA Study Solutions

DEPC-treated water	0.1% Diethylpyrocarbonate (DEPC) (v/v) in double-distilled water was stirred in loosely plugged bottle. Then autoclaved and stored at room temperature.

3.2.6. Immunofluorescence solutions

H33258 fluorochrome dye	1 mg/ml solution in double-distilled water and stored at -20 °C. Working solution was 1 µg/ml.
DAPI (4', 6-diamidino-2-phenylindole)	0.1-1 µg/ml (working solution in PBS).
4% paraformaldehyde	4 g paraformaldehyde, in 100 ml. PBS, Stir 4 hours at 58°C, pH 7.4. Stable at 4°C for a week.
Permeabization solution	100µl TritonX-100 in 100 ml PBS
BSA (Bovine serum albumin)	3% BSA in 1 X PBS (3 g in 100 ml).

3.2.7. Oxidative Stress Reagents

DCFH-DA Solution	10 mM HEPES (pH 7.5), 10 mM glucose, and 1 μM DCFH-DA (dissolved in methanol) in 1X PBS. Prepared freshly.

3.2.8. Estradiol, Tamoxifen and Retinoic acid Solutions

All-*trans*-retinoic acid (tRA), 17-β-estradiol (E2) and 4-hydroxy tamoxifen (4-OHT) were purchased from Sigma.

tRA was dissolved in DMSO as 10 mM stock solutions, E2 and 4-OHT was dissolved in ethanol as 1 mM stock solutions. All stock solutions were stored and protected from light at -20°C.

3.3. Equipment

Spectrophotometer	Nano Drop ND-1000
Horizontal electrophoresis apparatus	E-C Thermo Apparatus Corporation
Power supplies	Power-PAC200 and 300, Bio Rad
PCR machine	Techne, TC-512
Mini vertical gel system	Thermo EC120
Semi-dry transfer cell	Bio-Rad
Transilluminator	Vilber Lourmat, program Chemi-capt

Inverted light microscope, Axiovert 25	Zeiss
Flourescent microscope, AxioCam MRc5	Zeiss, Axiovision Rel 4.6
Hood	Holten
CO2 Incubator	Holten cell house

3.4. METHODS

3.4.1. Tissue Culture Studies

3.4.1.1. Cell lines and Growth conditions of cells:

Breast cancer-derived cell lines (T-47-D, BT-474, MCF 7, BT-20, MDA-MB-453, CAMA-1, SK-BR-3, MDA-MB-157, ZR-75-1, MDA-MB-468, MDA-MB-231 and HCC-1937; all from ATCC) were used in this study. T-47-D, BT-474, MCF-7, BT-20, MDA-MB-468, MDA-MB-453, MDA-MB-231, were grown in Dulbecco's modified Eagle's medium (DMEM) supplemented with 10% FCS and 50 mg/ml penicillin-streptomycin. CAMA-1 and MDA-MB-157 were cultivated in DMEM supplemented with 10% FCS, 50 mg/ml penicillin-streptomycin and 1% sodium pyruvate. ZR-75-1 and SK-BR-3 were cultivated in RPMI (glucose rich; 4.5g/L) medium (Sigma) and McCoy (Biochrom) medium accordingly, supplemented with 10% FCS and 50 mg/ml penicillin-streptomycin.

3.4.1.2. Thawing cell lines:

One vial of the frozen cell line from the liquid nitrogen tank was taken and immediately put into ice. The vial was left 1 minute on the bench to allow excess

nitrogen to evaporate and then placed into 37^{o}C water bath until the external part of the cell solution was thawed (takes approximately 1-2 minutes). The cells were resuspended gently using a pipette and transferred immediately into a 15 ml. sterile tube containing 10 ml cold fresh medium. The cells were centrifuged at 1500 rpm at 4^{o}C for 5 minutes. Supernatant was discarded and the pellet was resuspended in 10 ml 37^{o}C culture medium to be plated into 100 mm dish. After overnight incubation in a humidified incubator at 37°C supplied with 5% CO_2, culture mediums were replenished.

3.4.1.3. Subculturing of cells

The cells were passaged when they reached 80-90% confluence. The growth medium was aspirated and the cells were washed three times with 1x Phosphate buffer saline (PBS). Enough trypsin to cover the surface of the cells was added to the plate and waited 1-5 minutes until the cells are detached. The fresh medium was added and the suspension was pipetted gently to disperse the cells. The cells were transferred to either fresh petri dishes or fresh flasks using different dilutions (from 1:2 to 1:10) depending on requirements. All media and solutions used for culture were kept at 4°C (except stock solutions) and warmed to 37°C before use.

3.4.1.4. Cryopreservation of cell lines:

For cryopreservation cells should be in exponentially growing phase. 4x106cells/ml concentration of cells could be freezed in 1 ml of freezing medium. Cells were trypsinized and neutralized with growth medium. The cells were counted and precipitated at 1500 rpm for 5 min. The pellet was suspended in a freezing medium. Freezing medium: 10% DMSO, 10% FCS and 80% growth medium.1 ml of this solution was placed into 1 ml screw capped-cryotubes. The tubes were placed to -20°C immediately, and kept 2 hours at this temperature. Then tubes were moved to -80 °C and kept overnight. The next day, the tubes were transferred into the liquid nitrogen storage tank.

3.4.2. Protein studies

3.4.2.1. Protein extraction from cultured cells

Cells were grown to 70-80% confluency and washed with cold PBS three times. Then cells were scraped in cold PBS and centrifuged at 1500 rpm for 5 min at 4 °C. Cell pellet could be kept at -80°C or lysed immediately for the experiment. NP-40 lysis buffer were used to cell lysis.

NP-40 (Nonidet P-40) lysis buffer:

50µl 1M Tris pH=8.0
125µl 2M NaCl
10µl NP-40 (Igepal ca-630)
40µl 25X protease inhibitor
775 µl ddH2O

For lysis, the pellet was suspended and incubated in ice for 30 minutes in 4-5 volume of NP-40 lysis buffer. The lysate was centrifuged at 13.000 rpm for 30 minutes at 4°C. Supernatant was taken a new tube. After protein quantification, aliquots were stored at -80°C.

3.4.2.2. Bradford Assay for Protein Quantification

Standard curve for protein quantification

Tubes	**1 blank**	**2**	**3**	**4**	**5**	**6**	**7**	**8**
BSA (µl)	0	2.5	5	7.5	10	12.5	15	20
dH2O (µl)	100	97.5	95	92.5	90	87.5	85	80
Bradford(µl)	900	900	900	900	900	900	900	900

Protein sample preparation

Tubes	1 blank	2	3	4	5	6
Sample(µl)	0	2	2	2	2	2
dH2O(µl)	98	98	98	98	98	98
Bradford(µl)	900	900	900	900	900	900
Lysis buffer(µl)	2	-	-	-	-	-

SDS-polyacrlyamide gel for proteins

Acrlyamide concentration (%)	Linear range of separation (kD)
15	12-43
10	16-68
7.5	36-94
5	57-12

10% Resolving gel for SDS-Polyacrlyamide gel electrophoresis

Solution components	5 ml	10 ml	15 ml	20 ml	25 ml	30 ml	40 ml	50 ml
dH2O	2.6	5.3	7.9	10.6	13.2	15.9	21.2	26.5
30% Acrlyamide mix	1.0	2.0	3.0	4.0	5.0	6.0	8.0	10.0
1.5M Tris (pH 8.8)	1.3	2.5	3.8	5.0	6.3	7.5	10.0	12.5
10% SDS	0.05	0.1	0.15	0.2	0.25	0.3	0.4	0.5
10% APS	0.05	0.1	0.15	0.2	0.25	0.3	0.4	0.5
Temed	0.004	0.008	0.012	0.016	0.020	0.024	0.032	0.040

3.4.2.3. Immunoblot analyses

Cell pellets were incubated in NP-40 lyses buffer (50 mM Tris–HCl, pH 8.0, 250 mM NaCl, 0.1% Nonidet P-40 and 1Xprotease inhibitor cocktail (Roche) for 30 minutes in a cold room. Then cell lysates were cleared by centrifugation. Bradford assay was performed to quantify the protein concentration of the cell lysates. 30 µg of protein was denatured and resolved by SDS-PAGE using 10% or 12% gels. Then, proteins were transferred to the PVDF or nitrocellulose membranes. Membranes were treated for 1h with blocking solution (TBS containing 0.1% Tween-20 and 5% non-fat milk powder) and probed with primary antibody for 1hour. Next, membranes were washed three times with TBS-T and incubated with HRP conjugated secondary antibody for 1hour. Then, immunocomplexes were detected by ECL-plus (Amersham) kit on the membrane. α-tubulin was used as an internal control.

3.4.3. RNA studies

3.4.3.1. RNA extraction and cDNA synthesis

Total RNAs were extracted from cultured cells with NucleoSpin RNA II Kit (MN Macherey-Nagel, Duren, Germany) according to the manufacturer's protocol. Two micrograms of total RNA were reverse-transcribe into cDNA in a total volume of 20 µl using RevertAid First Strand cDNA synthesis kit (MBI Fermentas, Vilnius, Lithuania).

3.4.3.2. RT-PCR and Real-time PCR analysis

The PCR reactions were usually carried out with 1µl of cDNA, using the appropriate number of cycles and annealing temperature (Tm) provided in Table1. PCR products were analyzed on a 2% agarose gel and visualized with ethidium bromide under UV transillumination.

BioRad iCycler system was used to analyze Nox2 and Nox5 genes expression in breast cancer cell lines. Reactions were performed in a 20 µl volume with 2 µl of 1/3-diluted template cDNA, 10 pmol of forward and reverse primers, and 10 µl DyNAmo HS SYBR Green qPCR mix (Finnzymes). Same primer pairs for Nox2 and Nox5 were used for real-time PCR analysis, as listed in Table1. PCRs were incubated for 5 min 95°C, followed by 45 amplification cycles with 30 sec denaturation at 95°C, 30 sec annealing at 60°C, 30 sec extension at 72°C. Samples were analyzed in triplicate, and product purity was checked through dissociation curves at the end of real-time PCR cycles. Standard curve for each primer pair was performed by using five serial dilution points (2-fold dilutions) of a selected cell line cDNA. Primer amplification efficiency was calculated by using the formula; $E=2^{[-1/slope]}$. Real time RT-PCR results were evaluated by using $2^{-\Delta\Delta ct}$ method (Pfaffl, 2001), with a brief modification on the formula. The expression changes were calculated and compared as "Arbitrary Unit"s. The modified formula used was;

$$\text{Arbitrary unit} = [(E_{\text{Target gene}})^{\Delta CtTest(referance-sample)} / (E_{Actin})^{\Delta CtActin(referance-sample)}] * 1000$$

"Sample" represents breast cancer cell lines while "reference" represents ct value of negative controls. Because comparisons were performed between breast cancer cell lines and no exact control exists for each cell line we decided to use ct value of our negative control as a reference value. β-Actin was used as an housekeeping gene in the study.

3.4.4. Low-density clonogenic assay

Cells (20–60/cm^2 in 100mm plates or 150-200/cm^2 onto coverslips in six-well plates) were plated and grown 1–3 weeks to obtain isolated colonies formed with 100–1,000 cells. The medium was changed every 4 days, and colonies were subjected to SABG (Senescence associated β-galactosidase) staining.

3.4.5. SABG (Senescence associated β-galactosidase) assay

SABG activity was detected by using a described protocol (Dimri GP. *et al*., 1995). After eosin or nuclear fast red counterstaining, SABG positive cells were manually counted.

3.4.6. SABG and BrDU (Bromo deoxyuridine) incorporation assay co-staining

Sub-confluent cells were labeled with BrdU (10μg/ml) for 24 hour in freshly added culture medium. After BrDU labeling, SABG staining procedure was followed. BrDU assay was continued with 70% ice-cold methanol fixation for 10 min and then DNA denaturation in 2N HCl for 20 min. After cells were incubated with anti-BrdU antibody (Dako), the following steps were carried out with the DakoCytomation Strepavidin-HRP and Liquid DAP+Substrate chromogen system (Dako, CA, U.S.A.), according to the supplier's instructions.

3.4.7. Retinoic Acid treatment of breast cancer cell lines

Cells were seeded as low density (1500 cells/well) onto the coverslipts in six-well plates as duplicate. One day after seeding, 100 nM tRA (trans-Retinoic acid) treatments were started. Control plates were received only carrier which was DMSO. Every 2 days tRA and carrier was replaced. After 10 days experiment was stopped and plates were subjected to SABG staining. Then cells were stained with eosin as a counterstaining and mounted onto the slayts. SABG positive cells were counted manually under the light microscope in 4 different areas.

3.4.8. NAC (N-acetyl-L-cysteine) treatment

Cells were plated in low density (1000 cells/well) into six-well plates with normal medium. 48 hours later, experiment were started by removing the initial medium and followed by adding fresh medium supplemented with 10 mM NAC. Negative controls were carried out in medium supplemented with only ddH2O. Experiment

was continued until each colony reached 400-500 cells. NAC supplemented medium was removed 24 hour before SABG assay was performed.

3.4.9. Co-staining with DCFH-DA (2'-7'-dichlorodihydrofluorescein diacetate) and MitoTracker

Cells were seeded in six-well plates with low density (1000 cells/well). After colonies reached 300-400 cells, experiment were started. During this time, NAC treatment was carried out previously described protocol. Cells were washed with pre-warmed PBS for 3 times and incubated with DCFH-DA-MitoTracker reaction mixture which is composed of 10 mM HEPES (pH 7.5), 10 mM glucose, 1 µM DCFH-DA ve 125 nM MitoTraker in 1X PBS for 20 min at 37°C. Cells were washed 3 times with pre-warmed PBS again and analyzed under fluorescent microscope.

3.4.10. NBT (Nitro Blue Tetrazolium) assay

Cells were plated in 35 mm plates. Sub-confluent cells were washed with pre-warmed PBS for 3 times. Cells were incubated NBT (1.6 mg/ml) in 1xPBS for 45 min at 37°C. Then color change was observed under bright field microscope. Then experiment was continued with SABG assay.

3.4.11. Low density clonogenic assays and immunohistochemistry

Cells were seeded as low-density on coverslips in six-well plates (500-2000 cells, according to plating efficiency) allowed to grow in DMEM supplemented with 10% fetal calf serum, with medium change every three days, until they formed colonies of a few hundred cells. Depending on cell lines, this took one to two weeks. For BrdU assays, cells were labeled for 24hour prior to immunocytochemistry. For simple immunoperoxidase assays, cells were fixed with cold methanol for five minutes, and then blocked with 10% FCS in PBS for 1h at room temperature. This was followed by incubation with primary antibody for 1h. Cells were then washed with PBS three times and subjected to immunostaining using the Dako-Envision-dual-link system

and the Liquid DAP Substrate chromogen system (Dako, CA, USA), according to the manufacturer's instructions. Hematoxylin was used as a counter-stain when the visualization of cells was necessary. For SABG-immunoperoxidase co-staining studies, unfixed cells were first subjected to SABG assay, and then fixed prior to immunostaining assays. Hematoxylin counter-staining was omitted for co-staining experiments, unless cells were negative for SABG staining.

Table 1: Antibodies used in this study

	Antibody
Stem cell/progenitor marker	CD44
Luminal marker	CD24, ER and CK19
Myoepithelial marker	ASMA

3.4.12. Estrogen and tamoxifen treatment

Cells were seeded under low-density clonogenic conditions onto coverslips in six-well plates and then cultivated in standard culture medium for seven to eight days. Then, cells were fed with phenol red-free DMEM (Gibco) supplemented with 5% charcoal-stripped fetal calf serum for 48hour, followed by two successive 48h treatments with 10^{-9}M E2 (17β-estradiol; Sigma), 10^{-6}-10^{-9}M 4-OHT (4-Hydroxytamoxifen; Sigma) or an ethanol vehicle, under the same conditions. Colonies were then subjected to SABG assay. Each experimental condition was conducted in triplicate and experiments were repeated three times.

3.4.13. Generation of estrogen receptor-overexpressing clones

T47D-iso23 cells were transfected with the expression vector pCMV- ERα (Al-Otaibi *et al*., 2006) or an empty vector using FuGENE-6 (Roche). ER overexpressing

and control clones were selected with 500μg/ml G418 for three weeks. Isolated single-cell-derived colonies were picked and expanded in the presence of G418.

3.4.15. Lentiviral infection and generation of p21Cip1 knock-down clones

We used mission shRNA plasmid pLKO.1<-puro-p21 (NM_000389.2-640s1c1, Sigma) for p21cip1 knock-down. Control vector shRNA-pGIPz-SCR-puro and helper packaging mix (Invitrogen) were also used. HEK293T co-transfected with the appropriate vector and packaging mix, using CalPhos Mammalian Transfection Kit (Clontech), was following the manufacturer's instructions. After 48hour of culture, virus-containing culture media were collected, filtered and used to infect T47D-iso23 cells. After four hours of infection, stable cells were selected with 1 μg/ml puromycin for seven days.

3.4.16. Clinical Samples

Freshly frozen breast tumor specimens were collected at Ankara Numune Hospital. The use of the tissue material was approved by the Research Ethics Committee of Ankara Numune Research and Teaching Hospital, and consents were obtained in accordance with the Helsinki Declaration.

3.4.17. Nude mice tumorigenicity assays

For nude mouse xenotransplantation studies, MCF-7, T47D, CAMA-1, BT-20, HCC1937 and MDA-MB-453 cell lines were used. $5x10^6$ cells were injected subcutaneously into CD-1 *"*nude*"* mice (Charles River). Local tumor growth was monitored for 10 weeks at the injection sites. These experiments have been approved by the Bilkent University Animal Ethics Committee (Bil-AEC) and this study protocol complied with Bilkent University's guidelines on the humane care and use of laboratory animals.

3.4.18. Statistical analyses

Significant differences were evaluated using unpaired Student's t test for compared samples sizes of 10 or higher. Otherwise, one-tailed Fisher's exact test was used with 2×2 tables; $p < 0.05$ was considered statistically significant. On the graphical representation of the data, y axis error bars indicate the standard deviation for each point on the graph.

3.4.19. Cluster analysis

The two-channel microarray data containing 8102 cDNA genes/clones, generated by Sorlie *et al.* (2003) were downloaded from the Stanford Microarray Database (SMD) (http://genomewww. stanford.edu/MicroArray/). In the downloading process, "log (base 2) of R/G Normalized Ratio (median)" parameter was used for data filtering. We have median-centered expression values for each array. Arrays and genes with greater than 75% good data representing the amount of data passing the spot criteria were selected. Sixty-eight tissue samples were obtained according to this criterion and annotated with the subtypes described by the authors, found in "Supplementary Information" of the data set in SMD. The expression values of "500 gene signature," defined by the authors, were extracted from the data. Gene expression profiles of 31 breast cancer cell lines performed by Charafe-Jauffret *et al*., (2006) using the whole-genome cDNA microarray Affymetrix HGU-133 plus 2, was obtained from the "Supplementary Table" of the article. The authors filtered genes with low and poorly measured expression, and with low expression variation, retaining 15,293 genes. After log transformation of the data, we median normalized the arrays of the data in R language, using the Bioconductor biostatistical package (www.r-project.org/ and www.bioconductor.org/). The "500 gene signature" tumor data (Sorlie *et al*., 2003) and the normalized breast-cancer cell line data (Charafe-Jauffret *et al.*, 2006) were combined with respect to probe IDs using a set of customized perl routines (source codes are available upon request), as described (Gur-Dedeoglu *et al*., 2008). A set of 175 genes was common. "Median center" normalization of genes was made for the merged data set for the total samples. We performed unsupervised hierarchical

clustering with the 99 samples, including 31 breast cell line (Charafe-Jauffret *et al*., 2006) and 68 breast tumor samples (Sorlie *et al*., 2003) by pair-wise complete-linkage hierarchical clustering parameter, using the Gene-Pattern program. The Pearson correlation method was used for distance measurements.

Clustering was visualized by java treeview, again using Gene-Pattern (http://www.broad.mit.edu/cancer/software/genepattern/).

Table 2: List of gene-specific primers used for expression analysis of Nox genes

Genes	**Primer pairs (upper: forward, lower: reverse)**	**Tm,**	**Cycle**
Nox1	**5'-CATTCATATCCGAGCAGCAG-3'** **5'-CCAGCACAGCCACTTCATAC-3'**	**60**	**32**
Nox2	**5'-CACACATGCCTTTGAGTGGT-3'** **5'-GTGCACAGCAAAGTGATTGG-3'**	**60**	**32**
Nox3	**5'-ACTCCCTTCGCTGCTCTTCT-3'** **5'-CCGGTTTCCAGGGAGAGTA-3'**	**60**	**32**
Nox4	**5'-TCCTCGGTGGAAACTTTTGT-3'** **5-'TGTCCCATATGAGTTGTTCTGG-3'**	**60**	**32**
Nox5	**5'-CGGTCTTTCGAGTGGTTTGT-3'** **5'-TGGCCTTCATGTCATTCTTG-3'**	**60**	**32**
GAPDH	**5'-GGCTGAGAACGGGAAGCTTGTCAT-3'** **5'-CAGCCTTCTCCATGGTGGTGAAGA-3'**	**62**	**20**

CHAPTER 4. RESULTS

4.1. Spontaneous senescence in breast cancer cells

While analyzing clones from HCC-derived Huh7 cancer cell line, it is observed that some clones show characteristics of senescence and ceased proliferation in later passages. Then our analysis was extended to other HCC cell lines and breast cancer cell lines. During this screening, cells were plated at low density clonogenic conditions and were cultured until they accomplish 6-10 population doublings (PD). Next colonies were tested with senescence associated β-Gal (SABG) assay as described previously (Dimri GP. *et al*., 1995). This analysis showed us that two different SABG staining patterns can be observed on these cancer cell lines. One group could generate heterogeneously SABG positive progeny (Figure 9A) while other group generated significantly low or completely SABG negative progeny (Figure 9B) (Ozturk N. et al. 2006)

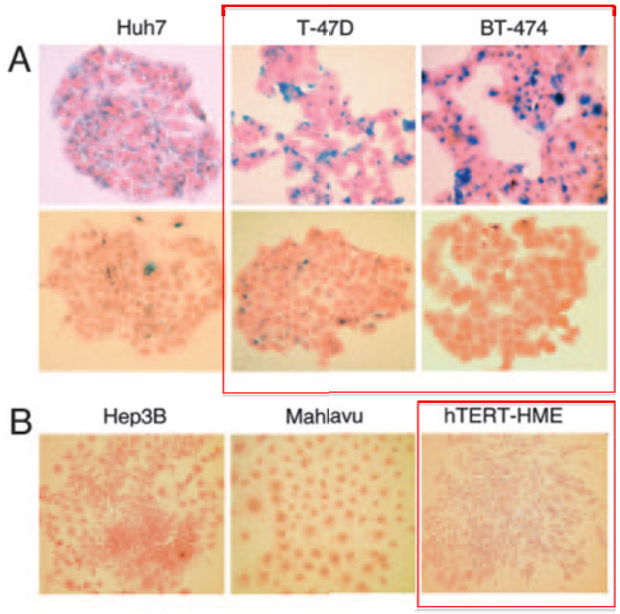

Figure 1: Analysis of senescence phenotype in HCC and breast cancer cell lines.

A) Heterogeneously SABG positive colonies, B) Low or completely SABG negative colonies in HCC and breast cancer cell lines (Ozturk N. *et al.* 2006).

4.1.1. Classification of breast cancer cell lines as senescent cell progenitor (SCP) and immortal cell progenitor (ICP) subtypes

Using low-density clonogenic assay and SABG staining, a panel of 12 breast cancer-derived cell lines, consist of luminal (n=7) and basal (n=5) subtypes, were screened (Table 3). This screening showed that only 5 out of 12 breast cancer cell lines present heterogeneous staining with SABG (Figure 10-11).

In clonogenic assay, cells were seeded in low density and cultured until they perform 6-10 PD. At the end of the assay each cell create a separate colony, each one has several hundred cells. Clonogenic assays are very good methods to detect stem/progenitor cells and properties of their progeny (Stingl J, 2009). This analysis enables us to classify our breast cancer cell line panel in to two categories according to their capacity to produce senescence progeny. First group of breast cancer cell lines produce progeny with high percentage of senescence (12-40%) whereas second group cannot generate considerable amount senescent cells in the colonies (<5%). The first group is named as "senescent cell progenitor" (SCP) subtype (T47D, BT474, ZR-75-1, Cama1 and MCF7) and the second group is called "immortal cell progenitor" (ICP) subtype (MDA-MB-453, BT20, SK-BR-3, MDA-MB-468, HCC1937, MDA-MB-231 and MDA-MB-157) (Figure 12).

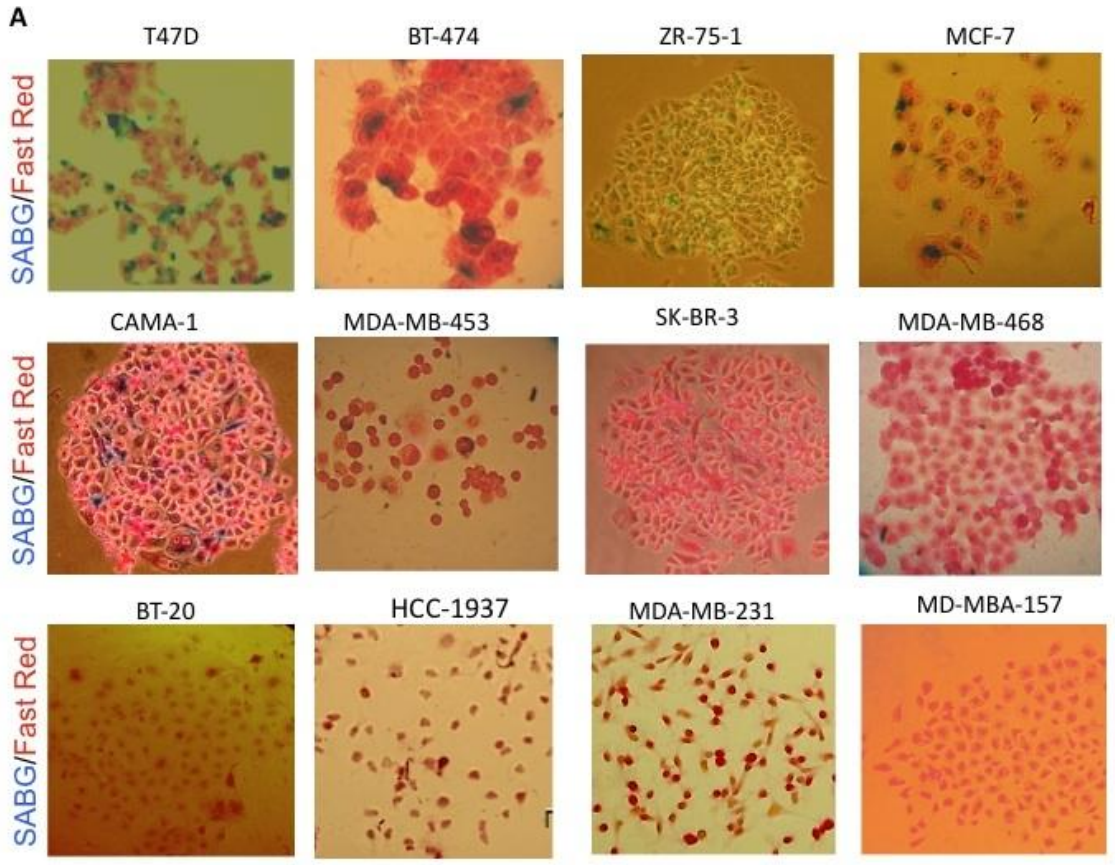

Figure 10: Representative pictures of SABG staining in breast cancer cell line panel. Five cell lines (T47D, BT-474, ZR-75-1, MCF7, and Cama1) show positive SABG staining whereas others (MDA-MB-453, BT20, SK-BR-3, MDA-MB-468, HCC1937, MDA-MB-231 and MDA-MB-157) present negative SABG staining.

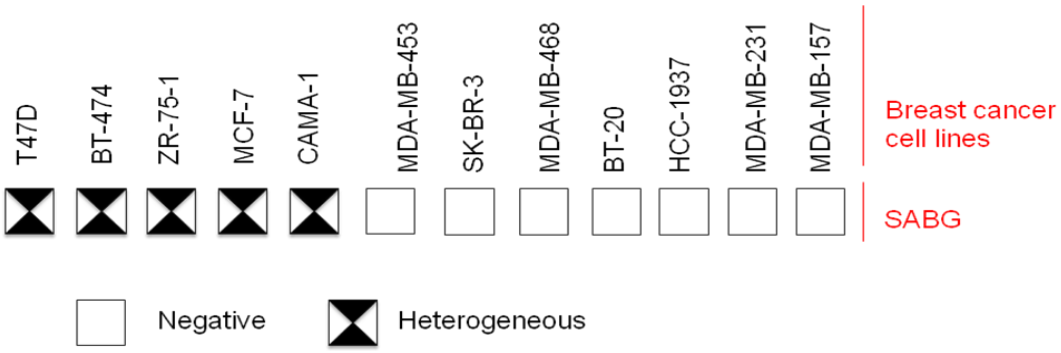

Figure 11: SABG staining results of breast cancer cell lines used in this study.

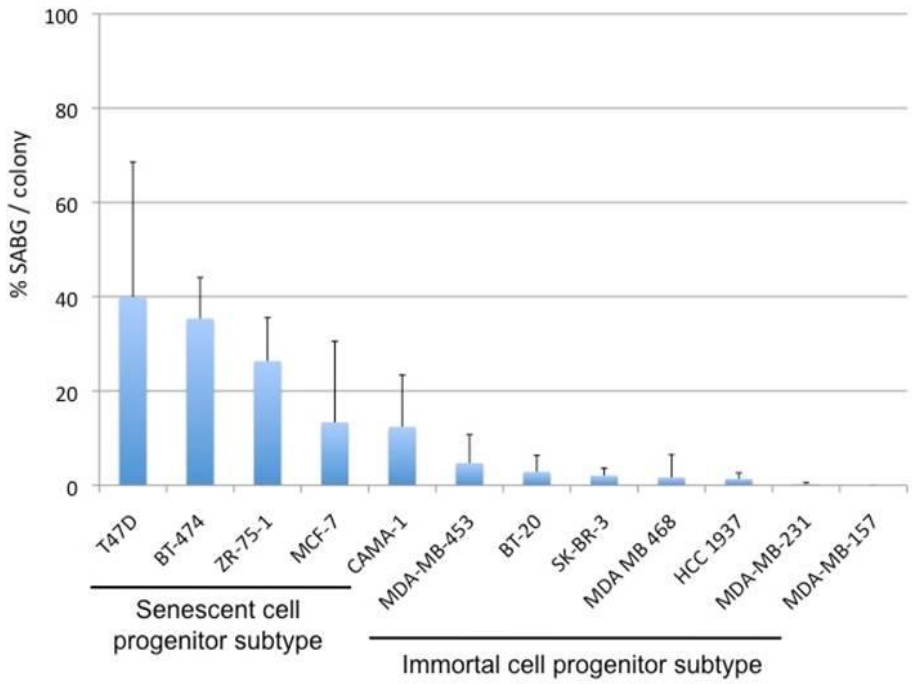

Figure 12: SABG index (% SABG positive cells/ colony) of breast cancer cell line panel.

First group of breast cancer cell lines which is named as SCP subtype produce progeny with high percentage of senescence (12-40%) whereas second group which is called ICP subtype cannot generate considerable amount senescent cells in the colonies (<5%).

To test whether the observed senescence phenotype in breast cancer-derived cell lines is intrinsic to cell line or due to the presence of side population, isogenic clones were generated from two breast cancer cell lines. T-47-D and BT-474 were selected to implement single cell cloning. Because previously these cell lines generated highest percentage of SABG positive progeny during SABG screening. From T-47-D and BT-474, 20 clones and 11 clones were established respectively. They were subjected to senescence associated β-galactosidase (SABG) screening. When highest percentage of SABG positive result was 61.46% in T-47-D isogenic clones, we can only get 52.7 % of SABG positive result in BT-474 isogenic clones (Figure 13). Then we choose 6 clones from T-47-D isogenic clones and 4 clones from BT-474

isogenic clones among the highest and lowest positive ones. These clones were maintained in the culture a long period of time (>60PD), but they did not fully entered senescence. Also none of them gained ICP type during this period. Their SABG indexes (percentage of SABG positive cells per colony) were remained around parental cell line. This result shows that senescence phenotype that is observed in breast cancer-derived cell lines is not related with replicative senescence. Breast cancer cell line clones (unlike our observation in Huh7 clones) do not enter totally senescence, but they maintained their senescent cell population in some fluctuated percentage.

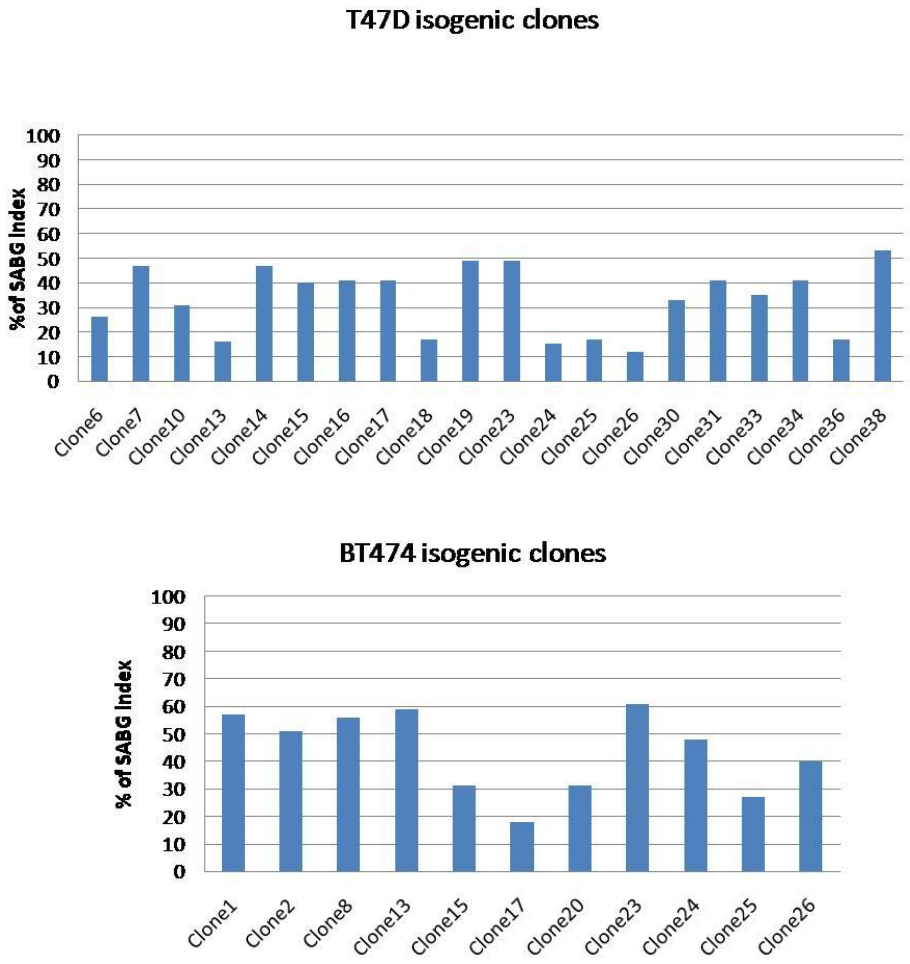

Figure 13: SABG index of T47D and BT-474 isogenic clones.

20 isogenic clones from T47D and 11 isogenic clones from BT-474 were established. All of the clones were subjected to SABG staining. Most of the clones showed similar SABG staining pattern like their parental cell lines.

To confirm senescent phenotype in SCP group with another test, long-term (24hour) BrdU incorporation assay was performed under mitogenic stimuli (Wei and Sedivy, 1999). In order to analyze senescence and BrdU correlation we performed co-staining. For this purpose first, cells were incubated with BrdU for 24 hour, then freshly stained with SABG, fixed and subjected to anti-BrdU staining, followed by DAB incubation. Under these conditions, senescent cells display blue staining, whereas DNA-synthesizing cells have brown nuclear staining. As shown in Figure 14, in two different cell lines, T-47D and CAMA-1, and clones T47D-iso23 and BT-474-iso23, SABG-positive blue cells and BrdU-positive brown cells can be distinguished by this double-staining method. The same figure also shows that most cells are blue or brown, indicating that they are either senescent (SABG+/BrdU-) or proliferating (SABG-/BrdU+) in response to mitogenic stimuli. This result indicates that SABG positive senescent cells were lost DNA synthesis ability irreversibly in this terminal differentiation stage.

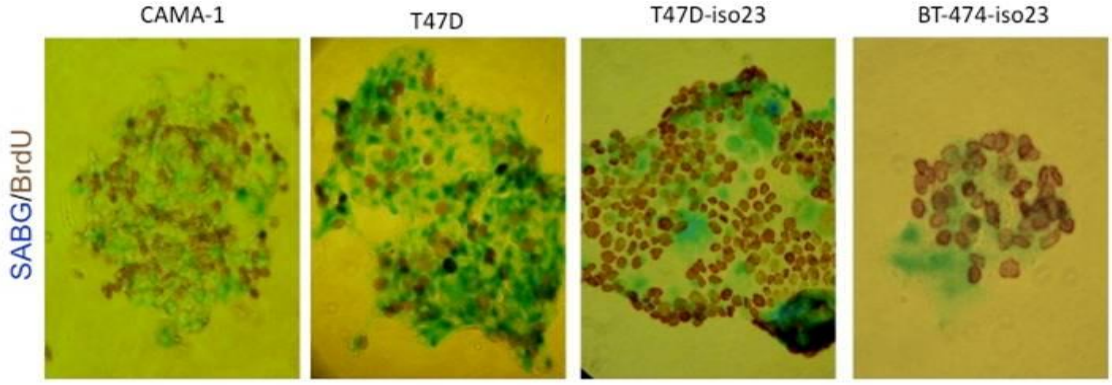

Figure 14: SABG and BrdU co-staining in Cama1, T47D, T47D-iso23 (isogenic clone of T47D) and BT-474-iso23 (isogenic clone of BT-474).

As seen in the picture, senescent cells presented blue SABG+ staining whereas no BrdU staining, indicating that they were not proliferating.

4.2. Role of oxidative stress in breast cancer cell senescence

4.2.1. ROS accumulation is related with senescence

Cellular senescence can be induced by different stimuli. One of them is oxidative stress. ROS are by-products of normal cell oxidative processes. ROS play different roles in cellular physiological functions like proliferation, apoptosis, differentiation and senescence.

We reasoned that senescence that we observed in breast cancer cell lines can be related with ROS accumulation in the cell. Therefore, we decided to co-stain our senescence-positive cell line, Cama-1, with oxidant-sensitive dye DCFH-DA and MitoTracker to show ROS accumulation. DCFH-DA is an oxidant-sensitive non-fluorescent dye that gives a fluorescence signal upon oxidation, and MitoTracker is a mitochondrion-selective probe that does not fluoresce until it is oxidized. MDA-MB-468 cell line, which is a senescence-negative cell line, was included to the study in order to compare the difference between senescence-positive and senescence-negative groups.

All the cells were seeded in low density clonogenic conditions. Cama-1 and MDA-MB-468 cells were treated with 10 mM NAC in order to prevent ROS accumulation in the cells. The media containing fresh NAC was added to the plates every three days and only ddH2O was added to the control plates. Half of the experiment was stopped at day 10 and other half was finalized at day 13. Then cells were co-stained with DCFH-DA and MitoTracker.

There wasn’t important difference in terms of ROS accumulation in control plates compared to the treatment received plates at Day 10 (Figure 15). But interestingly, high amount of ROS accumulation was observed at Day 13 in Cama-1 control plates compared to NAC treated plates (Figure 16). Importantly, 10 mM NAC treatment in Cama-1 cells caused statistically significant decrease in ROS accumulation (Figure 17). Another observation from this experiment was that there were no significant

experiment was that there were no significant changes in MitoTracker staining levels in Cama-1 control and treated plates. This result demonstrates that ROS accumulation is not of mitochondrial origin. There was also a low level of ROS accumulation in MDA-MB-468 cells. But this accumulation was not as significant as Cama-1 cells. Another point is there were no significant difference between control and treated plates in terms of their ROS accumulations.

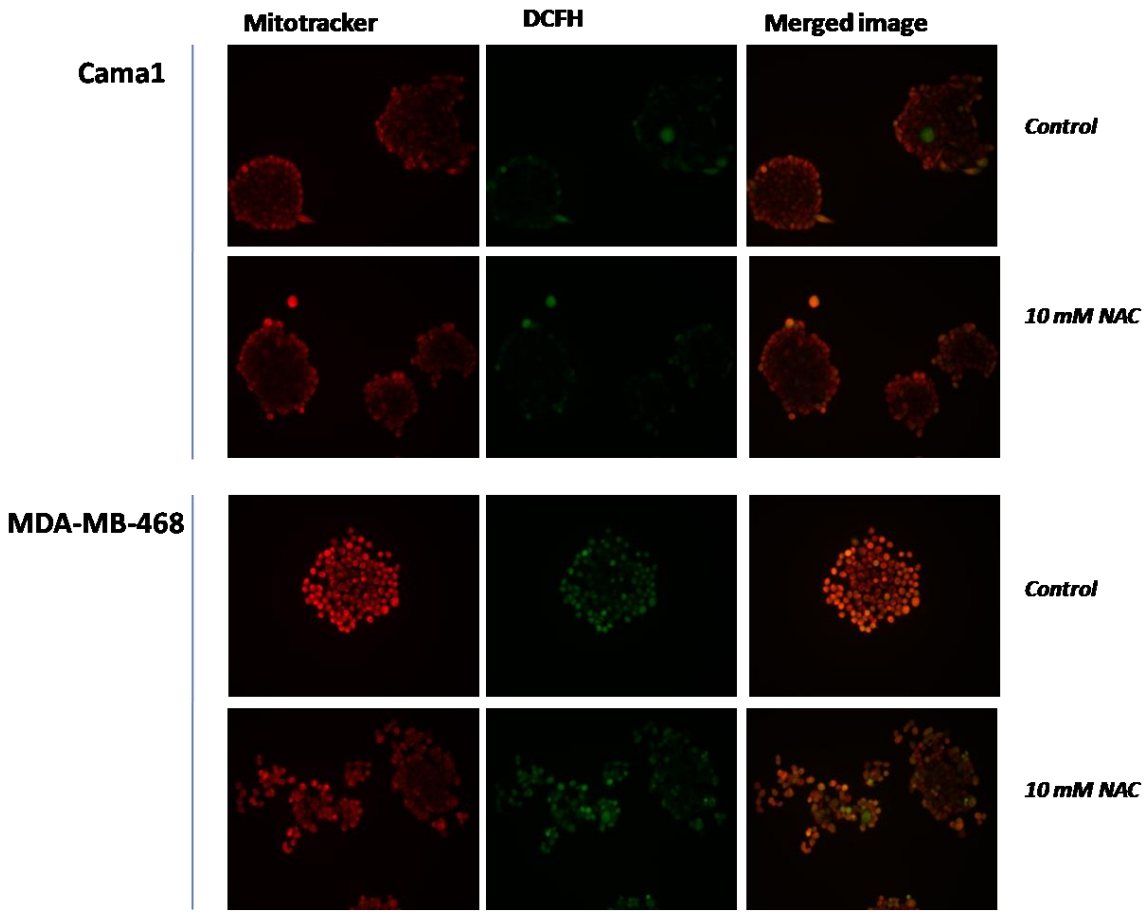

Figure 15: Co-staining with DCFH and Mitotracker in Cama1 and MDA-MB-468 cell lines at Day 10. No significant ROS accumulation was observed in Cama1 cells.

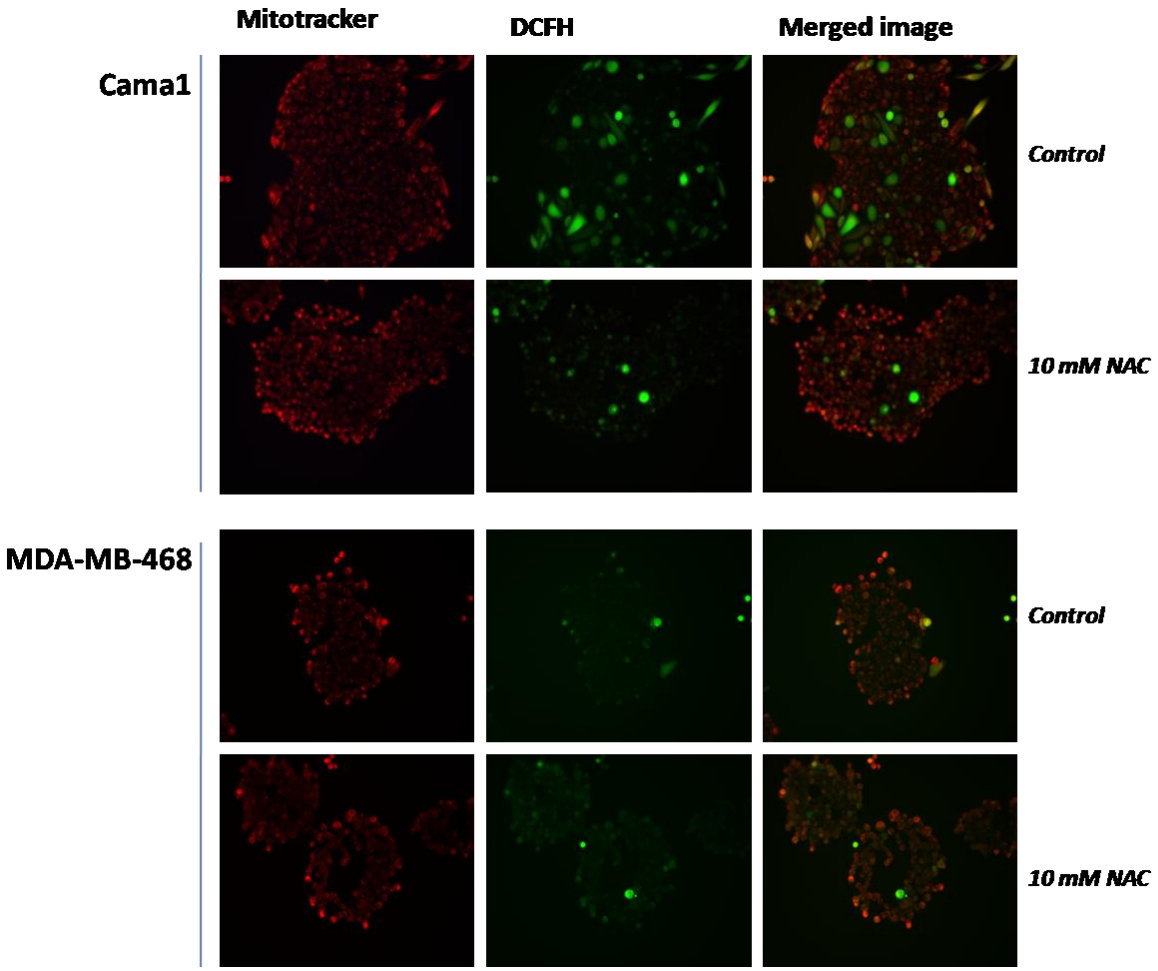

Figure 16: Co-staining with DCFH and Mitotracker in Cama1 and MDA-MB-468 cell lines at Day 13.

Increased level of ROS accumulation was observed at Day 13 in Cama-1 control cells compared to NAC treated cells. 10 mM NAC treatment in Cama-1 cells caused decrease in ROS accumulation. No major difference was seen between control and NAC treatment received cells in MDA-MB-468.

Mitotracker staining didn't present any significant variation in the plates suggesting that ROS accumulation is not originating from mitochondria.

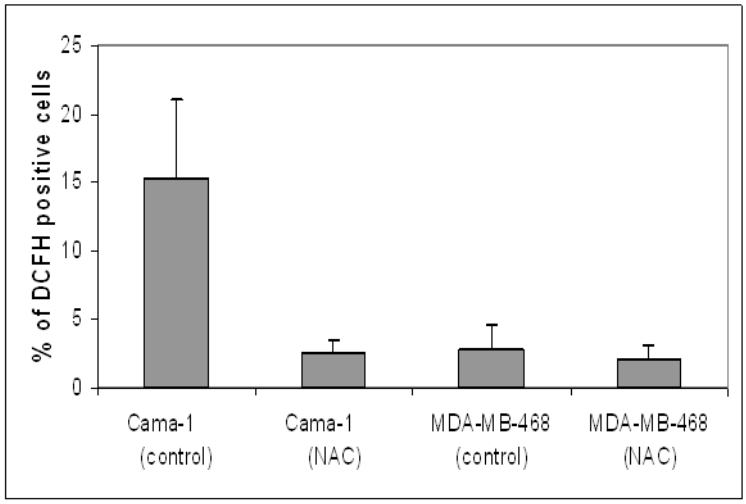

*p <0.0001.

Figure 17: Percentage of DCFH positive cells before and after NAC treatment in Cama1 and MDA-MB-468 plates at Day13.

High percentage of Cama1 cells show ROS accumulation compare to MDA-MB-468 cells. Also after 10mM NAC treatment ROS levels decrease significantly in Cama1 cells.

4.2.1.1. ROS accumulation was confirmed by co-staining with NBT and SABG

NBT assay was used to confirm our previous results where we observed ROS accumulation in Cama-1 cells.

Reduction of NBT (nitro blue tetrazolium) to formazan is one of the established methods to detect intracellular O_2^-generation. NBT is reduced by only O_2^-, which may act as electron donor or acceptor, but not by H_2O_2, which is an oxidizing agent. Moreover, NBT preferentially detects intracellular O_2^- (Berridge *et al*., 2005).

BT-474 cells were co-stained, which is again a senescence-positive cell line, with NBT and SABG (detail of co-staining is described in the methods section). As seen in the Figure 18, most of the SABG positive cells co-stained with NBT, and some of them stained only with NBT. SABG and NBT did not totally overlap. This can be

explained by the scenario that ROS accumulation starts and then ROS may activate some signaling pathways and this induces senescence response.

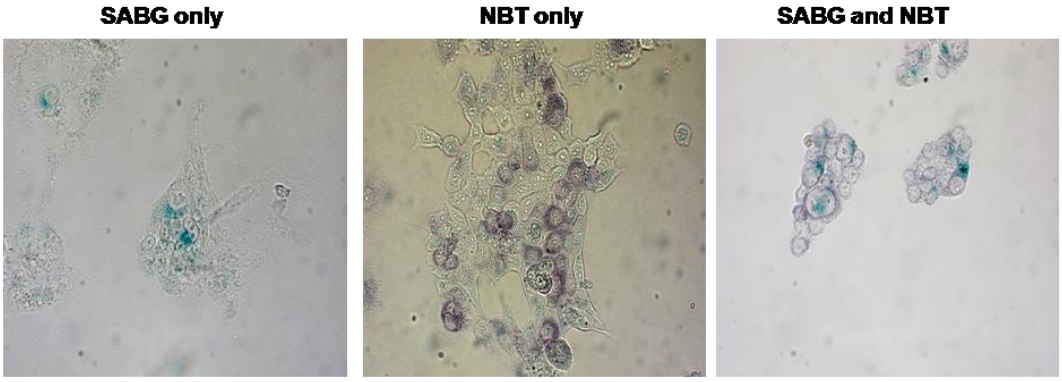

Figure 18: Co-staining of BT474 cells with NBT and SABG.

Most of the SABG positive cells overlapped with NBT stained cells. This demonstrates that senescence and ROS increase occurs in these cells at the same time.

4.2.2. Relationship between ROS accumulation and senescence

To understand whether 1) ROS accumulation is related with senescence, and 2) inhibition of ROS can reverse senescence phenotype, we decided to treat Cama-1 cells with NAC. NAC is reduced glutathione (GSH) provider for cells and a scavenger of ROS (Staal *et al*, 1990).

For this experiment Cama-1 cell line, which is one of the breast cancer cell lines from our SCP group, was chosen. Cells were seeded in low density and treated with 10mM NAC (experiment details are in the material-methods section). Only ddH2O was added to the control group. One set of experiment was stopped at day 10 and the other group was stopped at day 15. Then SABG assay was performed in order to check their senescence status. SABG positive cells were counted manually.

At Day 10, decrease in SABG index (percentage of SABG positive cells per colony) in either 10 mM or 20 mM NAC treated cells compare to untreated control was

observed. Also, similar very low level of SABG index was found at Day 15. But untreated control plates showed higher percentage of SABG index compare to day 10 control plates. This was probably because of the increase in ROS accumulation in these cells in the absence of NAC when the duration got increased (Figure 20). These results showed that by inhibition of ROS accumulation in Cama1 cells we were able to decrease the number of cells that enter senescence stage. This provides evidence that there is a relationship between ROS accumulation and senescence phenotype in Cama1 cell line, which is a representative of SCP group of breast cancer cell lines.

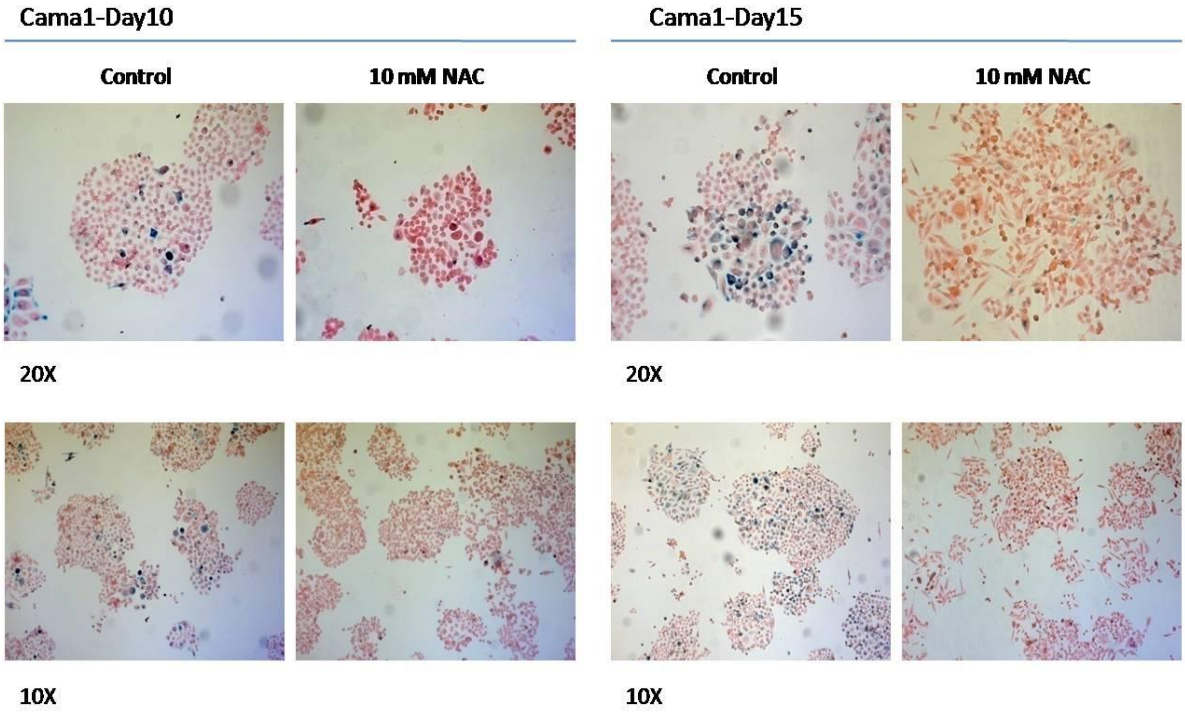

Figure 19: SABG staining of Cama1 cells after treatment of NAC.

NAC treatment protects cells from senescence both Day10 and Day15

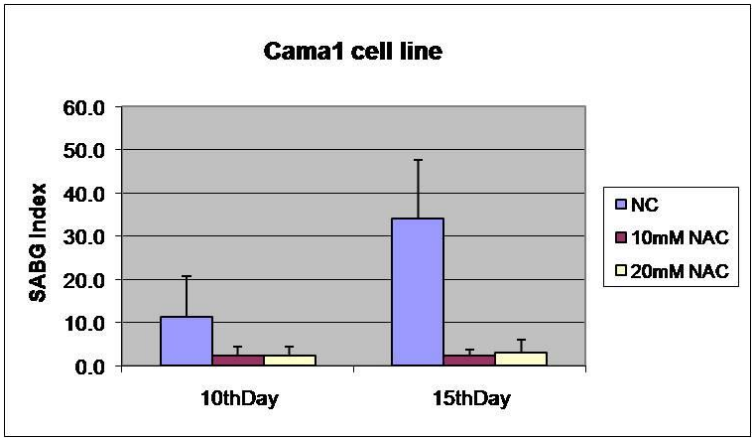

Figure 20: Quantification of SABG-positive cells in colonies from NAC treated and untreated Cama1 cell line.

Either 10 mM or 20 mM NAC protects cells from ROS accumulation and senescence. Also increase in SABG index of day 15 compare to SABG index of day 10 in untreated control plates could be the indicator of ROS accumulation.

4.2.3. Differential expression of NOX genes in breast cancer cell lines

Nox family of NAPDH oxidases is a family of enzymes whose physiological function is ROS generation. There are five important members of family of NAPDH oxidases, Nox1-5.

Previous experiments showed us that ROS accumulation in our senescence-positive breast cancer cell lines was from intracellular origin. Therefore, we wanted to analyze expression of Nox genes in our breast cancer cell line panel by using RT-PCR method. As seen in Figure 21, only Nox2 and Nox5 expressions were elevated in senescence-positive group of breast cancer cell lines compared to some of the cell lines in senescence-negative group. After this RT-PCR result, we wanted to extend and confirm our expression studies. Nox2 and Nox5 expression levels were evaluated by quantitative real-time PCR (qRT-PCR). qRT-PCR results were matched with previous RT-PCR results. qRT-PCR results were calculated as arbitrary unit. In Nox2, BT-474, T-47-D and Cama-1 showed increased expression. Only T-47-D presented substantial increase in expression compared to other cell lines in Nox5 (

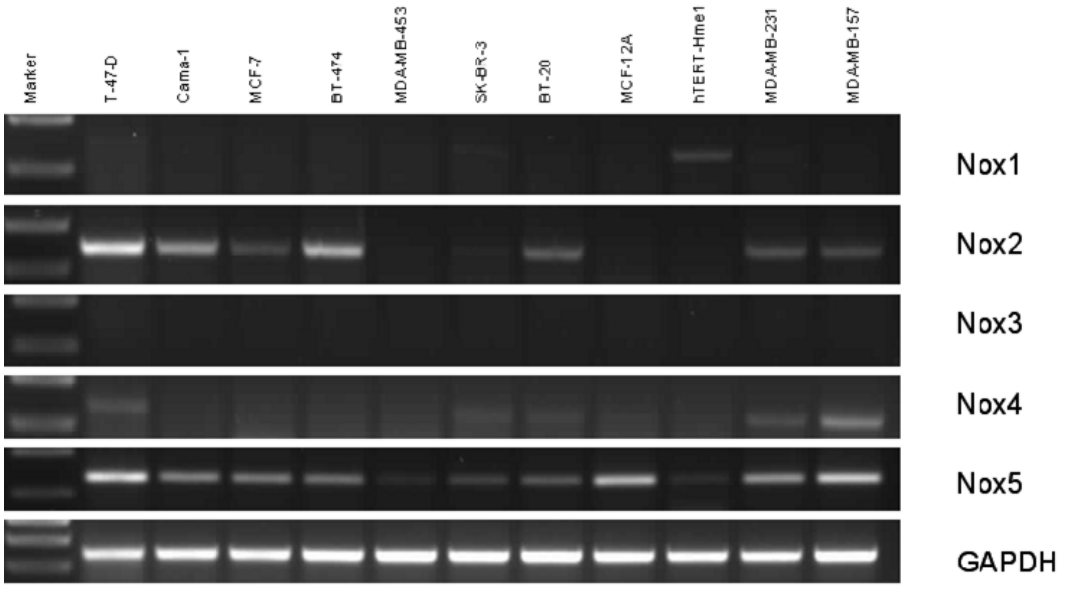

Figure 21: Expression analysis of Nox genes in breast cancer cell line panel by RT-PCR.

Data showed that expression of Nox2 and Nox5 were increased in senescence positive cell lines.

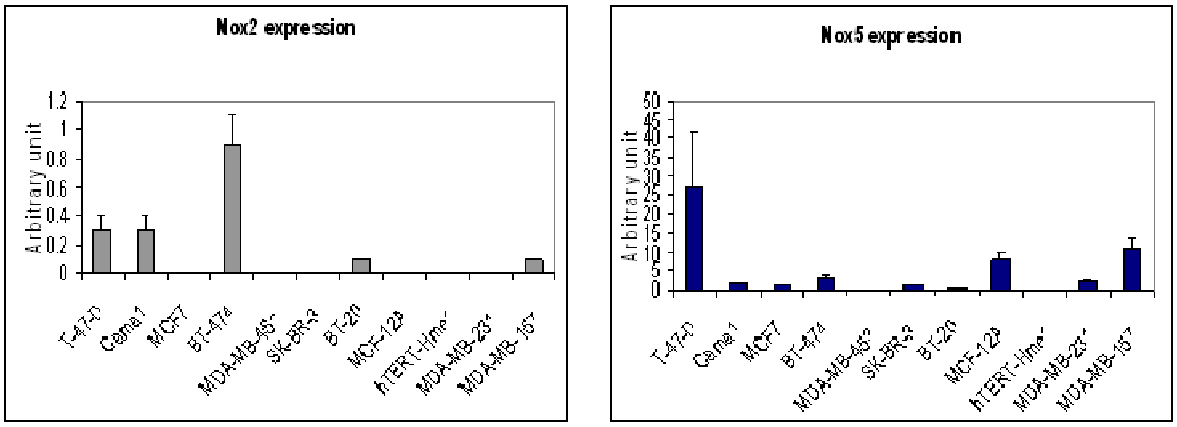

Figure 22: Real time PCR analysis of Nox2 and Nox5 expression in breast cancer cell lines.

BT474 showed highest expression of Nox2. In other senescence positive cell lines, except MCF7, high level of Nox2 expression was observed. Nox5 expression was very striking in T-47-D

4.3. Role of P16^{INK4a} and p21$^{WAF1/Cip1}$ in breast cancer senescence

P21/p53 and P16^{INK4a} /Rb pathways are two crucial pathways implicated in the senescence program. The cyclin-dependent kinase inhibitor p21 (also known as p21$^{WAF1/Cip1}$) has profound role in cell cycle arrest, differentiation and cellular senescence. P21$^{WAF1/Cip1}$ mediates these functions either through p53-dependent or independent of the classical p53 tumor suppressor pathway (Abbas T. and Dutta A., 2009).

4.3.1. P16^{INK4a}: No significant correlation between P16^{INK4a} expression and SCP phenotype.

P16^{INK4a} is a tumor suppressor and Cdk inhibitor. P16^{INK4a} blocks pRb phosphorylation by inhibiting cdk4 and cdk6 association with cyclin D. Failure in pRb phosphorylation and in E2F release cause G1 cell cycle arrest.

Therefore we wanted to examine expression status of p21^{Cip1} and P16^{INK4a} in our breast cancer cell line panel. We performed low density cloning assay and immunoperoxidase staining to detect p21^{Cip1} and P16^{INK4a} expression in the colony basis. Two SCP cell lines displayed heterogeneously positive P16^{INK4a} staining. On the other hand three of seven ICP cell lines displayed homogenously positive staining (Figure 23). We couldn't found any statistically significant association with P16^{INK4a} expression and SCP subtype ($p = 0.6893$).

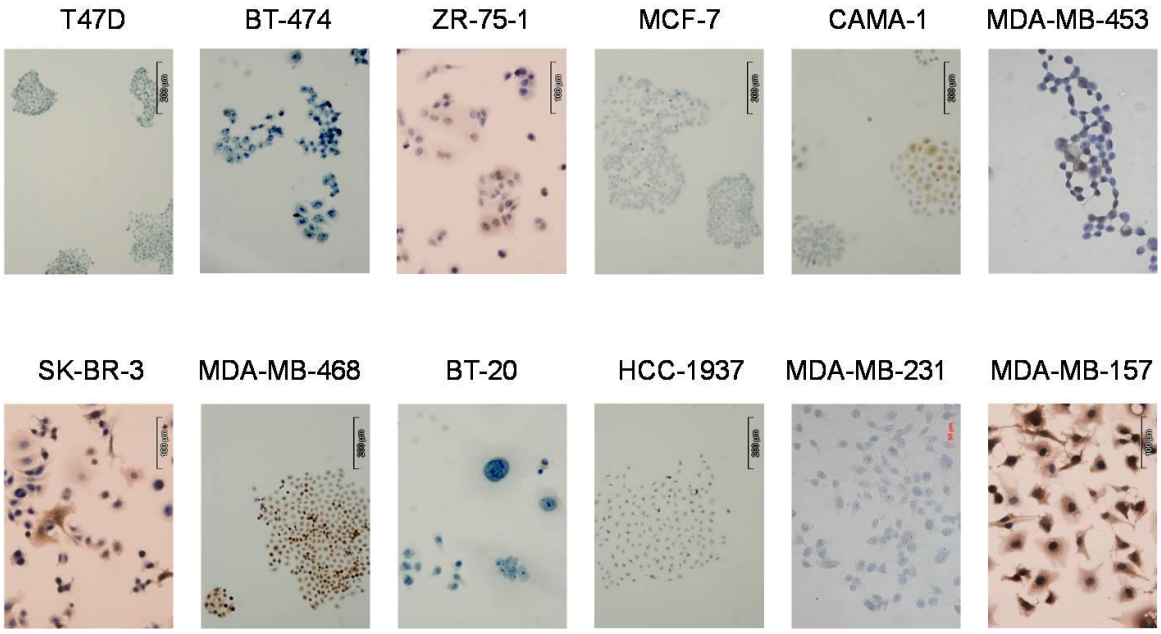

Figure 23: No significant correlation between P16INK4a expression and SCP phenotype.

P16^{INK4a} immunoperoxidase staining in breast cancer cell lines panel. From SCP subgroup ZR-75-1 and Cama1, from ICP group SK-BR-3 and MDA-MB-468 showed heterogeneous P16^{INK4a} staining. MDA-MB-157 was full positive for P16^{INK4a}. Results didn't show any correlation between SCP subgroup and P16^{INK4a} expression.

4.3.2. p21^{Cip1} expression correlates with SCP subgroup

p21^{Cip1} analysis showed that 4 out 5 SCP subtypes of cell lines express strong nuclear p21^{Cip1} heterogeneously. ICP subtype breast cancer cell lines were negative for the P21^{Cip1}expression (Figure 24). The association of p21^{Cip1} expression with the SCP subtype was statistically significant (p =0.0100)

These results suggested that there is a relationship between senescence and P21^{Cip1} expression. But Immunoperoxidase results didn't provide any correlation related with P16^{INK4a} expression and senescence phenotype in our breast cancer panel.

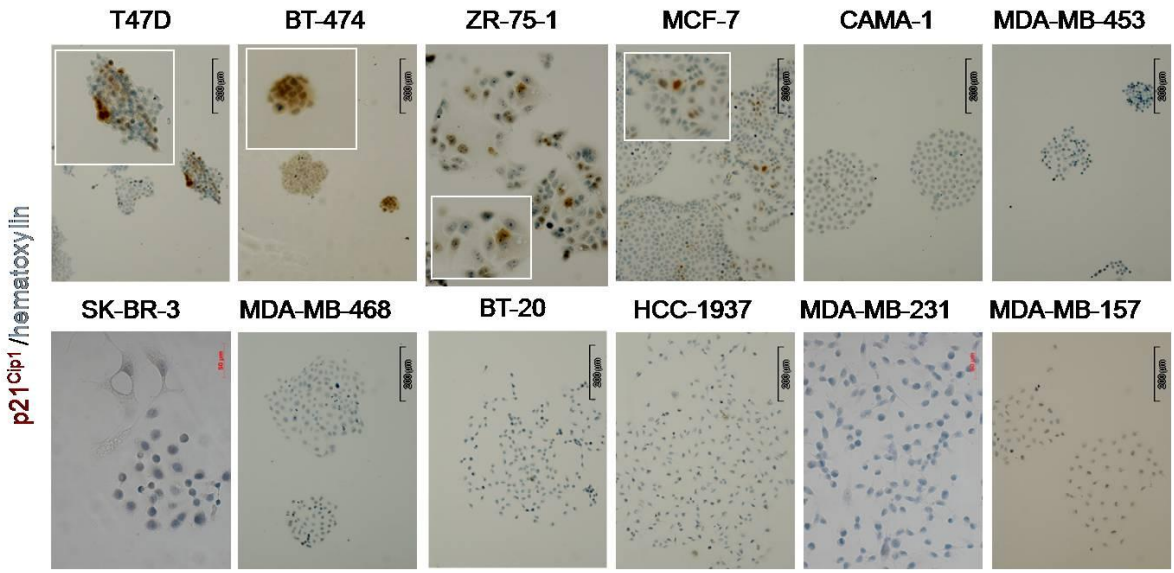

Figure 24: p21Cip1 correlate with SCP subgroup. $p21^{Cip1}$ immunoperoxidase staining in breast cancer cell lines panel.

$p21^{Cip1}$ analysis showed except Cama1 the entire SCP group of breast cancer cell lines expresses strong nuclear $p21^{Cip1}$ heterogeneously. All ICP subtype breast cancer cell lines were negative for the $P21^{Cip1}$expression. The association of $p21^{Cip1}$ expression with the SCP subtype was statistically significant.

To confirm relationship between senescence and $P21^{Cip1,}$ SABG and $p21^{Cip1}$ co-staining was performed in T47D cells. Co-staining showed that SABG positive staining mostly overlap with $p21^{Cip1}$ expression in T47D cells. Co-staining also carried out MDA-MB-231 cells. As expected MDA-MB-231 cells didn't showed any positive staining for either SABG or $p21^{Cip1}$ (Figure 25).

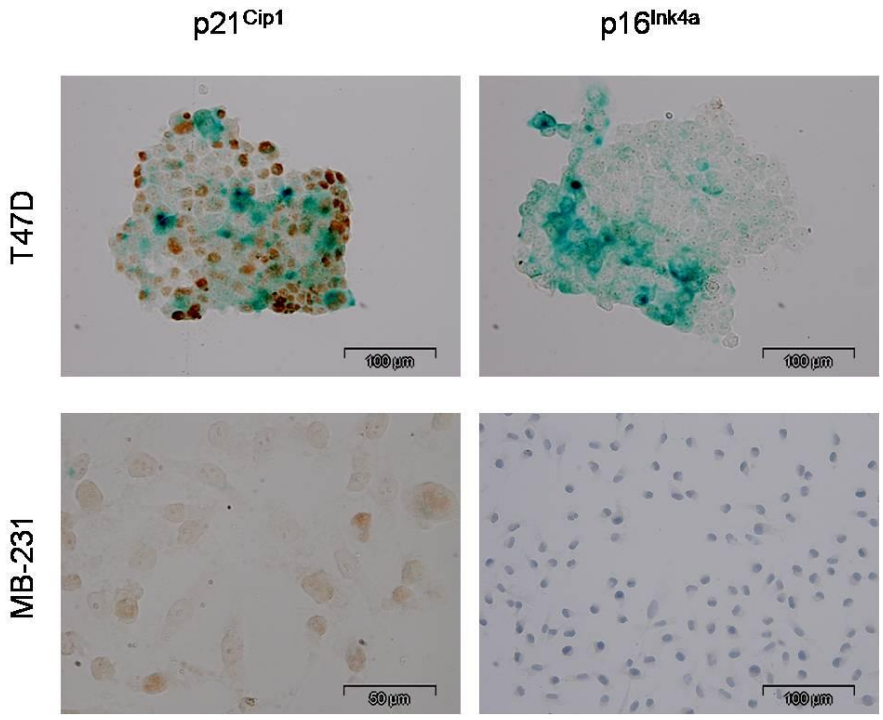

Figure 25: Co-staining of SABG and p21Cip1 in T47D and MDA-MB-231 cell lines. In T47D, SABG positive staining mostly overlaps with p21Cip1staining confirming that there is a relationship between senescence and p21Cip1.

4.3.3. p21^{Cip1} is partially responsible for senescent cell progenitor phenotype

Strong relationship between p21^{Cip1} and SCP subgroup of cell lines lead us further analyze the involvement of p21^{Cip1} in the senescent phenotype of these cell lines. We wanted to down-regulate p21^{Cip1} and checked its effect on the senescence.

For this purpose after infection of T47D with lentiviral vectors encoding p21^{Cip1} shRNA (T47D-p21sh) or a scrambled control (T47D-scr), two clones were generated. Western blot was confirmed successful p21^{Cip1} knockdown in T47D-p21sh cells (Figure 26B).Then we seeded both cell lines in low-density conditions. After 10 days, SABG and BrdU staining were performed. But because cells were formed tight clusters, it was difficult to evaluate SABG positive cells. For this reason we used BrdU staining instead of SABG to determine senescent cells (Figure 26C).

Colonies selected randomly and BrdU positive cells were counted manually (Figure 26D). The T47D-scr cell line generated BrdU+ progeny at a rate of 48±20% per colony (n=18). Under the same conditions, T47D-p21sh cells displayed BrdU+ progeny at a rate of 65±12% per colony (n=18), with a significant (p = 0.0043) increase in the number of cells escaping terminal arrest (Figure 26E).

These results display that $p21^{Cip1}$ was partially responsible for the induction of senescence observed in the progeny of T47D cells.

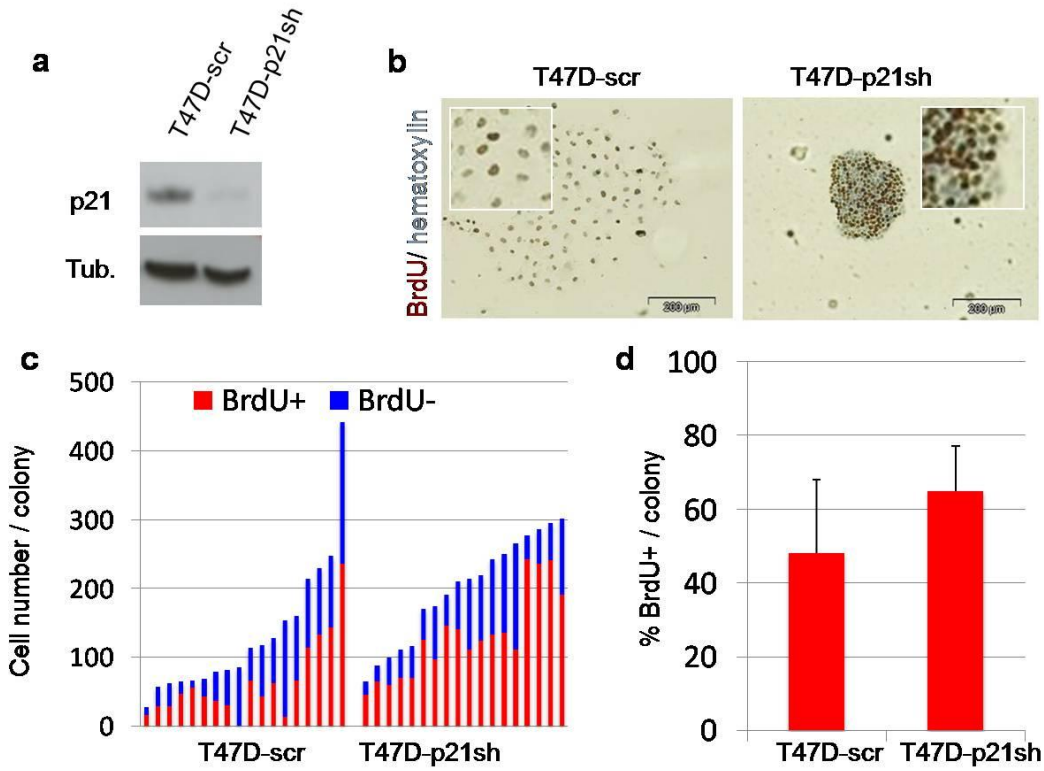

Figure 26: $p21^{Cip1}$ is partially responsible from senescence arrest in T47D cell line

A) $p21^{Cip1}$ is downregulated by lentiviral infection of $p21^{Cip1}$ shRNA. Down regulation was confirmed by western blot. B) Senescence is assessed by BrdU assay. Cells were seeded in low-density condition and cultivated 10 days in cell culture in order to generate colonies. Brown color staining represents BrdU incorporated

proliferating cells. BrdU incorporation increased in T47D-p21sh cells compare to T47D-scr (control) cells. C, D) Colonies selected randomly and cells counted manually from BrdU assay. T47D-p21sh cells generated BrdU positive cells at a rate of 65±12% per colony. But T47D-scr cells only displayed positive progeny at a rate of 48±20% per colony (n=18).

4.4. Role of ER in breast cancer senescence

4.4.1. ER expression and senescence

P53 pathway is one of the important pathways in cellular senescence. Even though $p21^{Cip1}$ is downstream target of p53, our T47D cell line does not express wild-type p53 (Table 4). Estrogen effects cell cycle progression through loss of $p21^{Cip1}$ (Cariou *et al*., 2000). E2 mediates p21 inhibition by c-myc (Mukherjee and Conrad, 2005). Myc gene is direct target of ER complex (Dubik and Shiu, 1992). Therefore, we wanted to check involvement of ER in senescence phenotype in breast cancer cell lines. First SABG and ER co-staining was performed in T47D and MDA-MB-231 cells. Results showed that T47D cells display strong nuclear ER immunoreactivity in most of the cells, but some of the cells were ER- (Figure 27). More interestingly, These ER- cells were SABG+, referring that the senescence occurred in T47D cells as a result of ER lost. In contrast to T47D, MDA-MB-231 cells do not show ER expression and SABG negative. Thus, the senescence susceptibility was restricted to ER+ T47D cells; however the senescent cells no longer expressed nuclear ER protein.

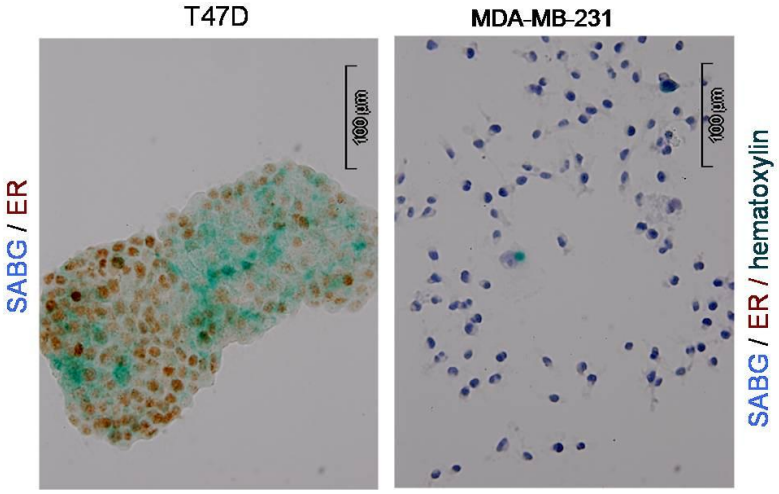

Figure 27: ER lost related with senescence phenotype in T47D cells.

T47D and MDA-MB-231 cells were co-stained with ER and SABG. Heterogenic ER expression was observed in T47D cells. Interestingly SABG positive cells were negative for ER expression. As expected MDA-MB-231 cells were negative for both ER and SABG.

4.4.2. Effect of Estrogen and Tamoxifen treatment

Next, we wanted to test whether experimental modification of ER activity in T47D cells could create any change in senescence response. Again cells were plated at low-density clonogenic conditions in complete DMEM, which contains weakly estrogenic phenol red (Berthois *et al*., 1986). Cells were cultured for seven days in order to obtain visible colonies. After seven days, culture medium was replaced with phenol-free DMEM complemented with charcoal-treated fetal calf serum, grown for two more days, then cultivated for four more days in the presence of E2 (10-9 M), 4-hydroxytamoxifen (OHT; 10-9 M to 10-6 M), or an ethanol vehicle as control. Later experiment was stopped and SABG assay was performed (Figure 28B). Total and SABG positive cells were counted from 20 randomly selected colonies in 4 different areas for each treatment. As seen on the figure, complementation of the medium with 10-9 M E2 caused inhibition of senescence almost 50%. Control cells generate colonies which display 31±13% SABG positivity on the other hand 10-9 M E2 treated cells displayed 17±18% SABG positivity in their colonies (Figure 28C).

When we compared control and E2 treatment inhibition in senescence was statistically significant ($p = 0.0093$).

In contrast to E2, OHT treatment of T47D cells creates a dose-dependent increase in the senescence response. At the maximum dose, 10-6 M OHT, we observed 90±13% SABG positivity in the colonies (Figure 28D), indicating that tamoxifen-mediated inactivation of ER can induce almost a complete senescence response in these cells ($p < 0.0001$). The increase in senescence rate was also significant with 10-7 M OHT ($p = 0.0002$). Our findings strongly suggested that the senescence observed in the SCP T47D cell line was due to a loss of expression and/or function of ER in a subpopulation of the progeny of these cells.

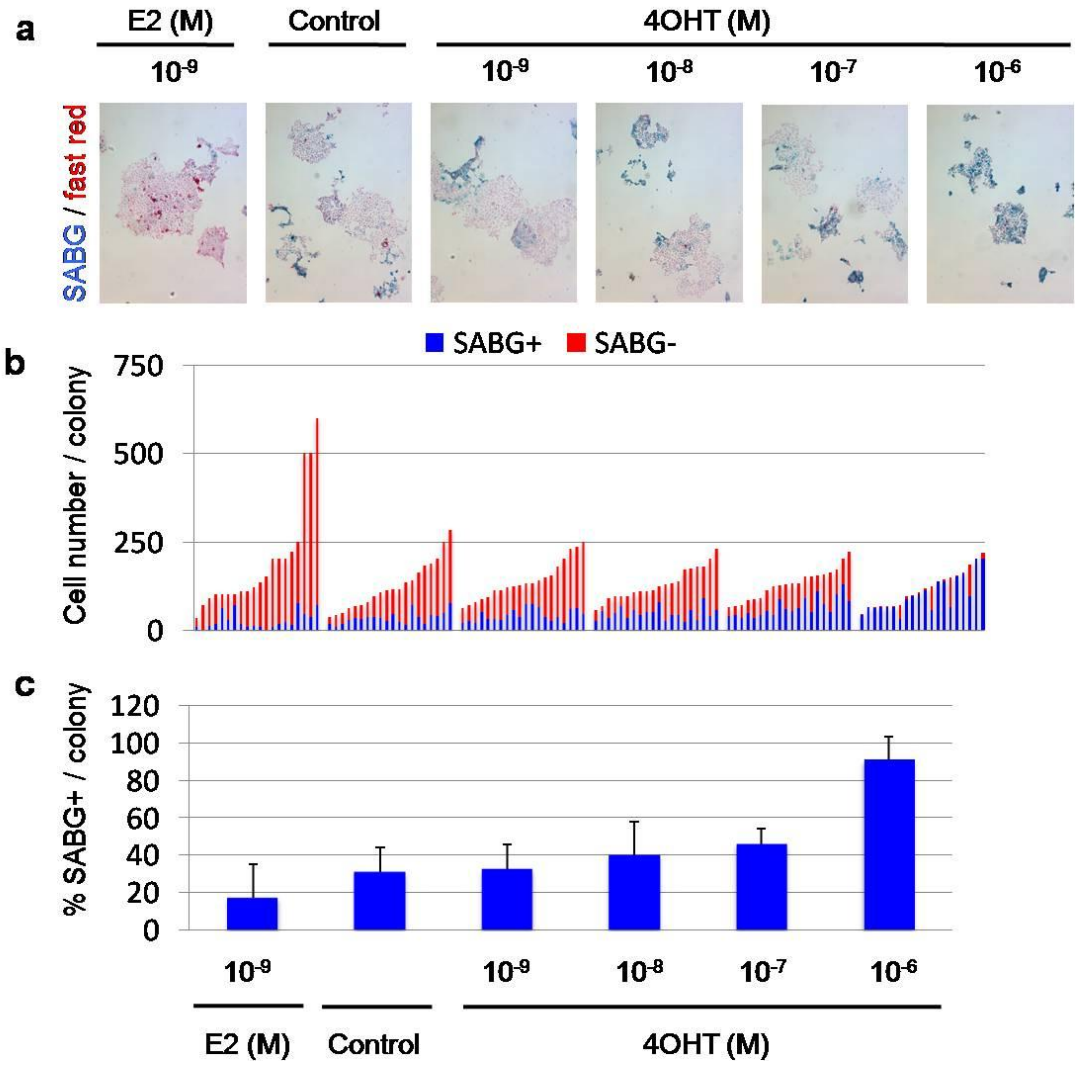

Figure 28: Estrogen treatment decreased generations of senescent progeny whereas Tamoxifen (4OHT) treatment increased

A) Cells were seeded in low density condition and cultured seven days in standard culture medium. Then culture medium replaced with replaced with phenol-free DMEM complemented with charcoal-treated fetal calf serum, grown for two more days, then cultivated for four more days in the presence of E2 (10^{-9} M),

B) 4-hydroxytamoxifen (OHT; 10^{-9} M to 10^{-6} M), or an ethanol vehicle as control. Later experiment was stopped and SABG assay was performed B) SABG positive and negative cells were counted from randomly selected colonies (n=20) and mean % SABG+ cells (± SD) were calculated

C) Inhibition by estrogen and activation by tamoxifen of senescence response was statistically significant ($p < 0.0001$) and ($p = 0.0002$)

4.4.3. Effect of ER overexpression

To confirm our results, we generated ER-overexpressing stable clones from T47D cell line. According to western blot result, three highest ER expressing clones were selected. Three other clones with endogenous expressions of ER were also selected from stable clones obtained with an empty vector (Figure 30A). BrdU assay was used for senescence response evaluation after low density cloning assay. Randomly selected colonies (n=10) from each clone were analyzed for total and BrdU+ number of cells (Figure 30B). Consistently higher levels of BrdU+ cells were observed with clones ectopically expressing the ER protein (Figure 30C). Overexpression of ER resulted in a significant increase in the BrdU+ progeny ($p = 0.034$). This finding is provided additional support to the previous data, which shows close relationship between ER expression and senescence in T47D cells. These results are indicating that acute lost of ER in T47D cells cause senescence phenotype. Also lack of senescent progeny in ER (-) MDA-MB-231 cells shows that ER expression and senescence could be possible factors responsible from good prognostic features of Luminal A group of breast cancers.

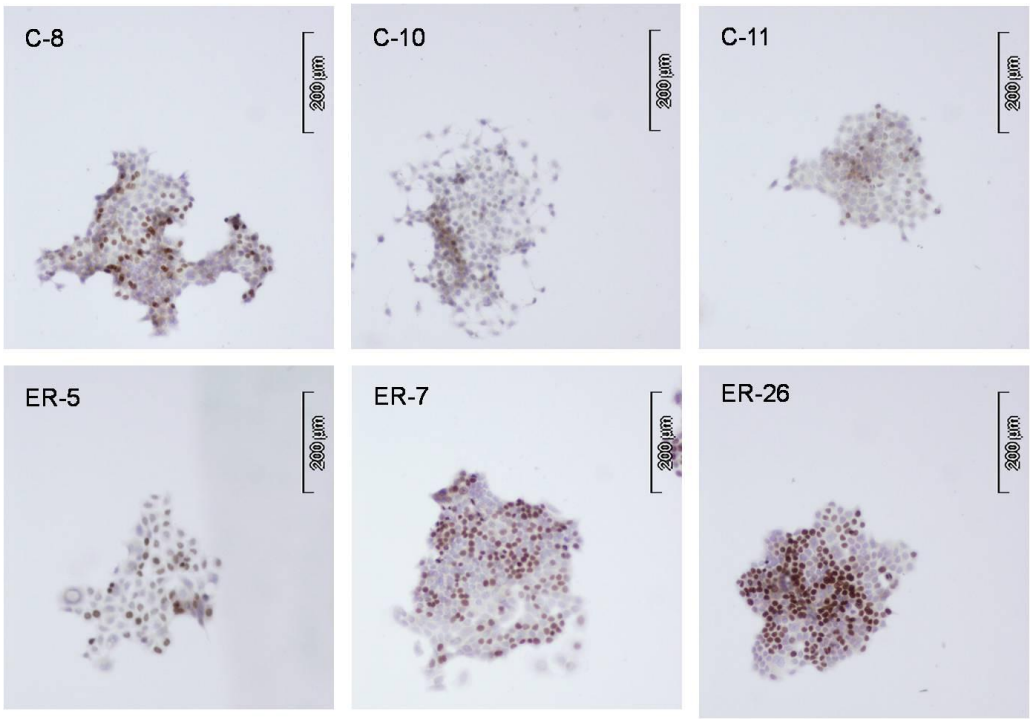

Figure 29: ER overexpression caused increased BrdU incorporation in T47D clones. 24 hour BrdU labeling and immunostaining in ER overexpressing clones (ER-5, ER-7, and ER-26) and control ones (C-8, C-10, C-11)

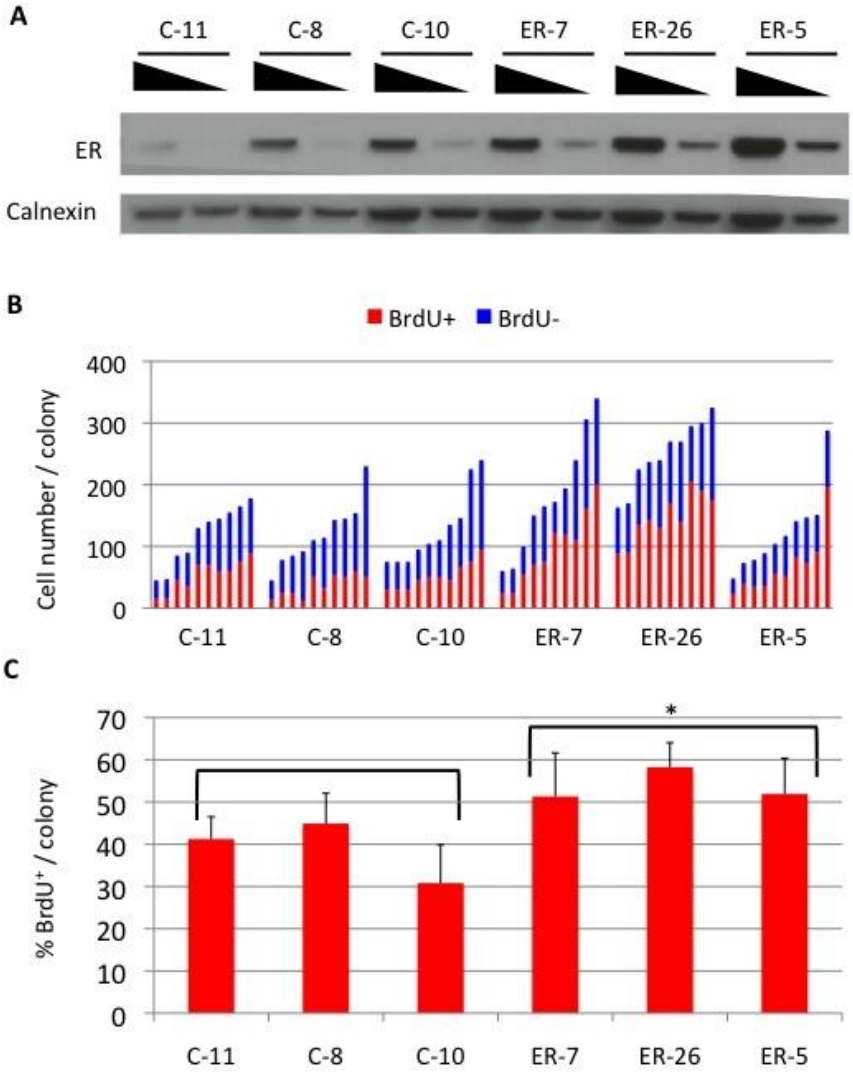

Figure 30: ER overexpression inhibits generation of senescent progeny in T47D cells

A) ER-overexpressing and control clones were established from T47D cells (C-8, C-10, C-11 are control, ER-5, ER-7, ER-26 are overexpression clones). ER expression levels were checked by western blot. Calnexin was used as loading control B) For BrdU assay; colonies were generated, labeled with BrdU for 24 hours and immunostained. BrdU positive cells quantified by manually C) Graphic present mean % BrdU+ cells per colony. ER overexpressed clones showed significant increased in BrdU ratio ($p=0.034$). (Error bars represent mean ± SD)

4.4.4. Senescence in ER+ tumors

All these data showed that there is a close relationship between ER expression and senescence in our ER+ cell line T47D. Also we wanted to analyze senescence phenotype in ER+ breast tissues to support our results with in vivo results. Breast tumor samples were collected from untreated patients. For obvious ethical reasons, it cannot be obtained fresh tumor tissues from tamoxifen treated patients. Therefore we analyzed small panel of 12 snapfrozen ER+ breast tumor tissues from 11 patients by SABG assay. The mean age of patients was 58±12 years, with a mixed menopause status (Table S2). Among these samples two tumors present SABG positive cells were scattered within the tumor area (%17)
(Figure 31). These result showed that ER+ tumors produce senescent progeny at a lower rate.

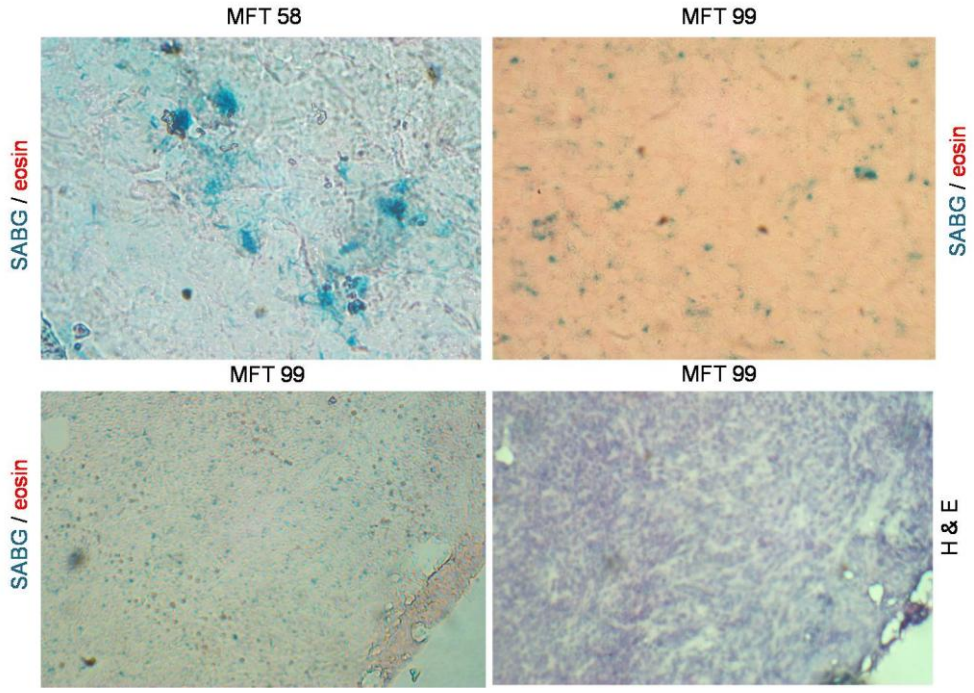

Figure 31: Detection of SABG+ senescent cells in estrogen receptor-positive breast tumors.

6µ thick snap-frozen tumor sections were used to detect SABG+ cells. H&E: hematoxylin-eosin staining

Sample Label	Patient age	Menopause	ER status	Grade	LN	Stage	Type	SABG
MFT29	58	Post-menopause	(+)	1	(+)	2	IDC	Negative
MFT46	64	Post-menopause	(+)	1	(+)	N/A	IDC	Negative
MFT55	68	Post-menopause	(+)	2	(-)	N/A	IDC	Negative
MFT58	**62**	**Post-menopause**	**(+)**	**3**	**(+)**	**2B**	**IDC**	**Positive**
MFT78	69	Post-menopause	(+)	2	(+)	N/A	IDC	Negative
MFT83	47	Post-menopause	(+)	2	(+)	2B	IDC	Negative
MFT88	60	Post-menopause	(+)	2	(+)	N/A	IDC	Negative
MFT90	32	Post-menopause	(+)	2	(+)	2B	IDC	Negative
MFT93	42	N/A	(+)	3	(+)	2A	IDC	Negative
MFT95	56	Post-menopause	(+)	3	(+)	N/A	IDC	Negative
MFT99 (right)	68	Post-menopause	(+)	2	(+)	2A	IDC	Negative
MFT99 (left)	**68**	**Post-menopause**	**(+)**	**2**	**(+)**	**1**	**IDC+ILC**	**Positive**
Mean	58							
SD	12							

N/A, not available.

Table 3: ER status, main pathological features of senescence staining (SABG) of breast tumors used in this study

4.5. Senescence as a major determinant of breast cancer molecular heterogeneity

4.5.1. Role of differentiation ability in SCP and ICP subtypes

Estrogen receptor expression in breast tumors is very important determinant for anti-estrogen therapies and for the prognosis. But even its importance we don't have enough knowledge about distribution of ER+cells among the mammary epithelial cell hierarchy. Previous observations suggest that normal ER+ cells may represent either relatively differentiated luminal cells with limited progenitor capacity, or primitive progenitors with stem cell properties in the luminal cell compartment Luminal restricted progenitors (Stingl and Caldas, 2007). According to our finding we hypothesize that we hypothesized that ER+ SCP cells may differ from ER- ICP cells by their differentiation potential.

To test this hypothesis we screened our 12 breast cancer cell lines by immunoperoxidase technique for their ability to generate stem/progenitor-like, luminal-like and myoepithelial-like cells. We used CD44 as a positive

stem/progenitor cell marker (Al-Hajj *et al*., 2003; Shipitsin *et al*., 2007), CD24, ER and CK19 as luminal lineage markers (Sleeman *et al.*, 2006; Shipitsin *et al*., 2007; Yeh and Mies, 2008) and ASMA as a myoepithelial lineage marker (Yeh and Mies, 2008) Representative pictures from marker studies are shown in Figure 33A-B and results are summarized in Figure 34. CD44 staining showed heterogeneous staining in all of the SCP cell lines. But 5 of the 7 cell lines from ICP subgroup only produced fully positive colonies. This result displays that these cell lines cannot produce CD44- cells. One cell line (MDA-MB-453) was totally negative for CD44. SK-BR-3 was showed heterogenic CD44 staining parallel to SCP group staining. When we compare the both subgroup's results in terms of ability of generate both CD44+ and CD44- progeny it is mostly associated with the SCP phenotype ($p = 0.0046$).

In ER immunostaining, all of SCP cell lines showed heterogeneous and mostly positive staining whereas all seven ICP cell lines never produced ER+ cells. ER expression was also significantly associated with the SCP subtype ($p = 0.0012$).
Moreover, we also found that ability to produce ASMA+ progeny was also significantly associated with the SCP subtype ($p = 0.0046$). ICP cell lines did not generate ASMA positive cells. Also we noticed that under low-density clonogenic conditions two SCP cell lines generate rare ASMA+ cells compare to under high-density conditions (Figure 32). This could be either ASMA+ cells are enhanced at high cell density, or these myoepithelial-like cells have limited survival ability under long-term culture conditions.

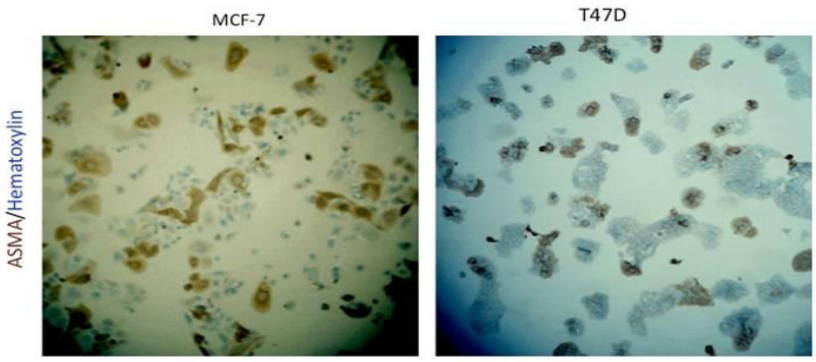

Figure 32: High density seeded MCF7 and T47D cells show more ASMA+ expression.

We did not find a strong association between the expression of CD24 and CK19 markers and cell subtype. All five SCP cell lines and three ICP cell lines generated heterogeneously staining colonies for CD24 expression. Similarly, all five SCP cell lines, as well as three ICP cell lines, expressed CK19, but homogenously.

A
CD44
CD24
CK19
ER
ASMA
T47D
BT-474
MCF-7
CAMA-1
ZR-75-1
Senescent cell
progenitor subtype

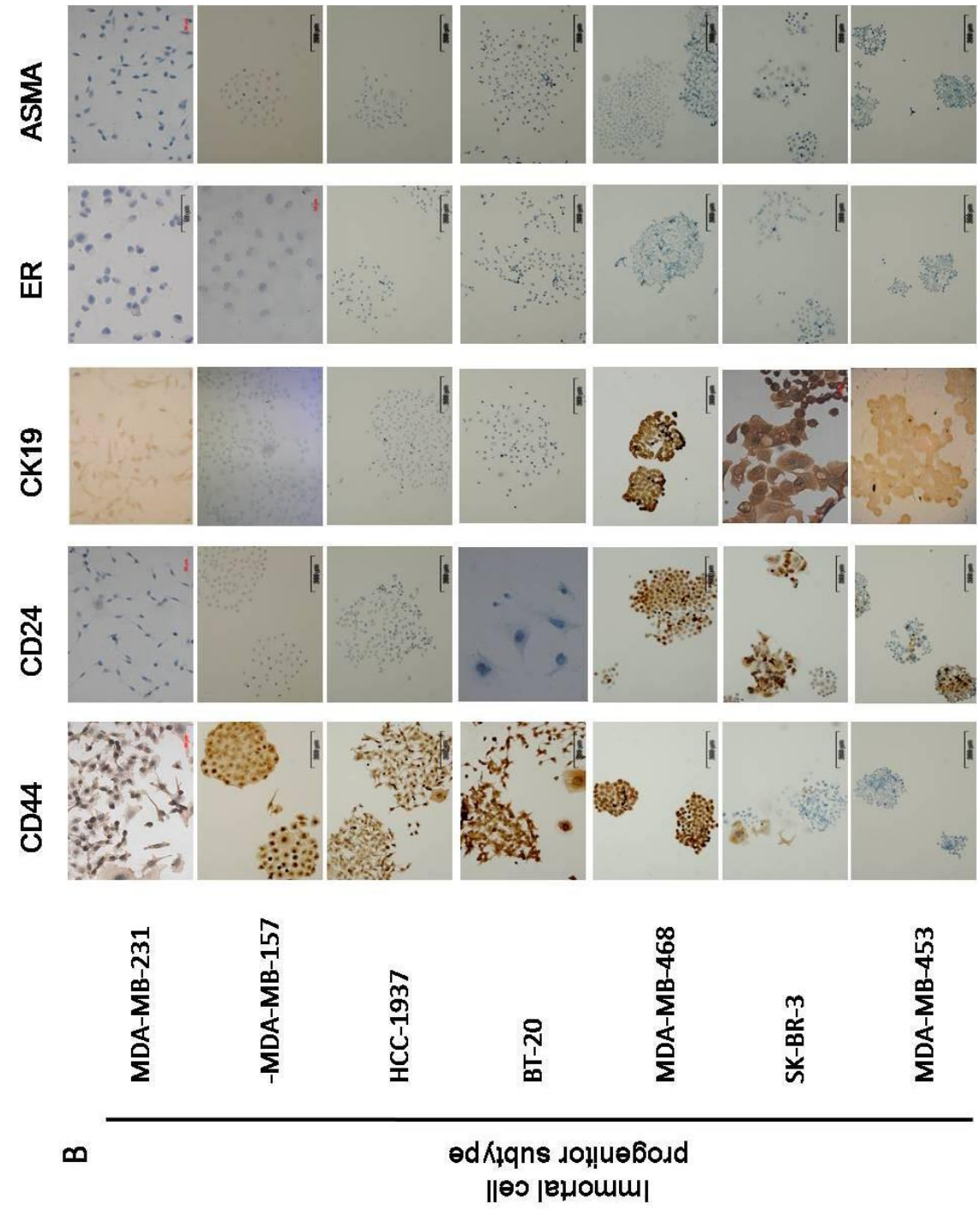

Figure 33: Representative pictures from marker studies A) Senescent Cell Progenitor subtype cell lines B) Immortal Cell Progenitor subtype cell lines

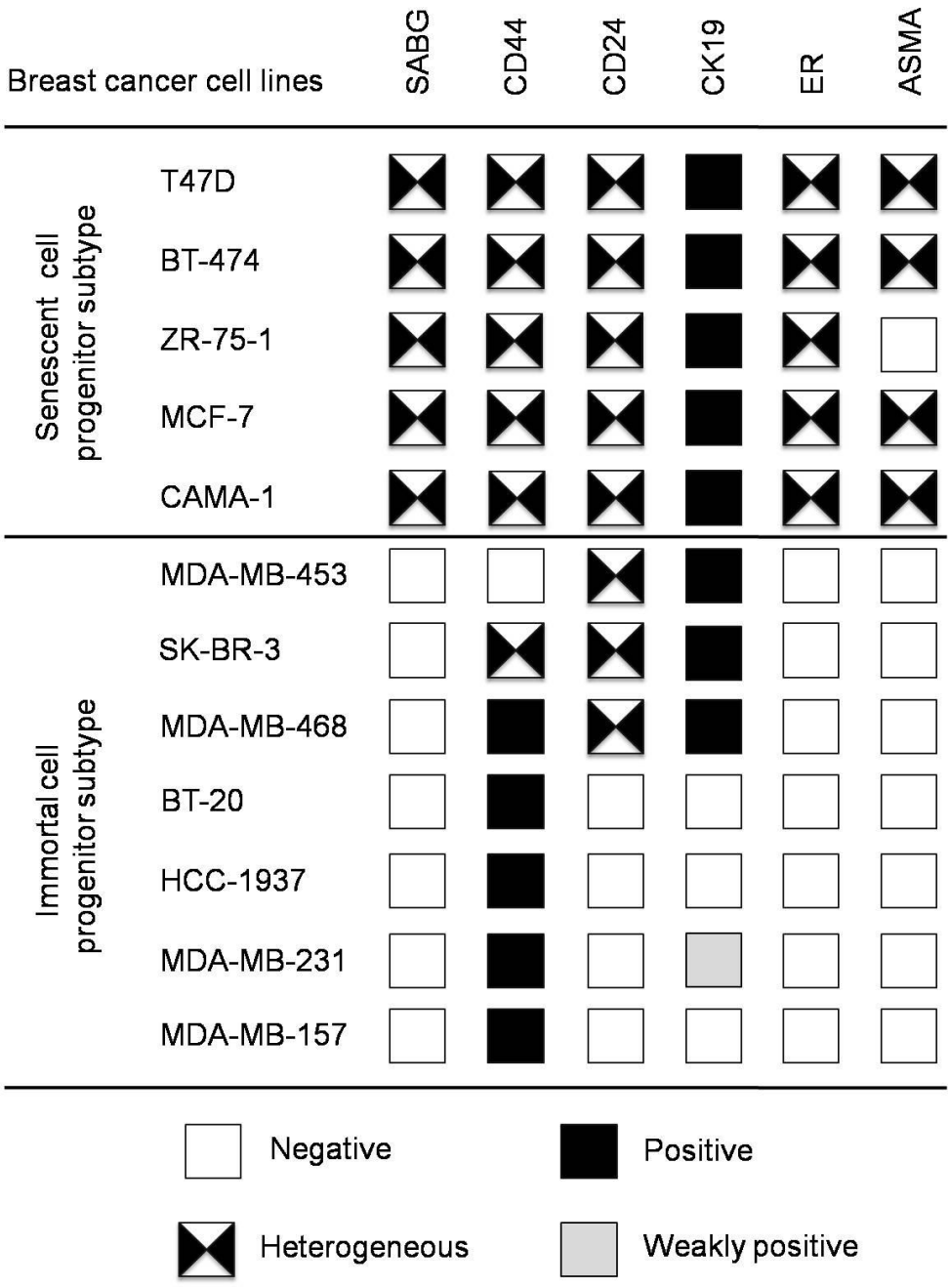

Figure 34: Summary of marker study results in breast cancer cell lines

4.5.2. Correlation of SCP and ICP subtypes with different breast tumor molecular subtypes

Gene expression profiling of breast cancer has been shown that breast cancer is not a single disease rather a group of molecularly distinct neoplastic disorder (Perou *et al.*, 2000; Sorlie *et al*., 2003; Sotiriou *et al.*, 2003; Sotiriou and Pusztai, 2009). Also each molecular subgroup has different prognosis and therapeutic response (Sorlie *et al.*, 2003; Sotiriou and Pusztai, 2009).

Therefore we wanted to analyze whether we could assign SCP and ICP cell lines to known molecular subtypes of breast tumors. For this study we conducted "hierarchical clustering" analysis which is a powerful technique for class discovery and prediction. The "intrinsic gene set" data generated by Sorlie et al. (2003) to classify breast tumors into five molecular subtypes was used to filter cell line data generated by Charafe-Jauffret *et al.* (2006). A set of 175 genes was common between the two data sets. Sixty-eight tumors and 31 cell lines were subjected to pair-wise complete-linkage hierarchical clustering and distance measurements. With this analysis we observed two main clusters; one consisting of basal and luminal B subtype, and the other consisting of luminal A, ERBB2+ and normal like subtypes. When we investigate the breast cell lines in these clusters, we have interestingly observed that all SCP cell lines exist in the second branch containing; luminal subtype A, ERBB2+ and normal like subtypes, and these cell lines were mainly close to luminal subtype A. On the other hand, ICP subtype breast cell lines were in the first branch containing basal and luminal B subtypes, except MDA-MB-453. Four cell lines clustered with Luminal A tumor subclass, and one cell line with normal-like subclass (Figure 35)

In other words, we have found SCP subgroup of breast cancer cell lines in perfect concordance with the luminal A, ERBB2 plus and normal like subtypes, and the five of ICP breast cancer cell lines in perfect concordance with the luminal B and basal subtypes ($p<0.01$, Fisher's exact test).Additionally, Luminal A tumors clustering with our SCP subtype cell lines display the longest tumor free, distant metastasis-free and overall survival rates. In contrast, basal and luminal B tumors clustering with our

ICP subtype cell lines have the worst prognosis, with shorter tumor-free, distant metastasis-free and overall survival times (Sorlie *et al*., 2003).

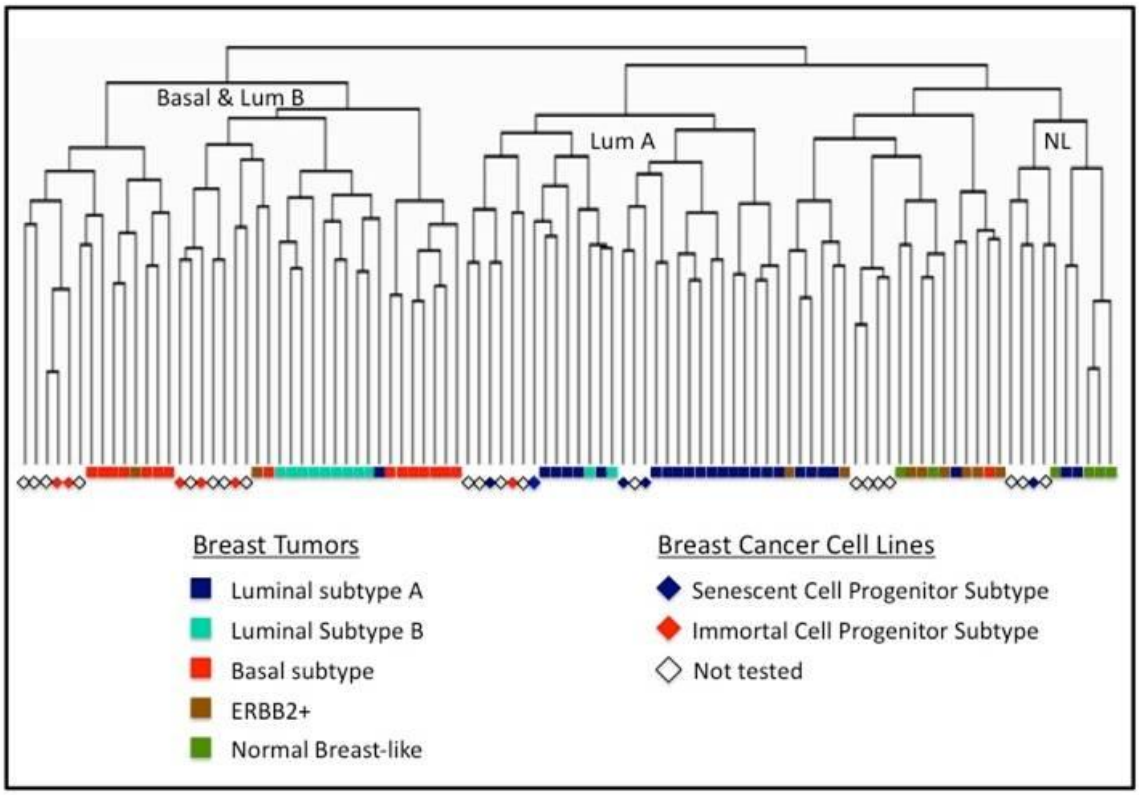

Figure 35: Unsupervised hierarchical clustering of breast tumor and cell line gene expression data from Sorlie *et al.* (2003) and Charafe-Jauffret *et al.* (2006).

Dendrogram displaying the relative organization of tumor and cell line data demonstrates that ICP cell lines cluster with basal and luminal A tumors in the same branch, except for MDA-MB-453. Senescent cell progenitor cell lines cluster with luminal A (BT-474, CAMA-1, MCF-7, T47D) and normal-like tumors (ZR-75-1). No data was available for MDA-MB-468. A dendrogram with sample IDs is provided in Figure 37. The "intrinsic gene set" data generated by Sorlie *et al.* (2003) was used to filter cell line data generated by Charafe-Jauffret et al. (2006). A set of 175 genes was common between the two data sets. Sixty-eight tumors and 31 cell lines were subjected to pair-wise complete linkage hierarchical clustering and distance measurements.

4.5.3. Differential tumorigenicity of SCP and ICP subtypes

With our cluster analysis result we observed that our SCP subgroup cell lines very well overlap with the luminal A type tumors which is a good prognostic group and ICP subgroup of cell lines overlap with the Luminal B and basal tumors which is bad prognostic group. Therefore we hypothesize that ability to generate differentiated and senescent progeny is indication of poor tumorigenicity and for ICP subgroup it is vice versa. To test this hypothesis we conducted nude mice tumorigenicity assay. Three SCP subgroup cell lines (MCF-7, T47D and CAMA-1) and three ICP subgroup cell lines (BT-20, HCC1937 and MDA-MB-453) were injected subcutaneously into CD1 “nude” mice. Tumor growth was monitored for 10 weeks at the injection sites. Nine animals implanted with SCP cell lines did not develop tumors and remained tumor-free for at least 10 weeks, whereas seven out of eight animals implanted with ICP cell lines developed subcutaneous tumors within five weeks of cell injection (Figure 36). We excluded one animal from the study, which died shortly after the cell injection of MDA-MB-453 ICP cell line. Data shows statistically significant difference between tumorigenicity of SCP subtype and ICP subtype cell lines ($p = 0.0002$). This result gives another invivo support to our hypothesis.

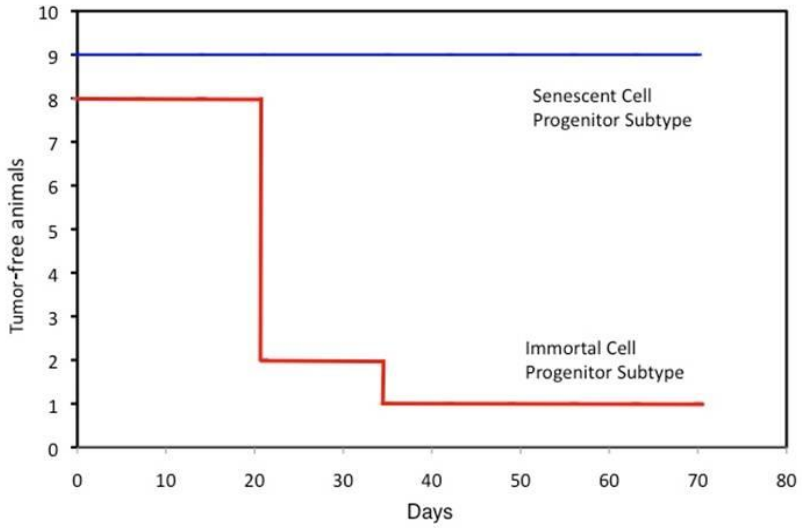

Figure 36: SCP subtype and ICP subtype shows differential tumorigenicity in nude mice.

5x106 cells were injected to the subcutaneous. Three SCP subgroup cell lines (MCF-7, T47D and CAMA-1) and three ICP subgroup cell lines (BT-20, HCC1937 and MDA-MB-453) were used in the study. Tumor growth was monitored for 10 weeks at the injection sites. Chart displays tumor-free survival following subcutaneous injection of cells.

Table 4: Gene clusters, genetic mutations and epigenetic changes of breast cancer cell lines

Cell Line	Gene Cluster[1]	PIK3CA (Ref. 2)	CCND1 (Ref. 1)	ERBB2 (Ref. 1)	KRAS BRAF (Ref. 2)	TP53 (Ref. 2, 8)	CDKN2A (Ref. 1,2, 7)	RB1 (Ref. 2)	PTEN (Ref. 2, 6)	NF2 (Ref. 2)
T47D	L	M/+				M/-	Met			
BT474	L	M/+	A	A		M/-	RNA (-)			
ZR-75-1	L		A			+/+	met		M/-	
MCF7	L	M/+				+/+	M/-			
CAMA-1	L		A			M/-	+/+		M/+	
MDA-MB-453	L	M/+				+/+	+/+		M/?	
SK-BR-3	L			A		M/-	unmet			
BT-20	BaA	M/M					M/-		M/-	
MDA-MB-468	BaA					M/-	+/+	M/-	M/?	
HCC1937	BaA	+/+				M/-	+/+		-/-	
MDA-MB-231	BaB				M/+	M/-	M/-			M/-
MDA-MB-157	BaB	+/+				M/-	+/+			

A, amplified; BaA, basal A; BaB, Basal B; L, luminal; M, mutated; met, promoter methylated; unmet, promoter unmethylated; +/+, wild-type; -/-, homozygous deletion; unknown.

[1] Neve *et al.* (2006); [2]From Sanger, COSMIC data; [3]Hollestelle *et al.* (2007); [4]Paz *et al.* (2003); [5]Runnebaum *et al.*(1991).

Gene clusters, genetic mutations and epigenetic changes of breast cancer cell lines used in this study

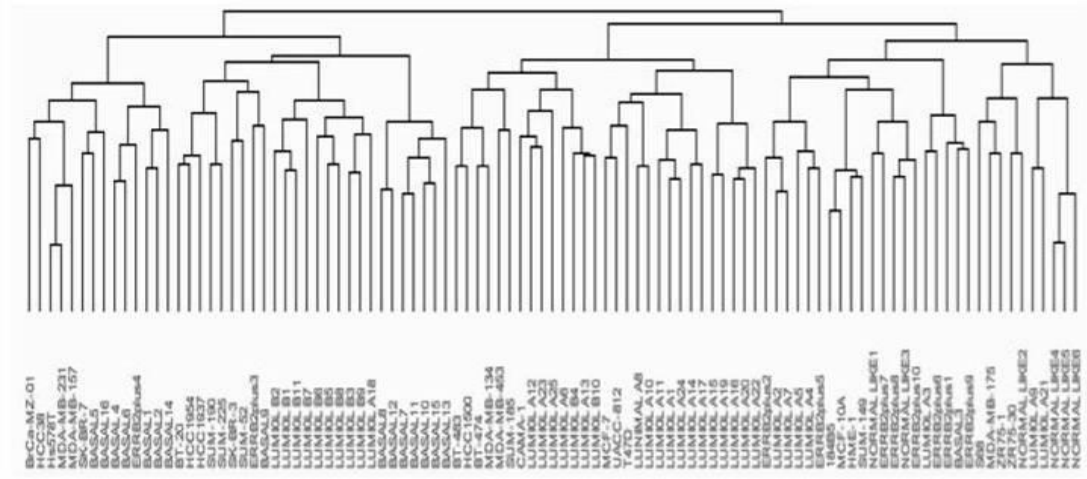

Figure 37: Unsupervised hierarchical clustering of breast tumor and cell line gene expression data.

This data is also described in Figure 35. Dendrogram shown here includes tumor and cell line sample IDs.

4.6. Effect of Retinoic acid in breast cancer cell senescence

Retinoids are physiological signaling molecules that play role in regulation of organismal development, tissue differentiation and cell death. Retinoids, natural or synthetic derivatives of vitamin A, act as regulators of transcription. Their effect on gene expression is mediated at the transcription level by binding to transcription factors formed through dimerization of retinoic acid receptors (RAR) and rexinoid receptors (RXR). These factors regulate transcription initiation by binding to retinoid response elements (RARE) in the promoters of target genes.

It has been shown that Retinoids cause senescent like changes and growth arrest in MCF7 cells (Chang *et al*., 1999; Docmanovic *et al*, 2002) and human neuroblastoma cells (Wainwrigth *et al.*, 2001).

We wanted to investigate the effect of Retinoids that causes differentiation associated with permanent growth arrest in our breast cancer cell lines. Therefore, we chose BT474, MCF7 (Napoli), Cama1 and BT-20 cell lines for low density cloning assay method. Cells were grown in the presence and absence of tRA until they generated colonies (10 days). As a tRA treatment dose, we applied 100nM tRA to the cells every 2 days, because this tRA dose was previously shown to successfully generate senescence in 6-9 days in MCF7 cells (Chang *et al.,* 1999). After tRA treatment, cells were subjected to SABG staining and manually counted to analyze their senescence status. The results obtained with SABG analysis showed that there was a measurable increase in SABG index and decrease in colony size of tRA treated MCF7 and Cama1 cells when compared with the untreated control group. Especially in Cama1 cells, anti-proliferative effect was more profound than senescent effect (Figure 38) (Cells in tRA treated colonies were ranging 3-1cells/colony where cells in control group 110-43cells/colony). tRA treatment did not make any drastic change on SABG staining status or colony size of BT474. In BT20, tRA treatment only resulted with decreased in colony size (Figure 39).

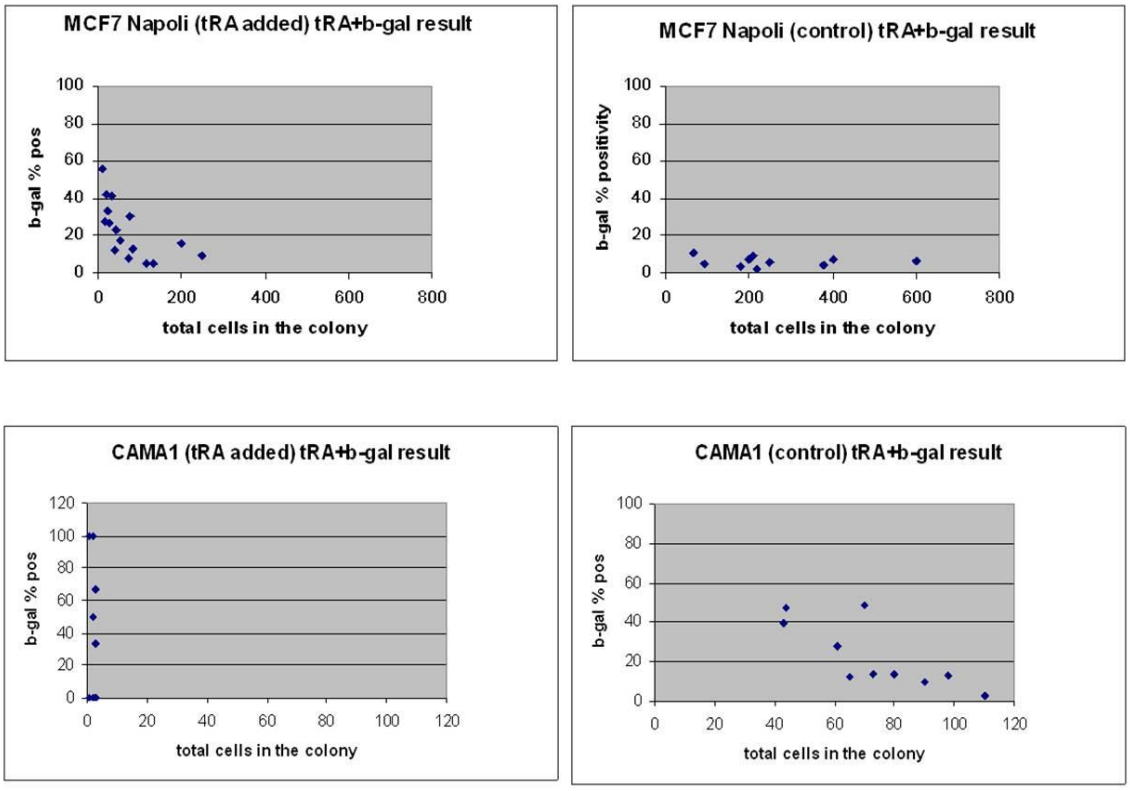

Figure 38: SABG index and colony size after tRA treatment in MCF7 and Cama1 cell lines for treated and untreated groups.

RA application into MCF7 and Cama-1 cells resulted with decreased in colony size and increased in SABG index. Effect of RA was more profound in Cama-1 cells. By RA treatment colony sizes of Cama-1 cells were decreased from ~ 100 cells/colony to ~ 3 cells/colony and most of the cells in colonies were SABG positive.

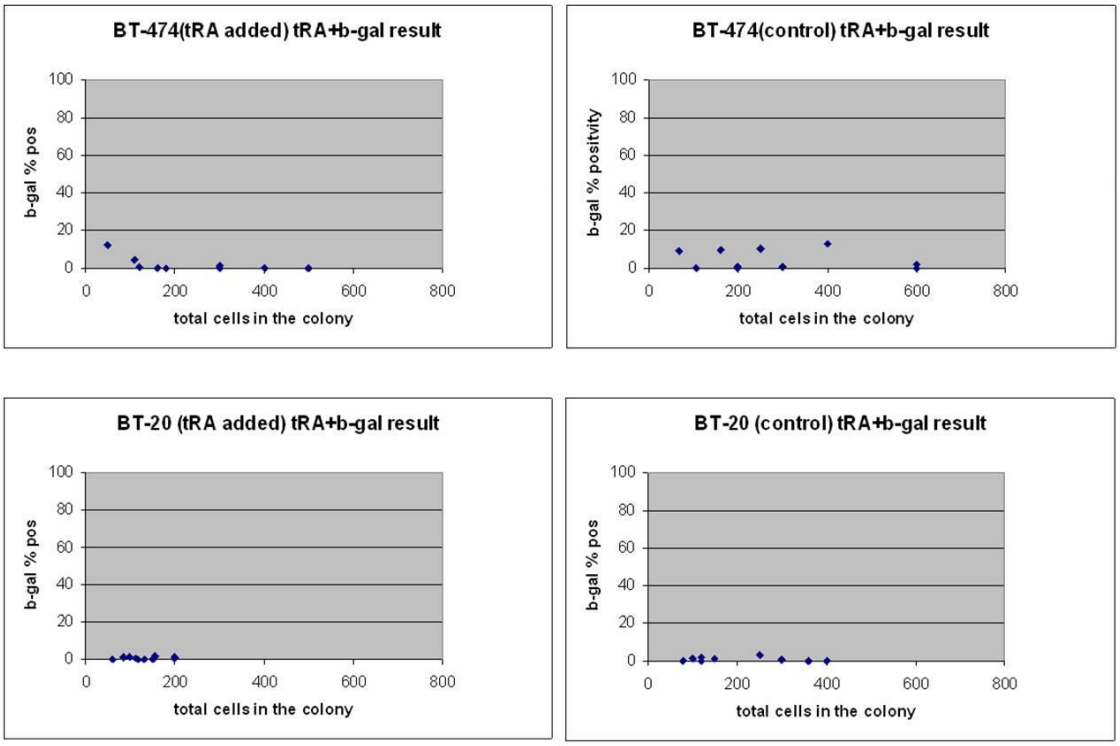

Figure 39: SABG index and colony size after tRA treatment in BT474 and BT20 cell lines for treated and untreated groups.

Not significant chances were observed either colony size or senescent index in BT-474 and BT-20 cell lines between tRA treated and untreated group.

Moreover, according to the results above, tRA dose was very high in Cama1 cells. It was totally blocked the proliferation of these cells. Then, we decided to use dose curve for tRA in Cama1 cells to find an optimal dose range to detect senescence effect more clearly. By performing dose curve for tRA, the dose range for senescence effect could be obtained within 1.5 - 0.75 nM tRA, which was a very low dose. As a result of these experiments, senescence induction and growth inhibition effect of tRA was observed not only in MCF7 cell line but also in Cama1 cell line. But the same effect was not observed in BT474, which is in the same molecular subgroup with MCF7 and Cama1. tRA didn't cause senescence induction but caused growth inhibition in BT20 cells (Figure 40).

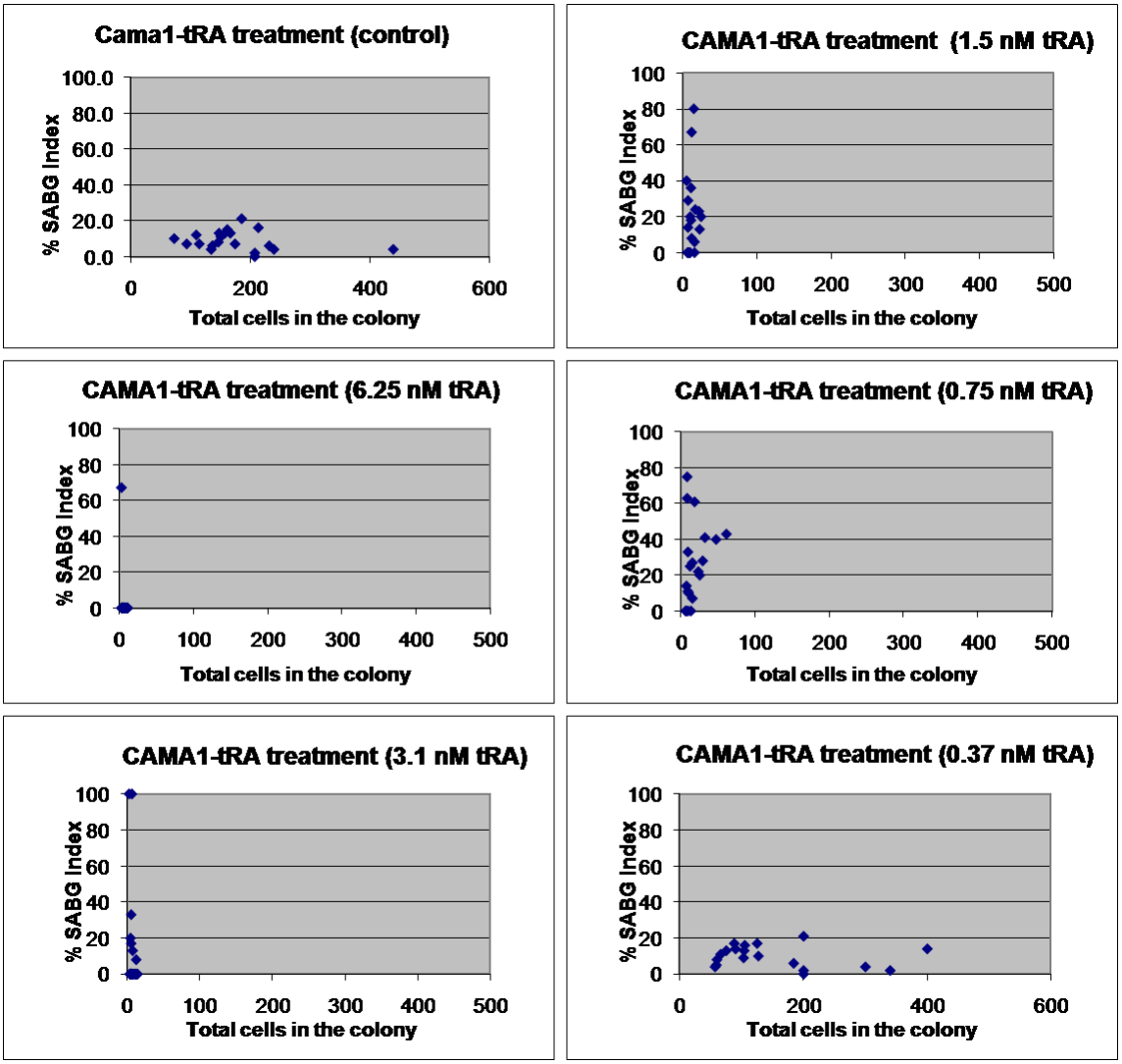

Figure 40: SABG index and colony size in Cama1 cells after different dose of tRA treatment.

Optimum senescence effect was obtained in 1.5 - 0.75 nM tRA dose range. In these doses less growth inhibition were observed. By this way senescence phenotype more clearly evaluated in Cama-1 cells.

CHAPTER 5. DISCUSSION AND FUTURE PERSPECTIVES

Most of the primary cells undergo a limited number of cell division and then they stop to proliferate which is known as senescence. It has been suggested that senescence presents a barrier against tumorigenesis. To become immortalized, human mammary epithelial cells should pass two senescence barriers known as "selection" and "crisis" (Romanov *et al*., 2001). $P21^{Cip1}$/p53 and $p16^{INK4a}$/Rb pathways have been shown to play crucial role in the induction of senescence (Ben-Porath and Weinberg, 2005).

In contrast to general characteristic of cancer, limitless capacity of proliferation, we observed senescence in a group of breast cancer cell lines, later we named it SCP (senescent cell progenitor) group. our breast cancer cell line panel was screened by using SABG assay as a senescence marker in low density clonogenic conditions. Low density cloning assay allowed us to follow progenies generated by a few hundred cells under the same experimental conditions. Clonogenic assays are very good methods to detect stem/progenitor cells and properties of their progeny (Stingl J, 2009). Our screening showed that our breast cancer cell line panel can be divided into two subgroups according to their ability to produce senescence progeny. First group is called SCP (senescent cell progenitor) group which produces high level of SABG positive cells and second group is called ICP (immortal cell progenitor) group which cannot generate SABG positive cells. Moreover, long time BrDU labeling and co-staining with SABG experiment showed that there was low incorporation of BrDU in senescent cells. This shows us that these senescent cells are differentiated cells.

Senescence that we observed in our breast cancer cell lines does not represent characteristics of replicative senescence. This is because, after generation of isogenic clones from SABG positive breast cancer cell lines, we couldn't observe fully senescence in these clones even after they passed many population doublings (>60) in the cell culture.

P53 and $p16^{INK4a}$/Rb are two main pathways for senescence. P53 mediates its effect by $p21^{Cip1}$. Therefore we analyzed whetherp16 and p21 expressions are related with SCP group of cell lines. All of the breast cancer cell lines were screened by immunoperoxidase assay in low density clonogenic conditions. There was no correlation found with p16 expression in SCP group. But importantly, it was found that 4 out of 5 SCP cell line shows strong, heterogenic, nuclear $p21^{Cip1}$ staining. Also, SABG and $p21^{Cip1}$ co-staining and SABG and $p16^{INK4a}$ co-staining were performed in T47D and MDA-MB-231 cell lines. $P21^{Cip1}$ positive cells were mostly senescent cells in T47D. MDA-MB-231 showed no staining for SABG and $p21^{Cip1}$. These results showed significant correlation between $p21^{Cip1}$ increase and SCP group. We confirmed these results by down regulating $p21^{Cip1}$ in T47D cell line. We observed increase in BrdU incorporation in T47D-p21sh clone compared to control clone (from 48±20% to 65±12% per colony). All these data indicated that $p21^{Cip1}$ is partially responsible from generation of progeny in SCP group.

ER expression is one of the important markers in breast cancer to evaluate the prognosis of the disease. $P21^{Cip1}$ is target of p53. E2 mediates $p21^{Cip1}$ inhibition by c-myc (Mukherjee and Conrad, 2005). Myc gene is direct target of ER complex (Dubik and Shiu, 1992). Therefore we hypothesize that ER receptor could play a role in the generation of senescent progeny in SCP group. First of all, our SCP group expresses ER, but ICP group of breast cancer cell lines don't express it. We checked whether senescence phenotype correlates with ER expression in SCP group. Co-staining of ER and SABG displayed that ER-negative cells were mostly in senescent state. Moreover, in T47D cells, estrogen treatment inhibits generation of senescent progeny whereas tamoxifen treatment (in 10^{-6}M concentration) increased it up to 90%. These results showed direct involvement of ER in senescence progeny generation in SCP group of breast cancer cell lines. We also confirmed our results by overexpressing ER in T47D cell lines. ER-overexpressing T47D clones increasingly incorporate BrdU compared to control clones. These data correlates well with the clinical data which shows good prognosis, good response to anti-estrogen treatment and relapse free survival for ER-positive Luminal-A group of breast cancer (Sorlie *et al.*, 2003).

Gene expression profiling of breast cancers revealed several subtypes of breast cancer (Perou *et al.,* 2000; Sorlie *et al.,* 2003). To understand whether our SCP and ICP subgroup correlated with this classification, we performed "hierarchical clustering" analysis on Sorlie *et al. (*2003) breast tumor data and Charafe-Jauffret *et al.* (2006) cell line data. With this analysis we observed two main clusters; one consisting of basal and luminal B subtype, and the other consisting of luminal A, ERBB2+ and normal like subtypes. We have found that SCP subgroup of breast cancer cell lines are in perfect concordance with the luminal A, ERBB2 plus and normal like subtypes, and the five of ICP breast cancer cell lines are in perfect concordance with the luminal B and basal subtypes. This shows that our SCP group is phenotypically similar to Luminal A group of breast cancers.

To test the tumorigenicity potential of our SCP and ICP group, we injected 3 cell lines from SCP group (MCF-7, T47D and CAMA-1) and 3 cell lines from ICP group (BT-20, HCC1937 and MDA-MB-453) subcutaneously into nude mice. SCP cell lines did not develop tumors and remained tumor-free for at least 10 weeks, whereas seven out of eight animals implanted with ICP cell lines developed subcutaneous tumors within five weeks of cell injection. This study results correlates with all the other data. Our SCP group cell lines are poorly tumorigenic and locate in Luminal A group breast cancer cluster and clinically this group has longest tumor-free, distant metastasis-free and overall survival rates. We also screened a small panel of breast tumor samples (12 snapfrozen ER+ breast tumor tissues from 11 patients) with SABG assay. These samples were from untreated patients. We detected positive SABG staining in only two tumor samples. It would be more informative to screen a bigger panel of breast tumor tissues.

Breast cancer is a heterogeneous disease in terms of histopathological and clinical features (Stingl and Caldas, 2007). Mammary epithelium consist of two epithelial lineages, luminal and myoepithelial cells. Recent studies indicate that mammary epithelium is organized hierarchically different cell that ranges from stem cells to differentiated cells (Stingl J, 2009). To understand differentiation ability of our breast cancer subtypes, we tested different marker expression status. We used CD44 as a

stem/progenitor cell marker, CD24, ER and CK19 as luminal lineage markers and ASMA as a myoepithelial lineage marker. SCP group of cell lines were heterogenous for all of the marker expressions. Only ZR-75-1 showed negative ASMA staining. It means that they contain $CD44^{+}/CD24^{-}$ stem cells and also differentiated cells. These cell lines can express epithelial marker (CK19) and as well as myoepithelial marker (ASMA). This result provides evidence that they have an ability to generate differentiated cells. This data is also important because it shows heterogenic characteristics and stem/progenitor potential of Luminal-A group of cancers. ICP group of cells (5/7) generated only $CD44^{+}$ and $CD24^{-}$ cells. They couldn't generate ASMA-positive cells. This can be interpreted as: "ICP group cell lines lost their differentiation ability and block in stem/progenitor cell stage". Therefore they are highly tumorigenic clinically. Moreover, MDA-MB-453, SK-BR-3 and MDA-MB-468 cell lines presented similar CK19 and CD24 staining pattern with SCP group in marker studies. But they are not SABG positive and don't express ER and ASMA. In addition CD44 expression in these three cell lines were vary. These results suggest that MDA-MB-453, SK-BR-3 and MDA-MB-468 cell lines still may retain partial differentiation ability but possibly not as much as SCP group. It is possible to think that these group could be prospective target to induce senescence and differentiation in order to decrease their tumorigenecity potential.

During my study we were also interested in other possible factors that could play role in senescence phenotype that we observed in our breast cancer cell lines. These are reactive oxygen species (ROS) and retinoids.

Cellular senescence can be induced by different stimuli. One of them is oxidative stress. We hypothesized that senescence that we observed in breast cancer cell lines can be related with ROS accumulation in the cell. Therefore, firstly, ROS accumulation in Cama1 and MDA-MB-468 cells were analyzed by DCFH and MitoTracker co-staining. Not at day 10 but at day 13, ROS accumulation in Cama1 cells were very strong and NAC treatment showed significant decrease in ROS level compared to no observable change in MDA-MB-468 cells. Also, MitoTracker staining which provides information about mitochondrial ROS didn't show any

difference neither in Cama1 nor in MDA-MB-468 cell line. This result suggests that there is a gradual intracellular ROS accumulation occuring in Cama1 cells and it is originated from intracellular source other than mitochondria. NBT (nitroblue tetrazolium) and SABG co-staining in BT-474 result provide evidence that senescence positive cells have ROS accumulation. To confirm our results we decided to check whether we can inhibit senescence by NAC which is a scavenger of ROS. Cama1 cells seeded at low density and treated with 10 mM NAC. Experiments were stopped at day 10 and 15 and next, SABG was performed. SABG results showed that there is a significant decrease in senescence with NAC treatment at day 15. Sources of cellular ROS include leakage from the mitochondrial electron transport chain, ROS-generating plasma membrane and cytosolic enzymes. NADPH oxidases (NOX) are membrane located electron-transporting enzymes. Their primary function is generation of reactive oxygen species (ROS). There is significant supporting evidence that the role of ROS which is produced by NADPH oxidases, is the regulation of intracellular signaling cascades in different types of cells (Droge W, 2002). Therefore we wanted to analyze the expression pattern of Nox genes (Nox1, Nox2, Nox3, Nox4 and Nox5) in our breast cancer cell line panel with RT-PCR. We found increased expression of Nox2 and Nox5 in two of the SCP subgroup of cell lines, but not in all of them. Real time PCR results also confirmed RT-PCR data. These results suggested that there is a correlation between ROS accumulation and senescence induction in SCP subgroup of cell lines. Increased level of ROS that we observed in Cama1 and BT-474 cells probably are not originated from mitochondria. Nox2 and Nox5 could be potential candidates. But increased expression in Nox2 and Nox5 were not observed in all SCP group. Therefore other cellular ROS providers might be considered for future experiments. According to our data, it may be possible to state that increased level of ROS triggers some redox-sensitive pathways, causing changes in gene expression and consequently senescence response. In addition, it has been shown that $p21^{Cip1}$ increased cellular ROS level both in normal fibroblasts and in p53-negative cancer cells and p21-induced senescence was rescued by using NAC (Macip *et al.*, 2002). This interesting finding correlates with our data even though their experiments were done in another type of cancer cell line.

Retinoids are physiological signaling molecules that play role in the regulation of organismal development, tissue differentiation and cell death. Retinoids have been used in the treatment of promyelocytic leukemia (APL) and premalignant diseases such as acute leukoplakia, actinic keratosis, cervical dysplasia and xeroderma pigmentosum (Altucci and Gronemeyer, 2001). It has been shown that retinoids cause senescent like changes and growth arrest in MCF7 cells (Chang *et al.,* 1999; Docmanovic *et al*, 2002) and human neuroblastoma cells (Wainwrigth *et al.,* 2001). Also Chang et al. detected senescence induction by retinoic acid treatment in vivo. They used H-Ras transformed MCF10ANeoT human breast epithelial cell line and transplanted in mammary gland of nude mice. 4-HPR (4-hydroxyphenyl retinamide) - threated mice developed less malignant tumors compared to untreated mice. Moreover, they observed high SABG staining in drug-treated tumor compare to untreated tumor (Chang *et al*., 1999). Since we consider our senescence phenotype as terminal differentiation stage in our SCP group cell lines, we hypothesized that retinoids could play a role in this phenomenon. 100nM tRA was applied into MCF7, Cama1, BT-474 and BT-20 cell lines in low density clonogenic conditions. Experiment was stopped at day 10 and subjected to SABG assay. RA treatment resulted in growth inhibition and senescence in MCF7 and Cama1 cell lines, showing no difference in BT-474 and some degree of growth inhibition in BT-20 cell line. But growth inhibition was very severe in Cama1 cell line. This result was very dramatic in Cama1 cell line. Some of the Cama1 colonies were 100% SABG-positive. But these colonies were very small. So we decided to use tRA dose curve in order to find optimum dose in which minimal growth inhibition and maximum senescence effect are observed. 1.5-0.75 nM range of tRA treatment in Cama1 cells resulted in high SABG index and less growth inhibition. This observation suggests that growth inhibitory effect of tRA is very prominent in Cama1 cells. But we still observed increased senescence response in 2 out of 3 SCP subgroup of cell lines. Probably it would be necessary to test other SCP group and ICP group cell lines with tRA treatment and compare tRA effect.

We think our results are important due to a couple of aspects. We provide evidence that Luminal A type of breast tumors has differentiation ability and senescence,

which is a terminal differentiation stage of cells, could be a reason of their good prognostic features. Senescence induction can be used in these cancers as a therapeutic approach. In this study, we also provide a group of cell lines as a model for future studies to explore senescence and differentiation mechanisms in more details.

REFERENCES

Abbas T, Dutta A, 2009. P21 in cancer: Intricate networks and multiple activities. *Nature Rev Cancer*, 9: 400-41

Al-Hajj M, Wicha MS, Benito-Hernandez A, Morrison SJ, Clarke MF, 2003 Prospective identification of tumorigenic breast cancer cells. *Proc. Natl. Acad. Sci*. 100:3983–3988

Allred DC, Mohsin SK, Fuqua SAW, 2001. Histological and biological evolution of human premalignant breast disease. *Endocr Relat Cancer*, **8**:47-61

Alotaibi H, Cankaya Yaman E, Demirpence E, Tazebay UH, 2006. Unliganded estrogen receptor-a activates transcription of the mammary gland Na+/I_ symporter gene. *Biochemical and Biophysical Research Communications.* 345, 1487–1496

Altucci L, Gronemeyer H, 2001. The promise of retinoids to fight against cancer. *Nat Rev Cancer*. (3):181-93

Barcellos-Hoff MH and Akhurst RJ, 2009. Transforming growth factor-β in breast cancer: too much, too late. *Breast Cancer Research*, 11(1):202

Beckmann MW, Niederacher D, Schnurch HG, Gusterson BA, Bender HG, 1997. Multistep carcinogenesis of breast cancer and tumor heterogeneity. *J Mol Med*. 75:429-439

Ben-Porath I and Weinberg RA, 2005. The signals and pathways activating cellular senescence. Int J of Biochemisty& Cell Biology 37:961-976

Ben-Porath I. and Weinberg R.A., 2004. When cells get stressed: an integrative view of cellular senescence, *The Journal of Clinical Investigation*, 113:8-13

Berridge MV, Herst PM, Tan AS., 2005. Tetrazolium dyes as tools in cell biology: new insights into their cellular reduction. *Biotechnol Annu Rev.*, 11:127-52

Berthois Y, Katzenellenbogen JA and Katzenellenbogen BS, 1986. Phenol red in tissue culture media is a weak estrogen: implications concerning the study of estrogen-responsive cells in culture. *Proc. Natl. Acad. Sci. U S A*, 83: 2496-2500.

Bodnar, AG et al. 1998. Extension of life span by introduction of telomerase into normal human cells. *Science*. 279, 349–352

Bonnet D, Dick JE, 1997. Human acute myeloid leukemia is organized as a hierarchy that originates from a primitive hematopoietic cell. *Nat. Med*. 3:730–737

Bowcock AM, 1999.Breast Cancer; Molecular Genetics, pathogenesis and Therapeutics. Humana Press.

Ceder JA, Jansson L, Ehrnstrom RA, Ronnstrand L, Abrahamsson PA, 2008. The characterization of epithelial and stromal subsets of candidate stem/progenitor cells in the human adult prostate. *Eur. Urol.* 53: 524–532

Chang BD, Broude EV, Dokmanovic M, Zhu H, Ruth A, Xuan Y, Kandel ES, Lausch E, Christov K, Roninson IB, 1999a. A Senescence-like Phenotype Distinguishes Tumor Cells That Undergo Terminal Proliferation Arrest after Exposure to Anticancer Agents. *Cancer Research* 59:3761–3767

Chang BD, Xuan Y, Broude EV, Zhu H, Schott B, Fang J, and Roninson IB, 1999b. *Oncogene*, 18: 4808-4818

Charafe-Jauffret E, Ginestier C, Monville F, Finetti P, Adelaide J, Cervera N, Fekairi S, Xerri L, Jacquemier J, Birnbaum D, Bertucci F., 2006.Gene expression profiling of breast cell lines identifies potential new basal markers, *Oncogene*. 25(15):2273-84

Chen Q and Ames BN, 1994. Senescence-like growth arrest induced by hydrogen peroxide in human diploid fibroblast F65 cells, *Proc. Natl. Acad. Sci*., 91(10):4130-4

Chen QM, Prowse KR, Tu VC, Purdom S, Linskens MH. 2001. Uncoupling the senescent phenotype from telomere shortening in hydrogen peroxidetreated fibroblasts. *Exp. Cell Res*. 265:294–303.

Collado M, Blasco MA, Serrano M. 2007. Cellular senescence in cancer and aging. *Cell*, 130:223-233

Collado M, Gil J, Efeyan A, Guerra C, Schuhmacher AJ, Barradas M, Benguria A, Zaballos A, Flores JM, Barbacid M et al. 2005. Tumor biology: senescence in premalignant tumors. *Nature,* 436:642

Cariou S, Donovan JC, Flanagan WM, Milic A, Bhattacharya N and Slingerland JM, 2000. Down-regulation of p21WAF1/CIP1 or p27Kip1 abrogates antiestrogen-mediated cell cycle arrest in human breast cancer cells. *Proc. Natl. Acad. Sci. U S A,* 97: 9042-9046.

Couse JF, Korach KS, 1999. Estrogen receptor null mice: What have we learned and where will they lead us. *Endocrine Reviews,* 20:321-344

Courtois-Cox S, Genther Williams SM, Reczek EE, Johnson BW, McGillicuddy LT, Johannessen CM, Hollstein PE, MacCollin M, Cichowski K. 2006. A negative feedback signaling network underlies oncogene-induced senescence. *Cancer Cell,* 10:459-472

d'Adda di Fagagna, F, et al., 2003. A DNA damage checkpoint response in telomere-initiated senescence. *Nature*, 426:194–198

d'Adda di Fagagna F, Teo SH, Jackson SP, 2004. Functional links between telomeres and proteins of the DNA-damage response. *Genes Dev.* 18:1781–1799

Dalerba P, Dylla SJ, Park IK, Liu R, Wang X, Cho RW, Hoey T, Gurney A, Huang EH, Simeone DM, Shelton AA, Parmiani G, Castelli C, Clarke MF. 2007. Phenotypic characterization of human colorectal cancer stem cells. *Proc Natl Acad Sci*., 104: 10158–10163

Datta S, Hoenerhoff MJ, Bommi P, Sainger R, Guo WJ, Dimri M, Band H, Band V, Green JE, Dimri GP. 2007. Bmi-1 cooperates with H-Ras to transform human mammary epithelial cells via dysregulation of multiple growth-regulatory pathways. *Cancer Res*. 67(21):10286-95

DiLeonardo A, Linke SP, Clarkin K, Wahl GM. 1994. DNA damage triggers a prolonged p53-dependent G1 arrest and long-term induction of Cip1 in normal human fibroblasts. *Genes Dev.* **8**:2540–2551

Di Micco R, Fumagalli M, Cicalese A, Piccinin S, Gasparini P, Luise C, Schurra C, Garre M, Nuciforo PG, Bensimon A et al. 2006. Oncogene-induced senescence is a DNA damage response triggered by DNA hyper-replication. *Nature*, 444:638-642

Dimri GP, Lee X, Basile G, Acosta M, Scott G, Roskelley C, Medrano EE, Linskens M, Rubelj I, Pereira-Smith O, et al. 1995. A biomarker that identifies senescent human cells in culture and in aging skin in vivo. *Proc Natl Acad Sci U S A.* 92(20):9363-7

Dimri GP, 2005.What has senescence got to do with cancer? *Cancer Cell,* 7(6):505-12

Dimri H, Band H, Band V, 2005. Mammary epithelial cell transformation: insights from cell culture and mouse models. *Breast Cancer Research*, 7:171-179

Docmanovic M, Chang BD, Fang J, Roninson IB 2002. Retinoid induced growth arrest of breast carcinoma cellsinvolves co-activation of multiple growth inhibitory genes. *Cancer Biol Ther* 1: 24-27

Droge W, 2002. Free radicals in the physiological control of cell function, *Physiological Review*, 82:47-95

Elenbaas B, Spirio L, Koerner F, Fleming MD, Zimonjic DB, Donaher JL, Popescu NC, Hahn WC, Weinberg RA, 2001. Human breast cancer cells generated by oncogenic transformation of primary mammary epithelial cells. *Genes Dev*, 15**:**50-65

Enmark E, Pelto-Huikko M, Grandien K, Lagercrantz S, Lagercrantz J, Fried G, Nordenskjold M, Gustafsson J-A. 1997. Human estrogen receptor β-gene structure, chromosomal location and expression pattern. *J Clin Endocrinol Metab*, 82:4258-426

Eramo A, Lotti F, Sette G, Pilozzi E, Biffoni M, Di Virgilio A, Conticello C, Ruco L, Peschle C, De Maria R. 2008. Identification and expansion of the tumorigenic lung cancer stem cell population. *Cell Death Differ*; 15: 504–514

Fürstenberger G and Senn HJ, 2002. Insulin-like growth factors and cancer. *Lancet Oncology*, 3(5):298-302

Geiszt M, Kopp JP, Varnai P, and Leto LT, 2000. Identification of Renox, an NAD(P)H oxidase in kidney, *Proc. Natl. Acad. Sci*., 97:8010–8014

Gur-Dedeoglu B, Konu O, Kir S, Ozturk AR, Bozkurt B, Ergul G, Yulug IG, 2008. A resampling-based meta-analysis for detection of differential gene expression in breast cancer. *BMC Cancer*, 8:396

Hagen TM, Yowe DL, Bartholomew JC, Wehr CM, Do KL, Park JY, Ames BN, 1997. Mitochondrial decay in hepatocyteas from old rats: membrane potential declines, heterogeneity and oxidant increase, *Proc. Natl. Acad. Sci*., 94(7):3064-9

Hahn WC, Dessain SK, Brooks MW, King JE, Elenbaas B, Sabatini DM, DeCaprio JA, Weinberg RA, 2002. Enumeration of the simian virus 40 early region elements necessary for human cell transformation. *Mol Cell Biol*, 22**:**2111-2123

Hanahan D, Weinberg RA, 2000. The Hallmarks of Cancer, *Cell*, 100(1):57-70

Harley CB, Futcher AB, Greider CW, 1990. Telomere shorten during egeing of human fibroblasts. *Nature*, 345:458-460

Hayflick L, Moorhead PS, 1961. The serial cultivation of human diploid cell strains, *Exp Cell Res*, 25:585-621

Henderson BE, Feigelson HS, 2000. Hormonal carcinogenesis. *Carcinogenesis* 21:427-433

Henderson BE, Ross R, Berstein L, 1988. Estrogens as a cause of human cancer: the Richard and Linda Rosenthal Foundation award lecture. *Cancer Research*, 48:246-253

Herbig U, Jobling, WA, Chen BP, Chen DJ, Sedivy, J. 2004. Telomere shortening triggers senescence of human cells through a pathway involving ATM, p53, and p21(CIP1), but not p16(INK4a). *Mol. Cell*, 14:501–513

Hollestelle A, Elstrodt F, Nagel JH, Kallemeijn WW, Schutte M, 2007. Phosphatidylinositol-3-OH kinase or RAS pathway mutations in human breast cancer cell lines. *Mol. Cancer Res.*, 5: 195-201.

Hu M, Polyak K, 2009.Microenviromental regulation of cancer development. Curr opinion in *Gen&Dev*, 18:27-34

Khan S, Guevara C, Fujii G, Parry D, 2004. p14ARF is a component of the p53 response following ionizing irradiation of normal human fibroblasts. *Oncogene*, 23(36):6040-6

Khan SA, Rogers MA, Obando JA, Tamsen A, 1994. Estrogen receptor expression of benign epithelium and its association with breast cancer. *Cancer Res*, **54**:993-997

Kenemans P, Verstraeten RA, Verheijen R.H.M., 2004. Oncogenic pathways in hereditary and sporadic breast cancer. *Maturitas* 49: 34–43

Kumar V, Green S, Stack G, Berry M, Jin JR, Chambon P, 1987. Functional domains of the human estrogen receptor**.** *Cell*, 51:941-951.

Lambeth DJ, 2004. Nox enzymes and the biology of reactive oxygen, *Nature Reviews Immunology*, 4: 181-189

Lawson JS, Field AS, Champion S, Tran D, Ishikura H, Trichopoulos D, 1999. Low oestrogen receptor α expression in normal human breast tissue underlies low breast cancer incidence in Japan. *Lancet*, 354:1787-1788

Lee AC, Fenster BE, Ito H, Takeda K, Bae NS, Hirai T, Yu ZX, Ferrans VJ, Howard BH, Finke T., 1999. Ras proteins induce senescence by altering the intracellular levels of reactive oxygen species. *J Bio Chem*, 274(12):7936-40

Li Y, Welm B, Podsypanina K, Huang S, Chamorro M, Zhang X, Rowlands T, Egeblad M, Cowin P, Werb Z, et al. 2003. Evidence that transgenes encoding components of the Wnt signaling pathway preferentially induce mammary cancers from progenitor cells. *Proc Natl Acad Sci*, 100**:**15853-15858

Lundberg AS, Hahn WC, Gupta P, and Weinberg RA, 2000. Genes invoved in senescence and immortalization, *Current opinon in cell biology*, 12:705-709

Li C, Heidt DG, Dalerba P, Burant CF, Zhang L, Adsay V, Wicha M, Clarke MF, Simeone DM, 2007. Identification of pancreatic cancer stem cells. *Cancer Res* 67:1030–1037

Macip S, Igarashi M, Fang L, Chen A, Pan Z, Lee SW and Aaronson SA, 2002. Inhibition of p21-mediated ROS accumulation can rescue p21-induced senescence. *EMBO J*., 21(9):2180-8

Mallette FA, Gaumont-Leclerc MF, Ferbeyre G, 2007. The DNA damage signaling pathway is a critical mediator of oncogene-induced senescence. *Genes Dev*, 21:43-48

McPherson K, Steel CM, Dixon JM, 2000. ABC of breast diseases. Breast cancer-epidemiology, risk factors, and genetics. *BMJ*, 321: 625-628

Melchor L, Benitez J, 2008. An integrative hypothesis about the origin and development of sporadic and familial breast cancer subtypes. *Carcinogenesis*, 29(8):1475-82

Michaloglou C, Vredeveld LC, Soengas MS, Denoyelle C, Kuilman T, van der Horst CM, Majoor DM, Shay JW, Mooi WJ, Peeper DS, 2005. BRAFE600-associated senescence-like cell cycle arrest of human naevi. *Nature*, 436:720-724

Mukherjee S and Conrad SE, 2005. c-Myc suppresses p21WAF1/CIP1 expression during estrogen signaling and antiestrogen resistance in human breast cancer cells. *J. Biol. Chem.*, 280:17617-17525.

Neve RM, Chin K, Fridlyand J, Yeh J, Baehner FL, Fevr, T, Clark L, Bayani N, Coppe JP, Tong F, Speed T, Spellman PT, DeVries S, Lapuk A, Wang, NJ, Kuo WL, Stilwell JL, Pinkel D, Albertson DG, Waldman FM, McCormick F, Dickson RB, Johnson MD, Lippman M, Ethier S, Gazdar A and Gray JW, 2006. A collection of breast cancer cell lines for the study of functionally distinct cancer subtypes. *Cancer Cell*, 10, 515-627.

Orr WC, Sohal RS, 1994. Extension of life-span by overexpression of superoxide dismutase and catalase in Drosophila melanogaster, *Science*, 263(5150):1128-30

Ozturk N, Erdal E, Mumcuoglu M, Akcali KC, Yalcin O, Senturk S, Arslan-Ergul A, Gur B, Yulug I, Cetin-Atalay R, Yakicier C, Yagci T, Tez M, Ozturk M, 2006. Reprogramming of replicative senescence in hepatocellular carcinoma-derived cells, *Proc. Natl. Acad. Sci*., 103(7):2178-83

Parkes TL, Elia AJ, Dickinson D, Hilliker AJ, Phillips JP, Boulianne GL, 1998. Extension of Drosophila lifespan by overexpression of human SOD1 in motoreneurons, *Nat Genet*, 19(2):171-4

Paz MF, Fraga MF, Avila S, Guo M, Pollan M, Herman JG, Esteller M, 2003. A systematic profile of DNA methylation in human cancer cell lines. *Cancer Res.*, 63: 1114-1121.

Pearson, M., Carbone, R., Sebastiani, C., Cioce, M., Fagioli, M., Saito, S., et al. 2000. PML regulates p53 acetylation and premature senescence induced by oncogenic Ras. *Nature*, 406:207–210.

Perou CM, Sørlie T, Eisen MB, van de Rijn M, Jeffrey SS, Rees CA, Pollack JR, Ross DT, Johnsen H, Akslen LA, Fluge O, Pergamenschikov A, Williams C, Zhu SX, Lønning PE, Børresen-Dale AL, Brown PO, Botstein D, 2000. Molecular portraits of human breast tumors. *Nature*, 406(6797):747-52.

Prince ME, Sivanandan R, Kaczorowski A, Wolf GT, Kaplan MJ, Dalerba P, Weissman IL, Clarke MF, Ailles LE, 2007. Identification of a subpopulation of cells with cancer stem cell properties in head and neck squamous cell carcinoma. *Proc Natl Acad Sci*, 104:973–978.

Reddel RR, 2000. The role of senescence and immortalization in carcinogenesis. *Carcinogenesis*, 21(3):477-84

Reya T, Morrison SJ, Clarke MF, Weissman IL, 2001. Stem cells, cancer, and cancer stem cells. *Nature*, 414(6859):105-11

Romanov RS, Kozakiewicz BK, Holst CR, Stampfer MR, Haupt LM, Tlsty TD, 2001. Normal human mammary cells spontaneously escape senescence and acquire genomic changes. *Nature* 409: 633-637

Runnebaum IB, Nagarajan M, Bowman M, Soto D, Sukumar S, 1991. Mutations in p53 as potential molecular markers for human breast cancer. *Proc. Natl. Acad. Sci. U S A*, 88: 10657-10661.

Satmpfer MR, Yawen P, 2003. Human epithelial cell immortalization as a step in carcinogenesis. *Cancer Letters*, 194:199-208

Schmitt CA, 2007. Cellular senescence and cancer treatment, *Biochimica et Biophysica Acta*, 1775:5-20

Serrano M, Lin AW, McCurrach ME, Beach D, Lowe SW, 1997. Oncogenic ras provokes premature cell senescence associated with accumulation of p53 and p16INK4a. *Cell*, 88:593–602

Shay JW and Roninson IB, 2004. Hallmarks of senescence in carcinogenesis and cancer therapy, *Oncogene*, 23:2919-2933

Shiose A, Kuroda J, Tsuruya K, Hirai M, Hirakata H, Naito S, Hattori M, Sakaki Y, Sumimoto H, 2001. A novel superoxide-producing NAD(P)H oxidase in kidney, *J Biol Chem*., 276(2):1417-23

Shipitsin M, Campbell LL, Argani P, Weremowicz S, Bloushtain-Qimron N, Yao J, Nikolskaya T, Serebryiskaya T, Beroukhim R, Hu M, Halushka MK, Sukumar S, Parker LM, Anderson KS, Harris LN, Garber JE, Richardson AL, Schnitt SJ, Nikolsky Y, Gelman RS and Polyak K, 2007. Molecular definition of breast tumor heterogeneity. *Cancer Cell*, 11: 259-273

Shoker BS, Jarvis C, Sibson DR, Walker C, Sloane JP, 1999. Oestrogen receptor expression in the normal and precancerous breast. *J Pathol*, 188:237-244

Sleeman KE, Kendrick H, Ashworth A, Isacke CM and Smalley MJ, 2006. CD24 staining of mouse mammary gland cells defines luminal epithelial, myoepithelial/basal and nonepithelial cells. *Breast Cancer Res*., 8: R7

Sørlie T, Perou CM, Tibshirani R, Aas T, Geisler S, Johnsen H, Hastie T, Eisen MB, van de Rijn M, Jeffrey SS, Thorsen T, Quist H, Matese JC, Brown PO, Botstein D,

Eystein Lønning P, Børresen-Dale AL, 2001. Gene expression patterns of breast carcinomas distinguish tumor subclasses with clinical implications. *Proc Natl Acad Sci U S A*. 98(19):10869-74.

Sorlie T, Tibshirani R, Parker J, Hastie T, Marron JS, Nobel A, Deng S, Johnsen H, Pesich R, Geisler S, Demeter J, Perou CM, Lonning PE, Brown PO, Borresen-Dale AL, Botstein D., 2003. Repeated observation of breast tumor subtypes in independent gene expression data sets, *Proc Natl Acad Sci*, 100(14):8418-23

Sotiriou C, Neo SY, McShane LM, Korn EL, Long PM, Jazaeri A, Martiat P, Fox SB, Harris AL, Liu ET, 2003. Breast cancer classification and prognosis based on gene expression profiles from a population-based study. *Proc Natl Acad Sci U S A*, 100(18):10393-8

Sotiriou C and Pusztai L, 2009. Gene-expression signatures in breast cancer. *N. Engl. J.Med.*, 360: 790-800.

Stingl J, Caldas C, 2007. Molecular heterogeneity of breast carcinomas and cancer stem cell hypothesis. *Nature Rev Cancer* 7:791-799

Stingl J, 2009. Detection and analysis of mammary gland stem cells. *J. Pathol.*, 217, 229-241

Staal FJ, Roederer M, Herzenberg L, 1990. Intracellular thiols regulate activation of nuclear factor κB and transcripion of human immunodeficiency virus. *Proc. Natl. Acad. Sci.*, 87:9943-9947

Thannickal VJ, Fanburg BL, 2000. Reactive oxygen species in cell signaling, *Am. J. Physiol. Lung Cell Mol. Physiol.*, 279:L1005-L1028

Wainwright LJ, Lasorella A, Iavarone A, 2001. Distinct mechanism of cell cycle arrest control the decision between differentiation and senescence in human neuroblastoma cells. *Proc Natl Acad Sci*, 98:9396-9400

Wei W. and Sedivy JM, 1999. Differentiation between senescence (M1) and crisis (M2) in human fibroblast cultures. *Exp. Cell. Res*., 253:519-522.

Werner H, Bruchim I, 2009. The insulin-like growth factor-I receptor as an oncogene. *Archives of Physiology and Biochemistry*, 115(2): 58–71

Yeh IT, and Mies C, 2008. Application of immunohistochemistry to breast lesions. *Arch Pathol. Lab. Med*., 132, 349-358.

Zhao JJ, Gjoerup OV, Subramanian RR, Cheng Y, Chen W, Roberts TM, Hahn WC, 2003. Human mammary epithelial cell transformation through the activation of phosphatidylinositol 3-kinase. *Cancer Cell*, 3:483-495.

Zhu J, Woods D, McMahon M, Bishop JM, 1998. Senescence of human fibroblasts induced by oncogenic Raf. *Genes & Development*, 12:2997–3007

PUBLICATIONS

International Journal of Cancer

The ability to generate differentiated and senescent progeny as a major determinant of breast cancer heterogeneity

Journal:	*International Journal of Cancer*
Manuscript ID:	IJC-09-1655
Wiley - Manuscript type:	Cancer Cell Biology
Date Submitted by the Author:	18-Jul-2009
Complete List of Authors:	Mumcuoglu, Mine; Bilkent University, Molecular Biology and Genetics Bagislar, Sevgi; Bilkent University, Molecular Biology and Genetics Yuzugullu, Haluk; Bilkent University, Molecular Biology and Genetics Alotaibi, Hani; Bilkent University, Molecular Biology and Genetics Senturk, Serif; Bilkent University, Molecular Biology and Genetics Gur-Dedeoglu, Bala; Bilkent University, Molecular Biology and Genetics Cingoz, Burcu; Bilkent University, Molecular Biology and Genetics Bozkurt, Betul; Ankara Numune Research and Teaching Hospital, Department of Surgery Tazebay, Uygar; Bilkent University, Molecular Biology and Genetics Yulug, Isik; Bilkent University, Molecular Biology and Genetics Akcali, Can; Bilkent University, Molecular Biology and Genetics Ozturk, Mehmet; Bilkent University, Department of Molecular Biology and Genetics; Institut Albert Bonniot – UJF, Centre de Recherche
Key Words:	senescence, differentiation, breast cancer heterogeneity

The ability to generate differentiated and senescent progeny as a major determinant of breast cancer heterogeneity

Short title: Differentiation and senescence in breast cancer

Mine Mumcuoglu[1], Sevgi Bagislar[1,2], Haluk Yuzugullu[1,2], Hani Alotaibi[1], Serif Senturk[1], Bala Gur-Dedeoglu[1], Burcu Cingoz[1], Betul Bozkurt[3], Uygar H. Tazebay[1], Isik G. Yulug[1], Can Akcali[1] and Mehmet Ozturk[1,2,4]

[1]Bilkent University, BilGen Genetics and Biotechnology Center - Department of Molecular Biology and Genetics, Ankara, 06800, Turkey; [2]INSERM - Université Joseph Fourrier, CRI U823, Grenoble, 38042, France; [3]Ankara Numune Research and Teaching Hospital, Department of Surgery, Ankara, Turkey.

[4]Corresponding Author:

Mehmet Ozturk, PhD

Centre de Recherche INSERM-UJF U823, Grenoble, France.

Phone: +33 476549410 Fax: +33 476549413 e-mail:ozturkm@ujf-grenoble.fr

Key words: senescence; differentiation; breast cancer heterogeneity

Abbreviations: 4OHT = 4-hydroxytamoxifen; E2 = 17β-estradiol; ER = estrogen receptor-α; ICP = immortal cell progenitor; PD = population doublings; SABG = senescence-associated β-galactosidase; SCP = senescent cell progenitor; TERT = telomerase reverse transcriptase.

Journal category: Cancer Cell Biology

Novelty and impact: Breast cancer heterogeneity is believed to be a sign of tumor initiation from different progenitor lineages involved in mammary epitheliogenesis. Here, we show that breast cancer cell lines clustering with luminal A/normal-like and basal/luminal B tumors respectively, differ from each other by the ability to generate differentiated and senescence-arrested progeny. Less tumorigenic senescent cell progenitor cell lines generate both luminal- and myoepithelial-like cells. In contrast, more tumorigenic immortal cell progenitor cell lines are defective in their ability to generate differentiated progeny. Our findings may have prognostic relevance and serve as a basis for therapeutic induction of differentiation and senescence in breast cancer.

Abstract

Breast cancer displays distinct subtypes, such as luminal A, luminal B, and basal-like. The prognosis and therapeutic response of each subtype is different. The mechanisms involved in the generation of these tumor types are poorly understood. Our aim was to test whether the ability to generate senescent progeny contributes to breast cancer heterogeneity. A panel of 12 breast cancer cell lines, 31 isogenic clones, and 12 breast tumors were used. We classified breast cancer cell lines into senescent cell progenitor (SCP) and immortal cell progenitor (ICP) subtypes. All ER+ cell lines tested, and some ER-positive (ER+) breast tumors displayed senescence. Acute loss and tamoxifen-mediated inactivation of ER triggered a robust senescence response in SCP type T47D cell line. In contrast, estrogen treatment and $p21^{Cip1}$ knockdown inhibited senescence. Breast cancer cell subtypes displayed divergent ability to produce differentiated progeny. The SCP subtype cells produced CD24+ or ER+ luminal-like and ASMA+ myoepithelial-like progeny, in addition to CD44+ stem/progenitor-like cells. In contrast, ICP cell lines acted as differentiation-defective stem/progenitor cells. Some cell lines generated only CD44+/CD24-/ ER-/ASMA- progenitor/stem-like cells, and others only CD24+/ER- luminal-like, but not ASMA+ myoepithelial-like cells. SCP cell lines were less tumorigenic, and they clustered with luminal A/normal like tumors. In contrast, ICP subtypes were more tumorigenic, and they clustered together with basal/luminal B tumors. Our results show that breast cancer cell lines clustering with luminal A/normal-like and basal/luminal B tumors respectively, differ from each other by the ability to generate differentiated and senescence-arrested progeny.

Human breast cancers are heterogeneous, both in their pathology and in their molecular profiles. First, the patterns of genetic changes such as chromosomal aberrations and gene mutations observed in breast tumors indicate that breast tumorigenesis does not follow a stepwise linear progression from well-differentiated to poorly differentiated tumors.[1] Second, gene expression analyses classify breast tumors into distinct subtypes, such as luminal A, luminal B, ERBB2-positive (ERBB2+) and basal-like.[2-4] The prognosis and therapeutic response of each subtype is different. Luminal A cancers are mostly estrogen receptor-α-positive (ER+) and sensitive to antiestrogen therapy, with best metastasis-free and overall survival rates. Luminal B tumors have incomplete antiestrogen response and lower survival rates. Basal-like and ERBB2+ tumors are ER- and display the worst survival rates.[3,4]

The mechanisms involved in the generation of different breast tumor types are poorly understood. According to one hypothesis, they may derive from different progenitor lineages involved in mammary epithelial cell differentiation.[1] The mammary gland is composed of differentiated luminal and myoepithelial cells that are generated from multilineage, luminal-restricted and myoepithelial-restricted progenitors originating from a hypothetical breast epithelial stem cell. Different types of breast cancers are proposed to originate from such stem or progenitor cells at different stages of commitment and differentiation, as observed in hematological malignancies.[1,5] In line with this hypothesis, CD44-positive/CD24-negative (CD44+/CD24-) mammary-tumor-initiating cells, also called "breast cancer stem cells" have been isolated from primary breast tumors,[6-8] and breast cancer cell lines.[7-12] Breast cancer stem cells have also been generated from human mammary epithelial cells through epithelial-mesenchymal transition.[13,14] CD44+ cells are more tumorigenic than CD44- cells. CD44+ mammary tumor-initiating cells represent a fraction of breast tumors, and they give rise to tumors composed of both CD44+ and CD44- cells, as observed in the original tumors.[6]

Breast cancer cell lines often reproduce the status of primary tumors. They harbor tumor-initiating cells at different rates and such tumor-initiating cells generate tumors composed of heterogeneous cell populations.[11,12] CD44+/CD24- cells have also been identified in normal mammary epithelium, in strong support of stem/progenitor cell origins for breast cancer.[15] Tumor-initiating cells have been identified from both luminal and basal-like cell lines.[9,11,12] Similarly, CD44+/CD24- stem-like cells were detected in both basal and non-basal breast tumors, with higher frequencies in basal tumors.[16] However, unlike hematological malignancies, specific stem- or progenitor cell-type origins have not been assigned to different breast tumor subtypes. It is also unknown if the differential prognosis and the therapeutic responses of distinct tumor subtypes can be related to tumor-progenitor cell types. If we assume that stem cells and downstream progenitor

cells at different stages of commitment have sensitively different progenitor potential, this should have a direct effect on tumor prognosis and therapeutic response. The lack of a comprehensive map of mammalian epitheliogenesis and the extreme heterogeneity of breast tumors appear to be the major obstacles in resolving these critical issues.

Here, we describe the use of cellular senescence as a mark of terminal differentiation to characterize the progenitor potential of breast cancer cells. Normal mammary epithelial cells undergo two successive senescence states, termed "stasis" and "agonescence," from which spontaneous immortalization has not been observed.[17,18] However, replicative immortality can be induced in these cells by ectopic expression of telomerase reverse transcriptase (*TERT*) and inactivation of senescence checkpoints.[19,20] Similarly, breast cancer cells can acquire immortalization by genetic/epigenetic inactivation of senescence checkpoints and reactivation of *TERT* expression.[18] The abundance of non-tumorigenic and differentiated cells both in breast tumors and cell lines strongly suggests that replicative immortality cannot be assigned to all cells within a tumor or a cancer cell line, and that spontaneous senescence after a limited number of population doublings (PD) is likely to occur. If this hypothesis is correct, then the rate of generation of senescent progeny may reflect the potential of a cancer stem/progenitor cell to produce terminally differentiated progeny. We tested this hypothesis using a panel of luminal and basal-like breast cancer cell lines (Table 1). Although a single cell line is not representative of breast tumor heterogeneity, a panel of cell lines might reproduce the heterogeneity that is observed in primary breast tumors, albeit with some limitations.[5,21] Therefore, we hoped that in vitro studies with a panel of cell lines might help to better understand breast tumor heterogeneity.

Our senescence tests allowed us to classify breast cancer cell lines as senescent cell progenitor (SCP) and immortal cell progenitor (ICP) subtypes. We also show that senescent progeny are observed exclusively in estrogen receptor-α (ER)-positive cells, as a result of ER inactivation, partly mediated with $p21^{Cip1}$ protein. The ability to produce senescent progeny was associated with the ability to produce luminal-like and myoepithelial-like progeny from stem/progenitor-like cells. In contrast, most of the cell lines lacking senescent progeny were also unable to generate differentiated progeny. Finally, we show that SCP subtype cell lines cluster with luminal A/normal-like breast tumor types and are less tumorigenic, whereas ICP subtype cell lines cluster with luminal B/basal-like tumor types and are more tumorigenic.

Material and Methodes

Clinical samples and cell lines

Freshly frozen tumor specimens were collected at Ankara Numune Hospital. The use of the tissue material was approved by the Research Ethics Committee of Ankara Numune Research and Teaching Hospital. Consents were obtained in accordance with the Helsinki Declaration. Breast cancer cell lines used in this study were listed in Table 1. The authenticity of cell lines was verified by short tandem repeat profiling, as recommended by ATCC (http://www.lgcstandards-atcc.org). Isogenic clones from T47D (n=20) and BT-474 (n=11) cell lines were obtained from single cell-derived colonies. Briefly, cells were plated in 96-well plates to obtain single colonies in less than 70% of wells. Isolated colonies were then tranferred to progressively larger wells, and to T25 flasks. Clones were subcultivated weekly at 1:4 dilution ratios, and maintained in culture for 25-30 passages to reach to >60 PD before testing.

Primary antibodies

The following antibodies were used: anti-CD44 (559046; BD Pharmingen), anti-CD24 (sc53660; Santa Cruz,), anti-ASMA (ab7817; Abcam), anti-CK19 (sc6278; Santa Cruz,), anti-$p21^{Cip1}$ (OP64; Calbiochem), anti-$p16^{Ink4a}$ (NA29, Calbiochem), anti-ERα (sc8002; Santa Cruz).

Low-density clonogenic assays

Cells were seeded as low-density on coverslips in six-well plates (500-2000 cells, according to plating efficiency) allowed to grow in DMEM supplemented with 10% fetal calf serum, with medium change every three days, until they formed colonies of a few hundred cells. Depending on cell lines, this took one to two weeks. For BrdU assays, cells were labeled for 24h prior to immunocytochemistry.

Immunocytochemistry

For simple immunoperoxidase assays, cells were fixed with cold methanol for five minutes, then blocked with 10% FCS in PBS for 1h. This was followed by incubation with primary antibody for 1h. Cells were then washed with PBS three times and subjected to immunostaining using the Dako-Envision-dual-link system and the Liquid DAP Substrate chromogen system (Dako, CA, USA), according to the manufacturer's instructions. Hematoxylin was used as a counter-stain when the visualization of cells was necessary. For SABG-immunoperoxidase co-staining studies, unfixed cells were first subjected to SABG assay, and then fixed prior to immunostaining assays.

Hematoxylin counter-staining was omitted for co-staining experiments, unless cells were negative for SABG staining.

Immunoblot analyses

Cell pellets were incubated in NP-40 lysis buffer [50 mM Tris–HCl, pH 8.0, 250 mM NaCl, 0.1% Nonidet P-40 and 1Xprotease inhibitor cocktail (Roche)] for 30 minutes in a cold room. Then cell lysates were cleared by centrifugation. Bradford assay was performed to quantify the protein concentration of the cell lysates. 30 µg of protein was denatured and resolved by SDS-PAGE using 10% or 12% gels. Then, proteins were transferred to the PVDF or nitrocellulose membranes. Membranes were treated for 1h with blocking solution tris-buffered saline containing 0.1% Tween-20 and 5% non-fat milk powder (TBS-T) and probed with primary antibody for 1h. Next, membranes were washed three times with TBS-T and incubated with HRP-conjugated secondary antibody for 1h. Then, immunocomplexes were detected by ECL-plus (Amersham) kit on the membrane. The α-tubulin was used as an internal control.

Senescence-associated beta-galactosidase (SABG) assay and BrdU/SABG co-staining

SABG activity was detected as described,[22] except that cells were counterstained with eosine or nuclear fast red, following SABG staining. For BrdU/SABG co-staining, cells were labeled with BrdU (10 µg/ml) for 24h in freshly added culture medium, and tested as described.[23] For co-staining, cells were first subjected to SABG assay, then fixed in 70% methanol and subjected to BrdU immunostaining.

Estrogen and tamoxifen treatment

Cells were seeded under low-density clonogenic conditions onto coverslips in six-well plates, and cultivated in standard culture medium for seven to eight days. Then, cells were fed with phenol red-free DMEM (Gibco) supplemented with 5% charcoal-stripped fetal calf serum for 48h, followed by two successive 48h treatments with 10^{-9} M E2 (17β-estradiol; Sigma), 10^{-6}-10^{-9} M 4OHT (4-hydroxytamoxifen; Sigma) or an ethanol vehicle, under the same conditions. Colonies were then subjected to SABG assay. Each experimental condition was conducted in triplicate and experiments were repeated three times.

Generation of estrogen receptor-overexpressing clones

T47D-iso23 cells were transfected with the expression vector pCMV- ERα (ref. 24) or an empty vector using FuGENE-6 (Roche). ER overexpressing and control clones were selected with 500μg/ml G418 for three weeks. Isolated single-cell-derived colonies were picked and expanded in the presence of G418.

Lentiviral infection and generation of $p21^{Cip1}$ knock-down clones

We used mission shRNA plasmid pLKO.1<-puro-p21 (NM_000389.2-640s1c1, Sigma) for $p21^{cip1}$ knockdown experiments. Control vector shRNA-pGIPz-SCR-puro and helper packaging mix (Invitrogen) were also used. HEK293T co-transfected with the appropriate vector and packaging mix, using CalPhos Mammalian Transfection Kit (Clontech), following the manufacturer's instructions. After 48h of culture, virus-containing culture media were collected, filtered and used to infect T47D-iso23 cells. After four hours of infection, stable cells were selected with 1 μg/ml puromycin for seven days.

Nude mice tumorigenicity assays

MCF-7, T47D, CAMA-1, BT-20, HCC1937 and MDA-MB-453 cells ($5x10^6$) were injected subcutaneously into CD-1 "*nude*" mice (Charles River). In order to minimise hormonal effects on tumor growth, male animals were used with no estrogen complementation. Local tumor growth was monitored for 10 weeks. All animal experiments were pre-approved by Bilkent University Animal Ethics Committee.

Cluster analysis

The two-channel microarray data containing 8102 cDNA genes/clones, generated by Sorlie et al.[2] were downloaded from the Stanford Microarray Database (SMD) (http://genome-www.stanford.edu/MicroArray/). In the downloading process, "log (base 2) of R/G Normalized Ratio (median)" parameter was used for data filtering. We have median-centered expression values for each array. We selected arrays and genes with greater than 75% good data (representing the amount of data passing the spot criteria). Sixty-eight tissue samples were obtained according to this criterion and annotated with the subtypes described by the authors, found in "Supplementary Information" of the data set in SMD. The expression values of "500 gene signature," defined by the authors, were extracted from the data. Gene expression profiles of 31 breast cancer cell lines performed by Charafe-Jauffret et al.,[25] using the whole-genome cDNA microarray Affymetrix

HGU-133 plus 2, was obtained from the "Supplementary Table" of the article. The authors filtered genes with low and poorly measured expression, and with low expression variation, retaining 15, 293 genes. After log transformation of the data, we median normalized the arrays of the data in R language, using the Bioconductor biostatistical package (www.r-project.org/ and www.bioconductor.org/). The "500 gene signature" tumor data[2] and the normalized breast-cancer cell line data[25] were combined with respect to probe IDs using a set of customized perl routines (source codes are available upon request). A set of 175 genes was common. "Median center" normalization of genes was made for the merged data set for the total samples. We performed unsupervised hierarchical clustering with the 99 samples, including 31 breast cell line[25] and 68 breast tumor [2] samples by pair-wise complete-linkage hierarchical clustering parameter, using the Gene-Pattern program. The Pearson correlation method was used for distance measurements. Clustering was visualized by java treeview, again using Gene-Pattern (http://www.broad.mit.edu/cancer/software/genepattern/).

Statistical analyses

Significant differences were evaluated using unpaired Student's t test for compared samples sizes of 10 or higher. Otherwise, one-tailed Fisher's exact test was used with 2×2 tables; $p < 0.05$ was considered statistically significant. On the graphical representation of the data, y axis error bars indicate the standard deviation for each point on the graph.

Results

Classification of breast cancer cell lines as senescent cell progenitor and immortal cell progenitor subtypes

Clonogenic assays have been successfully used to test the abilities of self-renewal and generation of phenotypically distinct progeny of mammary stem/progenitor cells.[26] We previously applied this technique to test the ability of cancer cells to produce progeny with replication-dependent senescence arrest.[23] Cells are plated under low-density clonogenic conditions and cultivated for one to two weeks until individual cells perform eight to ten PD and generate isolated colonies composed of several hundred cells. This method permits the tracing of progenies generated by a few hundred cells under the same experimental conditions. Here, we used low-density clonogenic assay to analyze a panel of 12 breast cancer cell lines, composed of luminal (n=7) and

basal (n=5) subtypes (Table 1). Our study classified the tested cell lines into two major subtypes. A group of cell lines generated colonies with high rates of senescence, while others did not produce appreciable amounts of senescent cells. Representative pictures of colonies subjected to SABG assay are shown in Fig. 1a. The percent of SABG+ progeny was calculated by manual counting of at least 10 different colonies for each cell line. Colonies derived from five cell lines generated SABG+ cells at high rates (means: 12-40%) Senescence rates were negligible (means: 0-5%) in the progeny of the remaining seven cell lines. The first group that we named here as "senescent cell progenitor" (SCP) subtype included T47D, BT-474, ZR-75-1, MCF-7 and CAMA-1 cell lines. The second group named "immortal cell progenitor" (ICP) subtype, included MDA-MB-453, BT-20, SK-BR-3, MDA-MB-468, HCC1937, MDA-MB-231 and MDA-MB-157 (Fig. 1b).

In order to verify whether the occurrence of senescent cells in the SCP group was intrinsic to each cell line or due to the presence of a side population, we generated clones from T47D (n=20) and BT-474 (n=11) cell lines, and subjected them to SABG assay at different intervals. All clones acted similarly to their respective parental cell lines with similar rates of SABG+ progeny. No clone gained the ICP phenotype. More importantly, none of the clones tested over a long period of time (>60 PD) entered full senescence (data not shown), unlike normal mammary epithelial cells that undergo two stages of senescence arrest over a period of ~20 PD (Ref. 18). We also confirmed the senescence phenotype by a supplementary test based on 24h BrdU labeling assay under mitogenic conditions.[27] In order to confirm the specificity of the BrdU assay, we performed co-staining for SABG and BrdU, as shown in Fig. 1c. Most of the time, individual cells of the colonies from CAMA-1, T47D, and clones T47D-iso23 and BT-474-iso23 displayed either SABG+/BrdU- or SABG-/BrdU+ staining. This indicated that SABG+ senescent cells were at the terminal differentiation stage with irreversible loss of DNA synthesis ability. Our observations also indicated that SABG and BrdU tests could be used alternatively to identify senescent (SABG+/BrdU-) and immortal (SABG-/BrdU+) cells under our experimental conditions.

Senescent cell progenitor phenotype is associated with $p21^{Cip1}$ expression

Both $p16^{Ink4a}$ and p53 have been shown to be mediators of senescence arrest in mammary epithelial cells.[17,19,20,28] The $p21^{Cip1}$ is the major effector of p53 for cell cycle arrest and senescence.[18] Therefore, we analyzed the expression of $p16^{Ink4a}$ and $p21^{Cip1}$ in the cell line panel. Heterogeneously and strongly positive nuclear $p21^{Cip1}$ immunoreactivity was observed in four of the five SCP cell lines, but not in any of the seven ICP cell lines (Fig. 2a). The association of $p21^{Cip1}$ expression with the SCP subtype was statistically significant ($p = 0.0100$). We also

compared the expression of $p16^{Ink4a}$. Two SCP cell lines displayed heterogeneously positive immunostaining, whereas three of seven ICP cell lines displayed homogenously positive staining (Supplementary Fig. S1). The difference of $p16^{Ink4a}$ expression between the two groups was not significant ($p = 0.6893$). These observations indicated that the SCP phenotype was associated with $p21^{Cip1}$ but not $p16^{Ink4a}$ expression in breast cancer cell lines.

To test whether $p21^{Cip1}$ was directly involved in the senescence observed in SCP cells, we first performed $p21^{Cip1}$/SABG staining in T47D-iso23 cells (hereafter termed T47D). A SABG+ signal was observed mostly in $p21^{Cip1}$-expressing cells (Supplementary Fig. S2). Next, we generated two derivative cell lines following infection of T47D with lentiviral vectors encoding $p21^{Cip1}$ shRNA (T47D-p21sh) or a scrambled control (T47D-scr). Following the demonstration of $p21^{Cip1}$ knockdown in T47D-p21sh cells by western blot assay (Fig. 2b), both cell lines were plated under low-density plating conditions, colonies were grown for 10 days, and subjected to SABG and BrdU stainings. It was not possible to quantify SABG+ cells in T47D-p21sh cells because they formed tight clusters in culture (data not shown). Therefore, we used BrdU staining as an alternative method for senescent cell quantification (Fig. 2c). Randomly selected colonies were counted for the number of BrdU+ and BrdU- cells (Fig. 2d). The T47D-scr cell line generated BrdU+ progeny at a rate of 48±20% per colony (n=18). Under the same conditions, T47D-p21sh cells displayed BrdU+ progeny at a rate of 65±12% per colony (n=18), with a significant ($p = 0.0043$) increase in the number of cells escaping terminal arrest (Fig. 2e). These results indicated that $p21^{Cip1}$ was partly responsible for the induction of senescence observed in the progeny of T47D cells.

The generation of senescent cell progeny is controlled by estrogen receptor

As stated above, $p21^{Cip1}$ is a downstream target of p53 for senescence, but T47D cells do not express wild-type p53 (Table 1). Estrogen inhibits $p21^{Cip1}$ expression[29] by c-Myc-mediated repression,[30] *MYC* gene being a direct target of ER complex.[31] Therefore, we tested whether ER could be involved in the senescence observed in T47D cells. Data shown in Fig. 3a indicated T47D cells displayed nuclear ER immunoreactivity in their great majority, but some progeny was ER-. More interestingly, these ER- cells tended to be SABG+, suggesting that the senescence occurred in T47D cells as a result of ER loss. MD-MBA-231 cells, on the other hand, did not express ER at all, and they were SABG-, as expected. Thus, the senescence susceptibility was restricted to ER+ T47D cells, however the senescent cells no longer expressed nuclear ER protein.

Next, we tested whether experimental modification of ER activity in T47D cells had any effect on senescence response. After plating at low-density clonogenic conditions, cells were grown

in regular cell culture medium that contained weakly estrogenic phenol red[32] for seven days in order to obtain visible colonies. Then, the culture medium was changed with phenol-free DMEM complemented with charcoal-treated fetal calf serum, grown for two more days, then cultivated for four more days in the presence of E2 (10^{-9} M), OHT (10^{-9} M to 10^{-6} M), or an ethanol vehicle as control. Colonies were subjected to SABG staining (Fig. 3b). Total and SABG+ cells were counted from 20 randomly selected colonies for each treatment (Fig. 3c). Colonies grown in a phenol-free charcoal-treated control medium complemented with an ethanol vehicle only displayed 31±13% SABG+ cells. Complementation of this medium with 10^{-9} M E2 generated colonies with 17±18% SABG+ cells. The inhibition of senescence by E2 was nearly 50% and statistically significant when compared to ethanol-complemented control cells ($p = 0.0093$). In contrast to E2, OHT provoked a dose-dependent increase in the proportion of SABG+ cells. At the maximum dose used (10^{-6} M OHT), 90±13% of colony-forming cells displayed SABG+ signal (Fig. 3d), indicating that tamoxifen-mediated inactivation of ER can induce almost a complete senescence response in these cells ($p < 0.0001$). The increase in senescence rate was also significant with 10^{-7} M OHT ($p = 0.0002$).

Our findings strongly suggested that the senescence observed in the SCP T47D cell line was due to a loss of expression and/or function of ER in a subpopulation of the progeny of these cells. For confirmatory reasons, we constructed ER-overexpressing stable clones from T47D cells. Three clones with the highest ER expression were selected. Three other clones with endogenous expressions of ER were also selected from stable clones obtained with an empty vector (Fig. 4a). Progeny obtained from these six clones was tested by BrdU assay (Supplementary Fig. S3). Randomly selected colonies (n=10) from each clone were evaluated for total and BrdU+ number of cells (Fig. 4b). Consistently higher levels of BrdU+ cells were observed with clones ectopically expressing the ER protein (Fig. 4c). Overexpression of ER resulted in a significant increase in the BrdU+ progeny ($p = 0.034$). The protective effect of ER overexpression was not as important as the senescence-promoting effects of ER inhibition, probably because endogenous levels of ER are already quite high in T47D cells and the phenol red in the standard culture medium is weakly estrogenic.[32] Nonetheless, these findings provide additional evidence of a close relationship between ER expression and senescence in T47D cells.

The detection of senescent cells in the progeny of the T47D cell line was correlated with a heterogeneous loss of nuclear ER expression. The lack of senescent progeny in the ER- MDA-MB-231 cell line indicates that senescence response is due to acute loss of ER in T47D cells, as, by definition, the growth of MDA-MB-231 cells is independent of ER expression.

The close relationship between ER and senescence in the ER+ T47D cell line, and the highly effective treatment of ER+ breast tumors with tamoxifen, which induced senescence in our experimental model, suggested that senescence induction might be a relevant mechanism involved in antiestrogen treatments. As fresh tumor tissues cannot be obtained from tamoxifen-treated patients for obvious ethical reasons, we analyzed untreated ER+ breast tumor samples for evidence of in vivo senescence. We screened a small panel of 12 snap-frozen ER+ breast tumor tissues from 11 patients for senescence by SABG assay. The mean age of patients was 58±12 yrs, with a mixed menopause status (Supplementary Table S1). Two tumors (17%) displayed SABG+ cells that were scattered within the tumor area (Supplementary Fig. S4). Thus, ER+ breast tumors also produced senescent progeny in vivo, but at a lower rate.

Senescent cell progenitor and immortal cell progenitor subtypes greatly differ in their ability to differentiate into luminal and myoepithelial cell types

The cellular specificity of ER among the mammary epithelial cell hierarchy is poorly understood. Previous data suggest that normal ER+ cells may represent either relatively differentiated luminal cells with limited progenitor capacity, or primitive progenitors with stem cell properties in the luminal cell compartment.[1,33,34] Based on the close association between senescence (that can be considered a manifestation of terminal differentiation) and loss of ER positivity, we hypothesized that ER+ SCP cells may differ from ER- ICP cells by their differentiation potential. We surveyed a few hundred single-cell-derived colonies from each of the 12 cell lines for production of stem/progenitor-like, luminal-like and myoepithelial-like cells. We used CD44 as a positive stem/progenitor cell marker,[6,15] CD24, ER and CK19 as luminal lineage markers[15,35,36] and ASMA as a myoepithelial lineage marker.[36]

Representative examples of marker studies by immunoperoxidase staining in SCP and ICP cell lines are shown in Fig. 5. All five SCP cell lines displayed a heterogeneous pattern of positivity with CD44; some colonies were fully positive, some fully negative and some others were composed of both positive and negative cells. CD44/CD24 double immunofluorescence studies with T47D cell line indicated that SCP cells produce also CD44+/CD24- stem/progenitor cells, as expected (data not shown). In sharp contrast, five of the seven ICP cell lines generated only fully positive CD44 colonies, indicating they never produced CD44- cells. One cell line was totally CD44-. Only one cell line displayed a pattern similar to that of SCP cell lines. The comparison of two subtypes indicated that the ability to generate both CD44+ and CD44- progeny is significantly associated with the SCP phenotype ($p = 0.0046$). All five SCP cell lines displayed heterogeneous,

but mostly positive ER immunostaining, whereas all seven ICP cell lines never generated ER+ cells. The expression of ER was also significantly associated with the SCP subtype ($p = 0.0012$). Furthermore, the ability to produce ASMA+ progeny was also significantly associated with the SCP subtype ($p = 0.0046$). The ICP cell lines did not generate ASMA+ cells, while four out of five SCP cell lines generated rare ASMA+ cells under low-density clonogenic conditions. Interestingly, the abundance of ASMA+ cells was much higher in the two SCP cell lines that were tested at high cell density (Supplementary Fig. S5). This suggests that either the production of ASMA+ cells is enhanced at high cell density, or these myoepithelial-like cells have limited survival ability under long-term culture conditions. We did not find a strong association between the expression of CD24 and CK19 markers and cell subtype. All five SCP cell lines and three ICP cell lines generated heterogeneously staining colonies for CD24 expression. Similarly, all five SCP cell lines, as well as three ICP cell lines, expressed CK19, but homogenously.

Typical features of senescent progenitor and immortal progenitor breast cancer cell lines

As summarized in Fig. 6, SCP and ICP subtype cell lines displayed several subtype-specific features. All SCP cell lines produced differentiated and senescent cells, in addition to putative CD44+/CD24- stem/progenitor cells. All of them produced ER+, and CD24+ luminal-like cells and most of them (n=4/5) also produced ASMA+ myoepithelial-like cells. In contrast, five of the seven ICP cell lines never produced CD44- cells, suggesting they cannot generate differentiated progeny under the experimental conditions tested. In confirmation of this hypothesis, four ICP cell lines only produced CD44+/CD24-/ER-/CK19-/ASMA- stem/progenitor-like, but never differentiated cells. Furthermore, all seven ICP cell lines were unable to produce ASMA+ myoepithelial-like, ER+ luminal-like or SABG+ senescent cells. CD24 and CD19 luminal lineage markers were expressed in only three cell lines, one of which remained fully positive for CD44 stem/progenitor marker.

Senescent and immortal cell progenitor breast cancer cell lines are phenocopies of luminal A/normal-like and basal/luminal B tumor subtypes

Distinct cell-type features associated with SCP and ICP subtypes suggest that they may be phenocopies of molecularly defined breast tumor subtypes.[2-4,37] As the prognosis and therapeutic response of each subtype is different,[3,4] we questioned whether we could assign SCP and ICP cell lines to known molecular subtypes of breast tumors. Using cell line and primary tumor gene expression datasets, we conducted hierarchical clustering analysis. The “intrinsic gene set” data generated by Sorlie et al.[3] to classify breast tumors into five molecular subtypes was used to filter

cell line data generated by Charafe-Jauffret et al.[25] A set of 175 genes was common between the two data sets. Sixty-eight tumors and 31 cell lines were subjected to pair-wise complete-linkage hierarchical clustering and distance measurements. This tumor-cell line combined analysis produced two major clusters. One cluster was composed of basal and luminal B subtype tumors and a group of cell lines that included five of six ICP cell lines. The other cluster included luminal A, ERBB2+ and normal-like subtype tumors and a set of cell lines that included all five SCP subtype cells. Four cell lines clustered with luminal A tumor subclass, and one cell line with normal-like subclass (Fig. 7a). A full list of clustered tumors and cell lines is provided in Supplementary Fig. S6.

Luminal A tumors clustering with our SCP subtype cell lines display the longest tumor-free, distant metastasis-free and overall survival rates. In contrast, basal and luminal B tumors clustering with our ICP subtype cell lines have the worst prognosis, with shorter tumor-free, distant metastasis-free and overall survival times.[3] Our cluster analysis suggests that the ability to generate differentiated and senescent progeny characterises breast cancers with poor tumorigenicity, and that the resistance to differentiation and senescence is indicative of more aggressive tumorigenicity. We compared in vivo intrinsic tumorigenic behavior of three SCP (MCF-7, T47D and CAMA-1) and three ICP (BT-20, HCC1937 and MDA-MB-453) cell lines in CD1 "nude" mice. In order to compare the intrinsic tumorigenicity of SCP and ICP cell lines independent of external hormonal inteference, we set up experimental conditions to minimise such effects. As estrogen interfered with sponatenous senescence arrest in T47D SCP cell line (Fig. 3), male animals in the absence of estrogen complementation were used for tumorigenicity studies. Nine animals implanted with SCP cell lines did not develop tumors and remained tumor-free for at least 10 weeks. In contrast, seven out of eight animals implanted with ICP cell lines developed subcutaneous tumors within five weeks of cell injection (Fig. 7b). One animal injected with MDA-MB-453 ICP cell line, which died very shortly after cell injection, was excluded from the analysis. The difference of tumorigenicity between SCP and ICP cell lines was statistically significant ($p = 0.0002$).

Discussion

In recent years, phenotypic heterogeneity of breast cancers has been correlated with genetic and molecular heterogeneity.[2,4] Breast cancer subtypes may represent cancers originating from different progenitor cells. Molecular and phenotypic heterogeneity and associated clinical manifestations of breast tumor subtypes have been related to the type of hypothetical tumor progenitor cells originating from a hypothetical mammary epithelial stem cell or from downstream progenitor

cells.[1,5] This hypothesis has not been fully validated, mainly because a hierarchical map of cells involved in mammary epitheliogenesis has not yet been established.

To better understand phenotypic differences between different breast cancer subtypes, we applied senescence as a surrogate marker for the potential to generate terminally differentiated progeny. We completed these studies with markers for breast stem/progenitor and differentiated luminal and myoepithelial lineage cells. The use of low-density clonogenic conditions allowed us to follow up the fate of a large number of single-cell-derived progeny for each cell line studied. Using these approaches, we draw several important conclusions. First, breast cancer cell lines form two distinct groups of SCP and ICP subtypes. The SCP cell lines produce both non-senescent and senescent progeny, whereas ICP cell lines produce only non-senescent progeny. Second, SCP and ICP cell lines are exclusively ER+ and ER- cell lines, respectively. Senescence occurs as a result of ER loss associated with $p21^{Cip1}$ induction. Experimental activation of ER by E2 protects from senescence, whereas its inactivation by tamoxifen aggravates it. Thus, senescence in ER-dependent cells appears to result from the loss of survival signals generated by transcriptional activity of ER. A similar type of senescence has been reported for lymphoma, osteosarcoma, and hepatocellular carcinoma tumors upon c-*MYC* inactivation.[38] Third, SCP cells generate ER+, CD24+ or CK19+ luminal-like, as well as ASMA+ myoepithelial-like progeny. These findings strongly suggest that most, if not all, SCP cells have the capacity to give rise to two major types of differentiated cells that are found in normal mammary epithelium. In sharp contrast, ICP cells never produce ER+ luminal-like or ASMA+ myoepithelial-like cells. Indeed, some ICP cells generate only CD44+ stem/progenitor-like cells and never CD44-, CD24+, CK19+, ER+ or ASMA+ cells. These findings indicate that ICP cells have limited differentiation ability, at least under in vitro conditions. The differentiation ability of ICP cells appears to be lost completely or partially, so while they self-renew as stem/progenitor-like cells, they do not differentiate fully. Fourth, SCP cell lines and luminal A/normal-like breast tumors form the same molecular cluster. This suggests that SCP cell lines are phenocopies of these relatively benign, antiestrogen-responsive luminal A tumors. The lack of tumorigenicity of SCP cell lines in "nude" mice correlates with better tumor-free and metastasis-free survival of patients with luminal A type tumors. The ICP cell lines cluster with luminal B/basal-like breast tumor subtypes, and they are highly tumorigenic, as expected for luminal B and basal-like tumors. Presently, it is unknown whether breast tumor subtypes that cluster with SCP or ICP cell lines are also composed of either differentiating or mostly self-renewing stem/progenitor cells. Recent studies reported that breast tumors may contain only CD44+, or only CD24+ cells, as well as mixed cell populations, and that CD44+ tumor cells express many stem-cell markers.[15,16] In addition, an association between basal-like breast cancer

and the presence of CD44+/CD24- cells has been established.[16]

The mechanisms of the differentiation block observed in ICP cell lines are not known. One might argue that cell lines that produce only CD44+, but never differentiation marker-positive cells cannot be defined as stem/progenitor cells by definition. However, such cell lines are not completely inert to differentiation stimuli, and may undergo differentiation under special conditions. For example, MDA-MB-231 and MDA-MB-468 cells (identified as ICP cell lines here) can be induced to differentiate into ER+ cells by Wnt5a treatment, and MDA-MB-231 cells become sensitive to tamoxifen.[39] The same study also showed ER promoter sequences are methylated in these two ICP cell lines. Wnt5a treatment induces ER promoter demethylation, providing evidence for epigenetic mechanisms involved in differentiation programs of breast cancer cells.

Most of the findings reported here are derived from in vitro studies performed with established cancer cell lines. Presently, it is unknown to what extent these findings are relevant also for breast tumors. We provide here some promising data that supports in vivo relevance of our conclusions. First, our cluster analyses associated the SCP cell types with luminal A and normal-like breast tumors, whereas the ICP cell types shared similar gene expression profile with luminal B/basal-like breast tumors. Second, our tumorigenicity experiments with three different cell lines from each group clearly showed that ICP cell lines displayed high tumorigenicity, in contrast to SCP cell lines that were less tumorigenic under the same conditions. The use of male animals without estrogen supplementation in these experiments allowed us to compare intrinsic tumorigenic potentials of SCP and ICP cell lines, with minimal interference of host animal estrogenic conditions. We preferred to use this model in order to maximise the contributions of cancer cell intrinsic features to the tumorigenic potential, with minimal interference of external hormonal factors. Therefore, the diffference in tumorigenic potential observed under our experimental conditions is likely to reflect in vivo behavior of cancer cells themselves, rather than their interaction with host hormonal factors. Obviously, ICP-like and SCP-like tumors in affected women may or may not display similar tumorigenic potentials depending on their hormonal status and treatment conditions. However, as most SCP-like luminal A or ER+ tumors are successfully treated with tamoxifen,[41] their less aggressive behavior could be related to their highly effective senescence response to tamoxifen treatment, as shown here with T47D cells under in vitro conditions (Fig. 3). It will be interesting to examine whether the success of anti-estrogenic treatments is indeed associated with senescence induction in breast tumors. If this is indeed the case, senescence-inducing treatments should be considered for breast cancer.

Conclusions

Our analyses reveal that in vitro ability to generate senescent progeny permits discrimination between cells that share molecular and tumorigenic similarities with luminal A subtype breast tumors from cells related to basal/luminal B subtype tumors. We also provide in vitro evidence for classification of breast cancers into two major groups based on the ability to generate differentiated progeny. Taken together, our results show that less-tumorigenic SCP cell lines generate both luminal- and myoepithelial-like cells. In contrast, more tumorigenic ICP cell lines are defective in their ability to generate differentiated progeny. Our findings may have prognostic relevance and serve as a basis for therapeutic induction of differentiation and senescence in breast cancer.

Acknowledgments

We thank Rana Nelson for editorial help, and Pelin Tozkoparan for technical help. This work was supported by TUBITAK, DPT and TUBA (Turkey). Additional funding was from Institut National de Cancer and INSERM (France).

References

1. Stingl J, Caldas C. Molecular heterogeneity of breast carcinomas and the cancer stem cell hypothesis. Nat Rev Cancer 2007;7:791-799.

2. Perou CM, Sorlie T, Eisen MB, van de Rijn M, Jeffrey SS, Rees CA, Pollack JR, Ross DT, Johnsen H, Akslen LA, Fluge O, Pergamenschikov A, Williams C, Zhu SX, Lonning PE, Borresen-Dale AL, Brown, PO, Botstein D. Molecular portraits of human breast tumours. Nature 2000;406:747-752.

3. Sorlie T, Tibshirani R, Parker J, Hastie T, Marron JS, Nobel A, Deng S, Johnsen H, Pesich R, Geisler S, Demeter J, Perou CM, Lonning PE, Brown PO, Borresen-Dale AL, Botstein D. Repeated observation of breast tumor subtypes in independent gene expression data sets. Proc Natl Acad Sci U S A 2003;100:8418-8423.

4. Sotiriou C, Pusztai L. Gene-expression signatures in breast cancer. N Engl J Med 2009;360:790-800.

5. Vargo-Gogola T, Rosen JM. Modelling breast cancer: one size does not fit all. Nat Rev Cancer 2007;7:659-672.

6. Al-hajj M, Wicha MS, Benito-Hernandez A, Morrison SJ, Clarke MF. Prospective identification of tumorigenic breast cancer cells. Proc Natl Acad Sci U S A 2003;100:3983-3988.

7. Ponti D, Costa A, Zaffaroni N, Pratesi G, Petrangolini G, Coradini D Pilotti S, Pierotti MA, Daidone MG. Isolation and in vitro propagation of tumorigenic breast cancer cells with stem/progenitor cell properties. Cancer Res 2005;65:5506-5511.

8. Yu F, Yao H, Zhu P, Zhang X, Pan Q, Gong C, Huang Y, Hu X, Su F, Lieberman J, Song E. let-7 regulates self renewal and tumorigenicity of breast cancer cells. Cell 2007;131:1109-1123.

9. Phillips TM, McBride WH, Pajonk F. The response of CD24(-/low)/CD44+ breast cancer-initiating cells to radiation. J Natl Cancer Inst 2006;98:1777-1785.

10. Zhou J, Wulfkuhle J, Zhang H, Gu P, Yang Y, Deng J, Margolick JB, Liotta LA, Petricoin E 3rd, Zhang Y. Activation of the PTEN/mTOR/STAT3 pathway in breast cancer stem-like cells is required for viability and maintenance. Proc Natl Acad Sci U S A 2007;104:16158-16163.

11. Fillmore CM, Kuperwasser C. Human breast cancer cell lines contain stem-like cells that self-renew, give rise to phenotypically diverse progeny and survive chemotherapy. Breast Cancer Res 2008;10:R25.

12. Charafe-Jauffret E, Ginestier C, Iovinom F, Wicinski J, Cervera N, Finetti P, Hur MH, Diebel

ME, Monville F, Dutcher J, Brown M, Viens P, Xerri L, Bertucci F, Stassi G, Dontu G, Birnbaum D, Wicha MS. Breast cancer cell lines contain functional cancer stem cells with metastatic capacity and a distinct molecular signature. Cancer Res 2009;69:1302-1313.

13. Mani SA, Guo W, Liao MJ, Eaton EN, Ayyanan A, Zhou AY, Brooks M, Reinhard F, Zhang CC, Shipitsin M, Campbell LL, Polyak K, Brisken C, Yang J, Weinberg RA. The epithelial-mesenchymal transition generates cells with properties of stem cells. Cell 2008;133:704-715.

14. Morel AP, Lièvre M, Thomas C, Hinkal G, Ansieau S, Puisieux A. Generation of breast cancer stem cells through epithelial-mesenchymal transition. PLoS ONE 2008;3:e2888.

15. Shipitsin M, Campbell LL, Argani P, Weremowicz S, Bloushtain-Qimron N, Yao J, Nikolskaya T, Serebryiskaya T, Beroukhim R, Hu M, Halushka MK, Sukumar S, Parker LM, Anderson KS, Harris LN, Garber JE, Richardson AL, Schnitt SJ, Nikolsky Y, Gelman RS, Polyak K. Molecular definition of breast tumor heterogeneity. Cancer Cell 2007;11:259-273.

16. Honeth G, Bendahl PO, Ringner M, Saal LH, Gruvberger-Saal SK, Lovgren K, Grabau D, Ferno, M, Borg A, Hegardtm C. The CD44+/CD24- phenotype is enriched in basal-like breast tumors. Breast Cancer Res 2008;10:R53.

17. Romanov SR, Kozakiewicz BK, Holst CR, Stampfer MR, Haupt LM, Tlsty TD. Normal human mammary epithelial cells spontaneously escape senescence and acquire genomic changes. Nature 2001;409:633-637.

18. Stampfer MR, Yaswen P. Human epithelial cell immortalization as a step in carcinogenesis. Cancer Lett 2003;194:199-208.

19. Kiyono T, Foster SA, Koop JI, McDougall JK, Galloway DA, Klingelhutz AJ. Both Rb/p16^{INK4a} inactivation and telomerase activity are required to immortalize human epithelial cells. Nature 1998;396:84-88.

20. Beausejour CM, Krtolica A, Galimi F, Narita M, Lowe SW, Yaswen P and Campisi, J. Reversal of human cellular senescence: roles of the p53 and p16 pathways. EMBO J 2003;22:4212-4222.

21. Neve RM, Chin K, Fridlyand J, Yeh J, Baehner FL, Fevr T, Clark L, Bayani N, Coppe JP, Tong F, Speed T, Spellman PT, DeVries S, Lapuk A, Wang NJ, Kuo WL, Stilwell JL, Pinkel D, Albertson DG, Waldman FM, McCormick F, Dickson RB, Johnson MD, Lippman M, Ethier S, Gazdar A, Gray JW. A collection of breast cancer cell lines for the study of functionally distinct cancer subtypes. Cancer Cell 2007;10:515-627.

22. Dimri GP, Lee X, Basile G, Acosta M, Scott G, Roskelley C, Medrano E E, Linskens M, Rubelj

I, Pereira-Smith O, Peacocket M, Campisi J. A biomarker that identifies senescent human cells in culture and in aging skin in vivo. Proc Natl Acad Sci U S A 1995;92:9363-9367.

23. Ozturk N, Erdal E, Mumcuoglu M, Akcali KC, Yalcin O, Senturk S, Arslan-Ergul A, Gur B, Yulug I, Cetin-Atalay R, Yakicier C, Yagci T, Tez M, Ozturk M. Reprogramming of replicative senescence in hepatocellular carcinoma-derived cells. Proc Natl Acad Sci U S A 1986;103:2178-2183.

24. Alotaibi H, Cankaya-Yaman E, Demirpence E, Tazebay UH. Unliganded estrogen receptor-a activates transcription of the mammary gland Na^+/I^- symporter gene. Biochem Biophys Res Commun 2006;345:1487–1496.

25. Charafe-Jauffret E, Ginestier C, Monvillem F, Finetti P, Adelaide J, Cervera N, Fekairi S, Xerri L, Jacquemier J, Birnbaum D, Bertucci F. Gene expression profiling of breast cell lines identifies potential new basal markers. Oncogene 2006;25:2273-2784.

26. Stingl J. Detection and analysis of mammary gland stem cells. J Pathol 2007;217:229-241.

27. Wei W, Sedivy JM. Differentiation between senescence (M1) and crisis (M2) in human fibroblast cultures. Exp Cell Res 2009;253:519-522.

28. Garbe JC, Holst CR, Bassett E, Tlsty T, Stampfer MR. Inactivation of p53 function in cultured human mammary epithelial cells turns the telomere-length dependent senescence barrier from agonescence into crisis. Cell Cycle 2007;6:1927-1936.

29. Cariou S, Donovan JC, Flanagan WM, Milic A, Bhattacharya N, Slingerland JM. Down-regulation of p21WAF1/CIP1 or p27Kip1 abrogates antiestrogen-mediated cell cycle arrest in human breast cancer cells. Proc Natl Acad Sci U S A 2000;97:9042-9046.

30. Mukherjee S, Conrad SE. c-Myc suppresses p21WAF1/CIP1 expression during estrogen signaling and antiestrogen resistance in human breast cancer cells. J Biol Chem 2005;280:17617-17525.

31. Dubik D, Shiu RP. Mechanism of estrogen activation of c-myc oncogene expression. Oncogene 1992;8:1587-1594.

32. Berthois Y, Katzenellenbogen JA, Katzenellenbogen BS. Phenol red in tissue culture media is a weak estrogen: implications concerning the study of estrogen-responsive cells in culture. Proc Natl Acad Sci U S A 1986;83:2496-2500.

33. Booth BW, Smith GH. Estrogen receptor-alpha and progesterone receptor are expressed in label-retaining mammary epithelial cells that divide asymmetrically and retain their template DNA strands. Breast Cancer Res 2006;8:R49.

34. Shyamala G, Chou YC, Cardiff RD, Vargis E. Effect of c-neu/ ErbB2 expression levels on estrogen receptor alpha-dependent proliferation in mammary epithelial cells: implications for breast cancer biology. Cancer Res 2006;66:10391-10398.

35. Sleeman KE, Kendrick H, Ashworth A, Isacke CM, Smalley MJ. CD24 staining of mouse mammary gland cells defines luminal epithelial, myoepithelial/basal and non-epithelial cells. Breast Cancer Res 2005;8:R7.

36. Yeh IT, Mies C. Application of immunohistochemistry to breast lesions. Arch Pathol Lab Med 2008;132:349-358.

37. Sotiriou C, Neo SY, McShane LM, Korn EL, Long PM, Jazaeri A, Martiat P, Fox SB, Harris AL, Liu ET. Breast cancer classification and prognosis based on gene expression profiles from a population-based study. Proc Natl Acad Sci U S A 2003;100:10393-10398.

38. Wu CH, van Riggelen J, Yetil A, Fan AC, Bachireddy P, Felsher DW. Cellular senescence is an important mechanism of tumor regression upon c-Myc inactivation. Proc Natl Acad Sci U S A 2007;104:13028-13033.

39. Ford CE, Ekstrom EJ, Andersson T. Wnt-5a signaling restores tamoxifen sensitivity in estrogen receptor-negative breast cancer cells. Proc Natl Acad Sci U S A 2009;106:3919-3924.

40. Xue W, Zender L, Miething C, Dickins RA, Hernando E, Krizhanovsky V, Cordon-Cardo C, Lowe SW. Senescence and tumour clearance is triggered by p53 restoration in murine liver carcinomas. Nature 2007;445:656-660.

41. Early Breast Cancer Trialists' Collaborative Group. Tamoxifen for early breast cancer: an overview of the randomised trials. Lancet 1998;351:1451-1467.

42. Hollestelle A, Elstrodt F, Nagel JH, Kallemeijn WW, Schutte M. Phosphatidylinositol-3-OH kinase or RAS pathway mutations in human breast cancer cell lines. Mol Cancer Res 2007;5:195-201.

43. Paz MF, Fraga MF, Avila S, Guo M, Pollan M, Herman JG, Esteller M. A systematic profile of DNA methylation in human cancer cell lines. Cancer Res 2003;63:1114-1121.

44. Runnebaum IB, Nagarajan M, Bowman M, Soto D, Sukumar S. Mutations in p53 as potential molecular markers for human breast cancer. Proc Natl Acad Sci U S A 1991;88:10657-10661.

Figure legends

Figure 1. Classification of breast cancer cell lines as senescent cell progenitor and immortal cell progenitor subtypes.

(**a**) Examples of SABG staining for senescence of breast cancer cell line colonies obtained after plating for low-density clonogenic conditions in 6-well plates. Breast cancer cell lines (Table S1) were plated to obtain a few hundred colonies with 1-2 weeks of cell culturing and were subjected to SABG assay, followed by counterstaining with nuclear fast red (except ZR-75-1). Pictures were slightly resized to visualize all cells of a colony. T47D, BT-474, ZR-75-1, MCF-7 and CAMA-1 generated mostly heterogeneous colonies with SABG+ and SABG- cells (shown here), but also fully negative or fully positive colonies. All other cell lines produced only SABG- colonies.

(**b**) Classification of breast cancer cell lines as senescent cell progenitor (SCP) and immortal cell progenitor (ICP) subtypes by quantification of the ability to generate senescent progeny. Cell lines with a mean of SABG+ cells superior to 10% were termed SCP, and the other cell lines as ICP. Colonies that were generated and stained as described in (**a**) were counted manually to calculate % SABG+ cells. At least 10 colonies were counted for each cell line. T47D and BT-474 senescence data were reported previously [23]. Error bars represent mean ± SD.

(**c**) SABG+ senescent cells display terminal growth arrest. Colonies were generated as described in (**a**), labeled with BrdU for 24h in the presence of freshly added culture medium, and subjected to SABG/BrdU double-staining (see Experimental Procedures). SABG+ cells are BrdU-, and vice versa. T47D-iso and BT-474-iso23 are clones derived from T47D and BT-474, respectively. Note that parental T47D and T47D-iso23 clones display similar staining features.

Figure 2. Senescent cell progenitor phenotype is associated with $p21^{Cip1}$ expression.

(**a**) Four of five senescent SCP cell lines (top four from left) generate colonies with heterogeneous expression of $p21^{Cip1}$, but not ICP cell lines. Colonies were immunostained for $p21^{Cip1}$, with hematoxylin used as counterstain. Insets: magnified views of $p21^{cip1}$+ cells.

(**b-e**) $p21^{Cip1}$ silencing inhibits the production of the terminally arrested progeny of SCP cells. T47D cells were infected with lentiviral vectors encoding $p21^{Cip1}$ shRNA or scrambled shRNA to generate T47D-p21sh and T47D-scr stable cell lines, and tested for $p21^{Cip1}$ knock-down by western blotting (**b**). Colonies were generated from respective cell lines, labeled with BrdU for 24h, immunostained for BrdU, and slightly counterstained with hematoxylin to visualize BrdU+ and negative cells. Insets: magnified views of cells (**c**). For quantification of % BrDU cells, individual colonies were manually counted. Each bar represents one colony (**d**). The silencing of $p21^{Cip1}$ caused a significant

increase in % ratios of BrdU+ cells (**e**; p = 0.0043). Mean % BrdU+ cells (± SD) were calculated from data presented in (**d**). Error bars represent mean ± SD. Tub. = Tubulin.

Figure 3. Generation of senescent cell progeny is controlled by estrogen receptor

(a) SCP cells (T47D) express nuclear ER, but their senescent progeny do not, as compared to ICP cells (MDA-MB-231), which do not express ER at all. Colonies generated from T47D and MDA-MB-231 cell lines, respectively, were co-stained for senescence by SABG and for ER expression by immunoperoxidase. MDA-MB-231 cells negative for both markers were counterstained with hematoxylin to visualize cells.

(b-d) The production of senescent progeny in SCP cells is inhibited by estrogen (E2), but enhanced by tamoxifen (4OHT) treatment. After plating in low-density clonogenic conditions, T47D cells were grown in standard cell culture medium for seven days, followed by phenol-free DMEM complemented with charcoal-treated fetal calf serum for two days, then cultivated for four days in the presence of E2, OHT, or an ethanol vehicle (control). Colonies were subjected to SABG staining (**b**). Total and SABG+ and SABG- cells were counted from 20 randomly selected colonies (**c**), and mean % SABG+ cells (± SD) were calculated (**d**). Error bars represent mean ± SD. The inhibition of senescence by E2 and its activation by OHT was statistically significant when compared to ethanol-complemented control cells (p values 0.0093, 0.0002 and <0.0001 for 10^{-9}M E2, 10^{-7} M OHT and 10^{-6} M OHT, respectively).

Figure 4. Overexpression of estrogen receptor inhibits the production of terminally arrested progeny.

ER-overexpressing (ER-5, ER-7, ER-26) and control (C-8, C-10, C-11) clones were established from T47D cells and tested for ER expression by western blotting using decreasing amounts of total proteins. Calnexin was used as loading control (**a**). Colonies were generated, labeled with BrdU for 24h and immunostained for BrdU (Fig. S3). For quantification of % BrDU cells, individual colonies were manually counted (**b**), and mean % BrdU+ cells were calculated (**c**). Error bars represent mean ± SD. Estrogen receptor overexpression caused a significant increase in % ratio of BrdU+ cells (*three ER clones *versus* three controls; p = 0.034).

Figure 5. Senescent cell progenitor and immortal cell progenitor subtypes greatly differ in their ability to differentiate into luminal and myoepithelial lineage cells.

Senescent cell progenitor and immortal cell progenitor subtype cell lines were studied by immunoperoxidase staining using CD44 and markers for luminal epithelial (CD24, CK19, ER) and myoepithelial (ASMA) lineages. Insets: magnified views of positive cells. Both subtypes have

CD44+ cells. Senescent cell progenitor cell lines produce CD44- cells, CD24+, CK19+ or ER+ luminal-like and ASMA+ myoepithelial-like cells (except ZR-75-1 for myoepithelial-like cells). Immortal cell progenitor cell lines produce only CD44+/CD24-/CK19-/ER-/ASMA- stem/progenitor cells (MDA-MB-231, MDA-MB-157, HCC-1937, BT-20), or cannot generate ER+ luminal-like and ASMA+ myoepithelial-like cells (MDA-MB-468, SK-BR-3, MDA-MB-453).

Figure 6. Typical features of senescent progenitor and immortal progenitor breast cancer cell lines.

Figure 7. Senescent and immortal cell progenitor breast cancer cell lines are phenocopies of luminal A/normal-like and basal/luminal B tumor subtypes.

(a) Unsupervised hierarchical clustering of breast tumor and cell line gene expression data from Sorlie et al [2] and Charafe-Jauffret et al [25]. Dendrogram displaying the relative organization of tumor and cell line data demonstrates that ICP cell lines cluster with basal and luminal A tumors in the same branch, except for MDA-MB-453. Senescent cell progenitor cell lines cluster with luminal A (BT-474, CAMA-1, MCF-7, T47D) and normal-like tumors (ZR-75-1). No data was available for MDA-MB-468. A dendrogram with sample IDs is provided in Supplementary Fig. S6. The "intrinsic gene set" data generated by Sorlie et al [2] was used to filter cell line data generated by Charafe-Jauffret et al [25]. A set of 175 genes was common between the two data sets. Sixty-eight tumors and 31 cell lines were subjected to pair-wise complete-linkage hierarchical clustering and distance measurements.

(b) Immortal cell progenitor cell lines, but not senescent cell progenitor cell lines, form subcutaneous tumors in "nude" mice. Chart displays tumor-free survival following subcutaneous injection of $5x10^6$ cells. Three SCP (MCF-7, T47D and CAMA-1) and three ICP (BT-20, HCC1937 and MDA-MB-453) cell lines were used in triplicate. One animal died shortly after the injection of MDA-MB-453 cells. The difference in tumorigenicity was statistically significant ($p = 0.0002$).

Table 1: Gene clusters, genetic mutations and epigenetic changes of breast cancer cell lines used in this study

Cell Line	Gene Cluster	*PIK3CA*	*CCND1*	*ERBB2*	*KRAS* *BRAF*	*TP53*	*CDKN2A*	*RB1*	*PTEN*	*NF2*
T47D	L	M/+				M/-	met			
BT474	L	M/+	A	A		M/-	RNA (-)			
ZR-75-1	L		A			+/+	met		M/-	
MCF7	L	M/+				+/+	M/-			
CAMA-1	L		A			M/-	+/+		M/+	
MDA-MB-453	L	M/+				+/+	+/+		M/?	
SK-BR-3	L			A		M/-	unmet			
BT-20	BaA	M/M					M/-		M/-	
MDA-MB-468	BaA					M/ -	+/+	M/-	M/?	
HCC1937	BaA	+/+				M/-	+/+		-/-	
MDA-MB-231	BaB				M/+ M/+	M/-	M/-			M/-
MDA-MB-157	BaB	+/+				M/-	+/+			
References	21	Sanger[1]	21	21	Sanger[1]	Sanger[1], 44	Sanger[1], 21, 43	Sanger[1]	Sanger[1], 42	Sanger[1]

A, amplified; BaA, basal A; BaB, Basal B; L, luminal; M, mutated; met, promoter methylated; unmet, promoter unmethylated; +/+, wild-type; -/-, homozygous deletion; ?, unknown. [1]From Sanger COSMIC data (http://www.sanger.ac.uk/genetics/CGP/cosmic/).

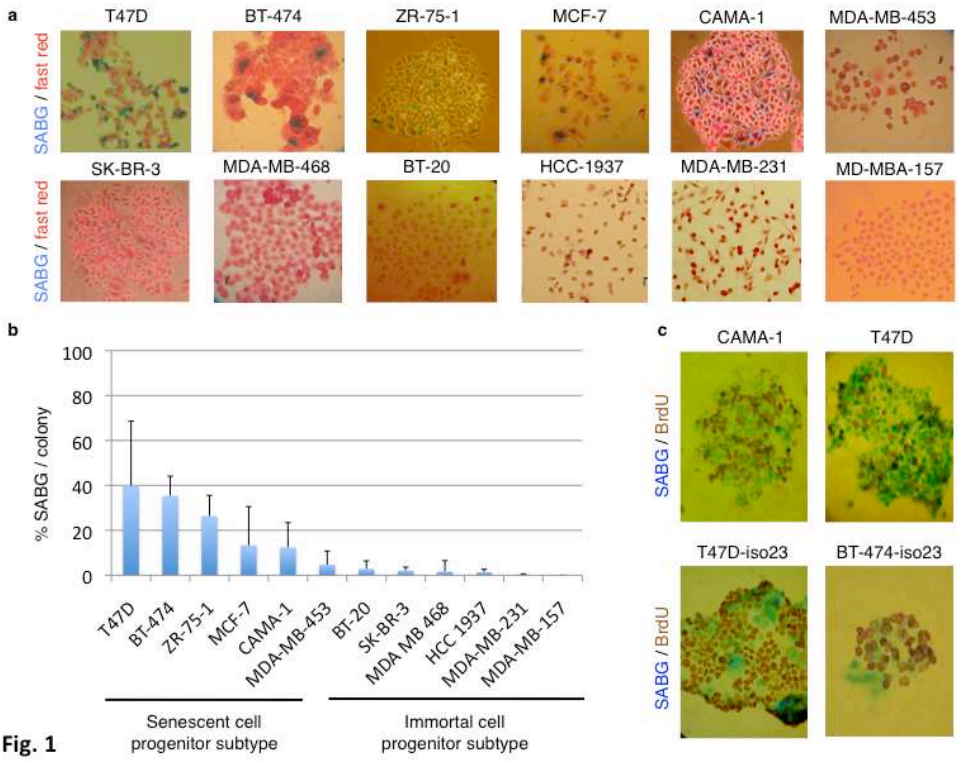

Fig. 1

278x215mm (72 x 72 DPI)

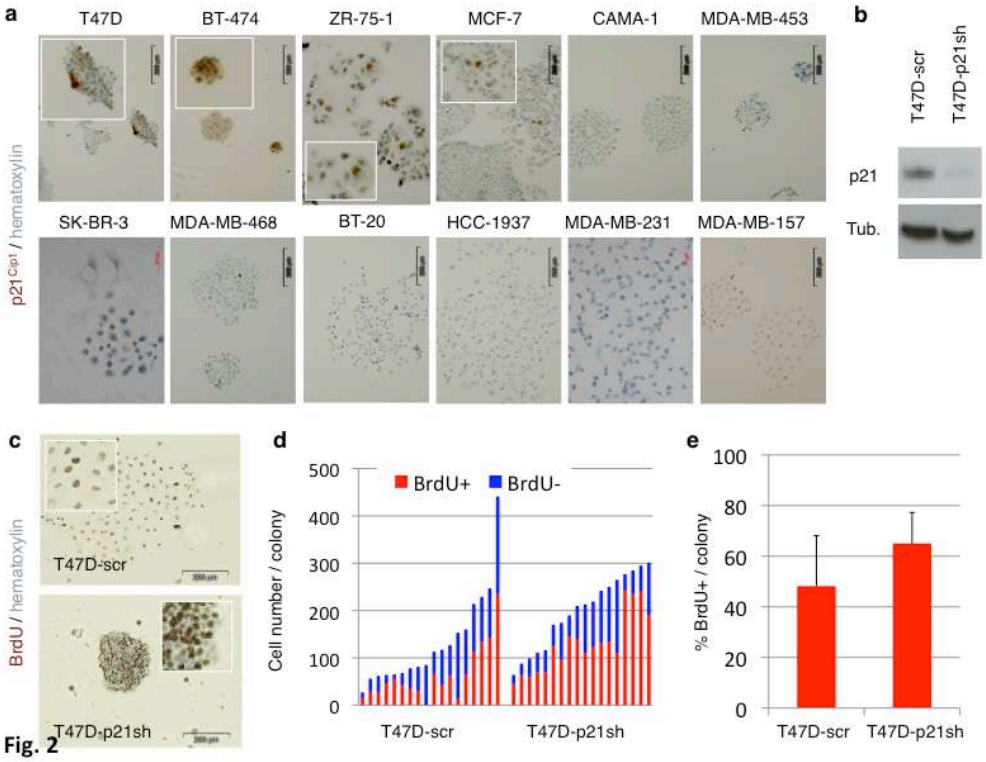

Fig. 2

278x215mm (72 x 72 DPI)

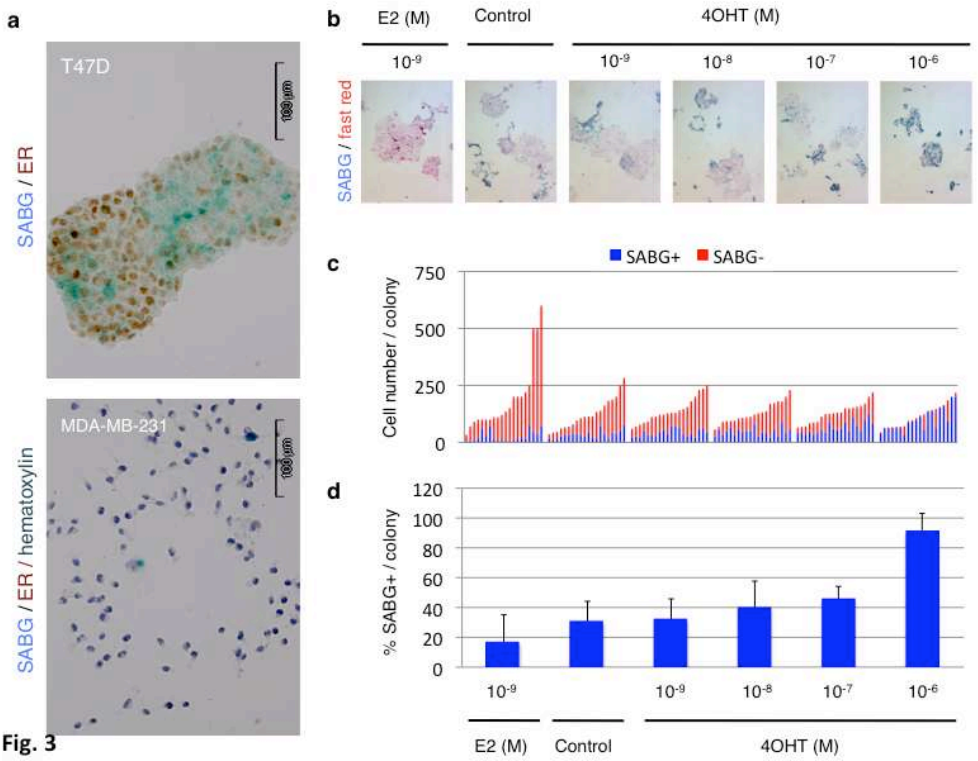

Fig. 3

278x215mm (72 x 72 DPI)

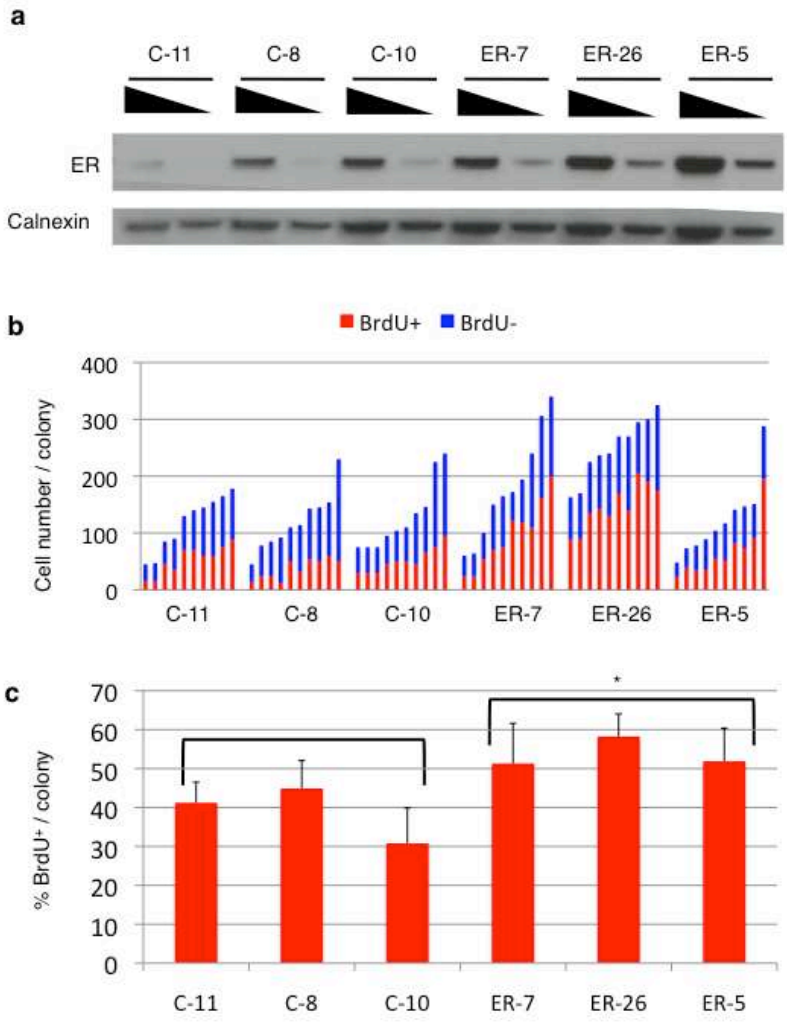

Fig. 4

215x278mm (72 x 72 DPI)

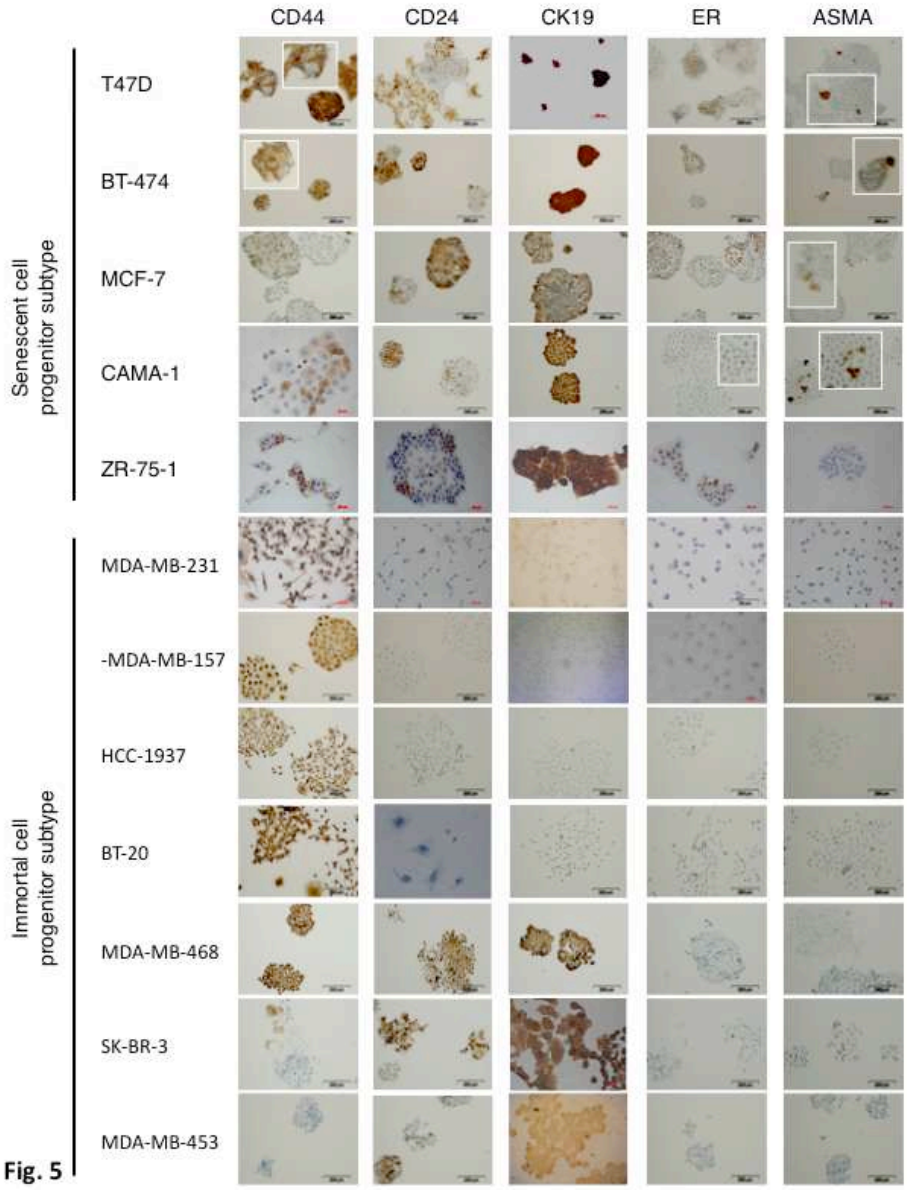

Fig. 5

215x278mm (72 x 72 DPI)

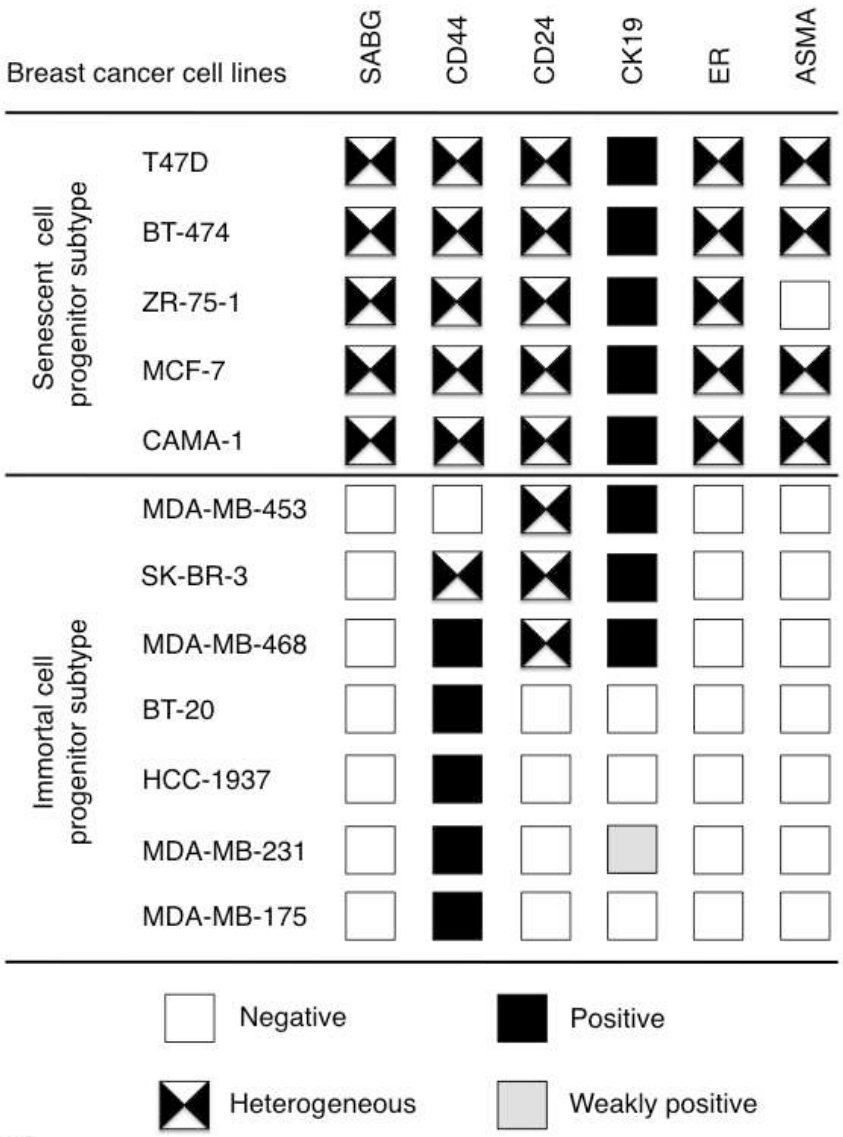

Fig. 6

215x278mm (72 x 72 DPI)

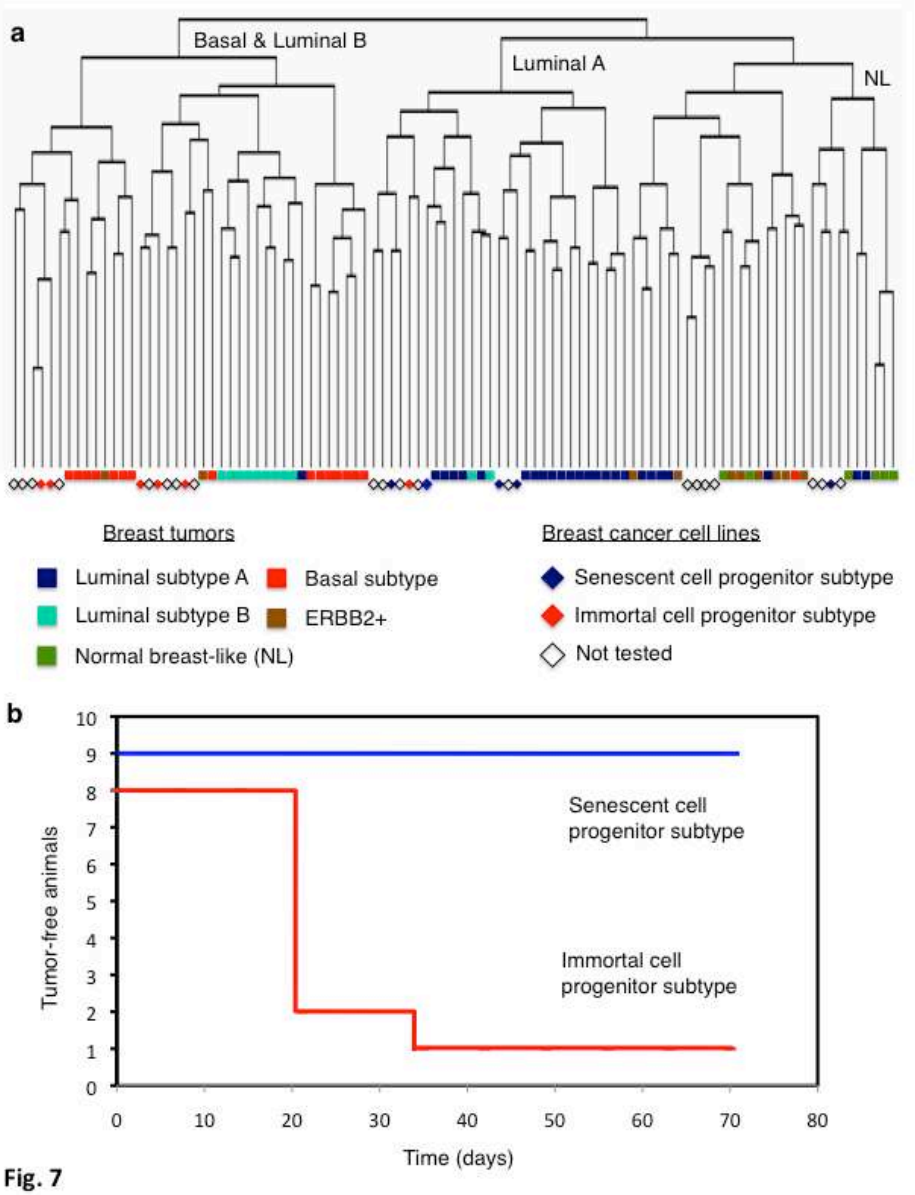

Fig. 7

215x278mm (72 x 72 DPI)

Reprogramming of replicative senescence in hepatocellular carcinoma-derived cells

Nuri Ozturk*, Esra Erdal*†, Mine Mumcuoglu*, Kamil C. Akcali*, Ozden Yalcin*‡, Serif Senturk*, Ayca Arslan-Ergul*, Bala Gur*, Isik Yulug*, Rengul Cetin-Atalay*, Cengiz Yakicier*, Tamer Yagci*, Mesut Tez§, and Mehmet Ozturk*¶‖

*Department of Molecular Biology and Genetics, Bilkent University, Bilkent, Ankara 06800, Turkey; and §Department of 5th Surgery, Numune Training and Research Hospital, Sihhiye, Ankara 06100, Turkey

Communicated by Aziz Sancar, University of North Carolina, Chapel Hill, NC, December 18, 2005 (received for review October 10, 2005)

Tumor cells have the capacity to proliferate indefinitely that is qualified as replicative immortality. This ability contrasts with the intrinsic control of the number of cell divisions in human somatic tissues by a mechanism called replicative senescence. Replicative immortality is acquired by inactivation of p53 and $p16^{INK4a}$ genes and reactivation of hTERT gene expression. It is unknown whether the cancer cell replicative immortality is reversible. Here, we show the spontaneous induction of replicative senescence in p53-and $p16^{INK4a}$-deficient hepatocellular carcinoma cells. This phenomenon is characterized with hTERT repression, telomere shortening, senescence arrest, and tumor suppression. SIP1 gene (*ZFHX1B*) is partly responsible for replicative senescence, because short hairpin RNA-mediated SIP1 inactivation released hTERT repression and rescued clonal hepatocellular carcinoma cells from senescence arrest.

immortality | liver cancer | SIP1 | telomerase | p53

Tumor cells are clonal (1), and tumorigenesis usually requires three to six independent mutations in the progeny of precancerous cells (2). For this to occur, preneoplastic somatic cells would need to breach the replicative senescence barriers. Replicative senescence is a telomere-dependent process that sets a limit to the successive rounds of cell division in human somatic cells (3). Progressive telomere shortening is observed in almost all dividing normal cells. This phenomenon is linked to the lack of efficient *hTERT* expression that is observed in most human somatic cells (3). Replicative senescence (permanent growth arrest also called M_1 stage) is believed to be initiated by a DNA damage-type signal generated by critically shortened telomeres, or by the loss of telomere integrity, leading to the activation of cell cycle checkpoint pathways involving p53, $p16^{INK4a}$, and/or retinoblastoma (pRb) proteins (4, 5). In the absence of functional p53 and $p16^{INK4a}$/pRb pathway responses, telomeres continue to shorten resulting in crisis (also called M2 stage). Cells that bypass the M_2 stage by reactivating *hTERT* expression gain the ability for indefinite cell proliferation, also called immortality (3, 4, 6). There is accumulating evidence that cancer cells undergo a similar process during carcinogenesis to acquire immortality. Telomerase activity associated with *hTERT* reexpression is observed in ≈80% of human tumors (7), and senescence controlling *p53* and $p16^{INK4A}$ genes are commonly inactivated in the majority of human cancers (8). Moreover, experimental transformation of normal human cells to tumor cells requires hTERT-mediated immortalization, as well as inactivation of *p53* and *pRb* genes (9).

Aberrant expression of hTERT, together with the loss of p53 and $p16^{INK4a}$/pRb control mechanisms, suggests that the replicative immortality is a permanent and irreversible characteristic of cancer cells. Although some cancer cells may react to extrinsic factors by a senescence-like stress response, this response is immediate, telomere-independent, and cannot be qualified as replicative senescence (10). Experimental inactivation of telomerase activity in cancer cells mostly results in cell death (11), whereas ectopic expression of p53, $p16^{INK4a}$, or pRb provokes an immediate senescence-like growth arrest or cell death (10). Thus, to date there is no experimental evidence for spontaneous reprogramming of replicative senescence in immortalized cancer cells. Using hepatocellular carcinoma (HCC)-derived Huh7 cells as a model system, here we show that cancer cells with replicative immortality are able to spontaneously generate progeny with replicative senescence. Thus, we provide preliminary evidence for the reversibility of cancer cell immortality. The replicative senescence of cancer cells shares many features with normal cell replicative senescence such as repression of *hTERT* expression, telomere shortening, and permanent growth arrest with morphological hallmarks of senescence. However, the *p53* gene is mutated, whereas $p16^{INK4a}$ promoter is hypermethylated in these cells. Thus, we show that fully malignant and tumorigenic HCC cells that display aberrant hTERT expression and lack functional *p53* and $p16^{INK4a}$ genes are able to revert from replicative immortality to replicative senescence by an intrinsic mechanism. Furthermore, we demonstrate that the *SIP1* gene, encoding a zinc-finger homeodomain transcription factor protein involved in TGF-β signaling (12, 13) and *hTERT* regulation (14), serves as a molecular switch between replicative immortality and replicative senescence fates in HCC cells.

Results

When analyzing clones from established cancer cell lines, we observed that some clones change morphology and cease proliferation at late passages with features reminiscent of cellular senescence (data not shown). We reasoned that this could be an indication for generation of progeny programmed for replicative senescence. We surveyed a panel of HCC and breast carcinoma cell lines and hTERT-immortalized human mammary epithelial cells (hTERT-HME). Plated at low clonogenic density, cells were maintained in culture until they performed 6–10 population doublings (PD), and tested for senescence-associated β-galactosidase (SABG) activity (15). Different cancer cell lines generated progeny with greatly contrasting SABG staining patterns. The first group, represented here by HCC-derived Huh7 and breast cancer-derived T-47D and BT-474 cell lines, generated heterogeneously staining colonies. Cells of some colonies were mostly positive for SABG, but others displayed significantly diminished or complete lack of staining (Fig. 1*A*). The second group, represented by HCC-derived Hep3B and Mahlavu, and hTERT-HME generated only SABG-negative colonies (Fig. 1*B*). Manual counting of randomly selected colonies demonstrated that mean SABG-labeling indexes for Huh7,

Conflict of interest statement: No conflicts declared.

Abbreviations: HCC, hepatocellular carcinoma; PD, population doubling; SABG, senescence-associated β-galactosidase; shRNA, short hairpin RNA.

†Present address: Department of Medical Biology and Genetics, Faculty of Medicine, Dokuz Eylul University, 35210 Izmir, Turkey.

‡Present address: Swiss Institute for Experimental Cancer Research, Ch. des Boveresses 155, CH-1066 Epalinges, Lausanne, Switzerland.

¶To whom correspondence should be addressed. E-mail: ozturk@fen.bilkent.edu.tr.

www.pnas.org/cgi/doi/10.1073/pnas.0510877103

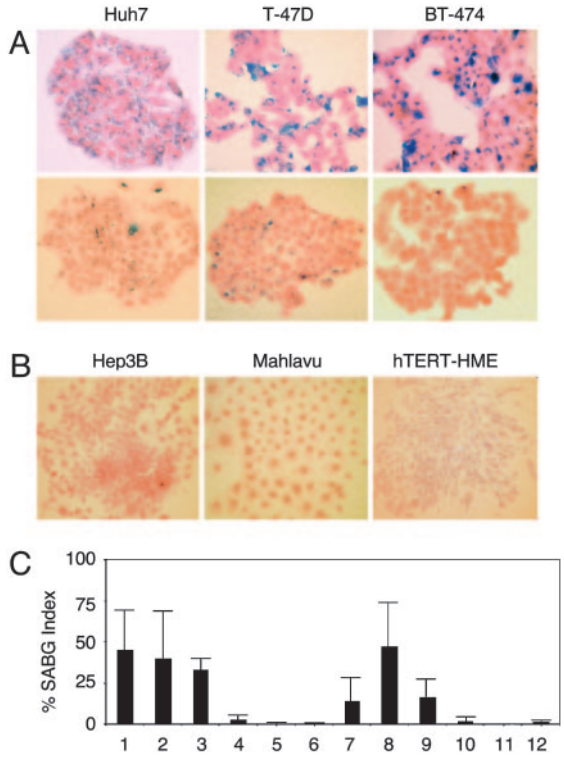

Fig. 1. Established human cancer cell lines generate senescence-associated β-galactosidase (SABG)-expressing progeny. (*A*) Representative pictures of HCC (Huh7) and breast cancer (T-47D and BT-474) cell lines that generate both SABG-positive (*Upper*) and SABG-negative (*Lower*) colonies. (*B*) Representative pictures of HCC (Hep3B and Mahlavu) and telomerase-immortalized mammary epithelial (hTERT-HME) cell lines that generate only SABG-negative colonies. Cells were plated at clonogenic density to generate colonies with 6–10 population doublings, and stained for SABG activity (blue), followed by eosin counterstaining (red). (*C*) Quantification of SABG-positive cells in colonies. Randomly selected colonies ($n \geq 10$) obtained from parental (lanes 1–6) cell lines and expanded clones (lanes 7–12) were counted to calculate the average % SABG positive cells per colony (% SABG index). Lanes 1–6 designate Huh7, T-47D, BT-474, Hep3B, Mahlavu, and hTERT-HME, respectively. Lanes 7–9 are Huh7-derived C1, C3, and C11 clones, and lanes 10–12 are Hep3B-derived 3B-C6, 3B-C11, and 3B-C13 clones. Error bars indicate SD.

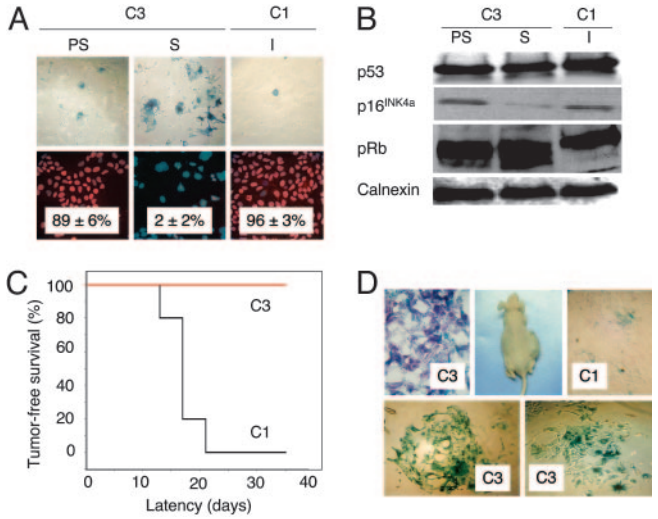

Fig. 2. p53-and p16^{INK4a}-deficient Huh7 cells generate progeny that undergo *in vitro* and *in vivo* replicative senescence resulting in loss of tumorigenicity. (*A*) Huh7-derived clones C3 and C1 were tested for replicative senescence arrest by SABG and BrdUrd staining at different passages. Presenescent C3 and immortal C1 cells display low SABG staining (*Upper*) and high BrdUrd incorporation (*Lower*), whereas senescent C3 cells are fully positive for SABG (*Upper*) and fail to incorporate BrdUrd into DNA after mitogenic stimuli (*Lower*). (*B*) p53 and p16^{INK4a} protein levels show no increase in senescent C3 cells, compared to presenescent C3 and immortal C1 cells, but senescent C3 cells display partial hypophosphorylation of pRb. Calnexin was used as a loading control. Proteins were tested by Western blotting. PS, presenescent (PD 57); S, senescent (PD 80); I, immortal (PD 179). (*C*) C1 cells (black line) were fully tumorigenic, but C3 cells (red line) were not in *nude* mice. (*D*) C1 tumors displayed low SABG staining (*Upper Right*), whereas implanted C3 cells remaining at the injection site are fully positive for SABG *in situ* (*Upper Left*), as well as after short-term *in vitro* selection (*Lower*). Animals were injected with presenescent C3 (PD 59) and immortal C1 (PD 119) cells, and tumors and nontumorigenic cell samples were collected at day 35 and analyzed.

T-47D and BT-474 progenies were 45 ± 23%, 40 ± 29%, and 33 ± 7%, respectively (Fig. 1*C*, lanes 1–3). In contrast, Hep3B, Mahlavu, and hTERT-HME progenies displayed <3 ± 3% mean SABG-labeling indexes (Fig. 1*C*, lanes 4–6). Clones from representative cell lines were expanded and subjected to the same analysis. SABG-staining patterns of all clones tested were closely similar to the patterns of their respective parental cell lines. For example, mean SABG staining indexes of Huh7-derived clones were 14 ± 15%, 47 ± 27%, and 17 ± 11% (Fig. 1*C*, lanes 7–9), whereas Hep3B-derived clones generated <2 ± 3% SABG-positive progenies (Fig. 1*C*, lanes 10–12). We speculated that the first group of cell lines comprised progenies in different stages of replicative senescence process at the time of analysis, whereas the second group of cell lines were composed mostly of immortal cells. The results obtained with the first group were unexpected. These cell lines have been established >20 years ago (16–18) and expanded in culture over many years, with PD well beyond the known senescence barriers for normal human cells (3), but they were still capable of generating presumably senescent progeny.

The study of a potentially active replicative senescence program in the progeny of immortal cancer cell lines requires the long-term follow up of single cell-derived clones. To this end, we chose to focus our investigations on Huh7 cell line. We expanded different Huh7-derived clones in long-term culture and examined their potential to undergo replicative senescence. Some clones performed >100 PD in culture with stable proliferation rates and heterogeneous SABG staining, whereas others sustained a limited number of PD, then entered a growth arrest phase with full SABG staining patterns. For example, C3 clone performed only 80 PD, whereas C1 clone replicated >150 PD. Permanently arrested C3 cells (PD 80) displayed enlarged size, flattened shape, and fully positive SABG staining, whereas early passage C3 (PD 57) and C1 (PD 179) cells displayed normal morphology with heterogeneous SABG staining (Fig. 2*A Upper*). Normal human cells at replicative senescence (M_1) are refractory to mitotic stimulation and display <5% BrdUrd index (19). Growth-arrested C3 cells displayed very low BrdUrd staining (2 ± 2%), in contrast to early passage C3 and late passage C1 cells, which exhibited 89 ± 6%, and 96 ± 3% BrdUrd indexes, respectively (Fig. 2*A Lower*). Senescent C3 cells remained growth arrested, but alive when maintained in culture for at least 3 months, with no emergence of immortal clones (data not shown).

Biological mechanisms of replicative senescence observed here are of particular interest, because senescence-regulatory *p53* is inactivated (20–22) and *p16^{INK4a}* promoter is hypermethylated (23) in Huh7 cells. Accordingly, there was no change in p53 levels, whereas the low level p16^{INK4a} expression did not increase, but decreased in senescent C3 (PD 80) cells, when compared to presenescent C3 (PD 57) or immortal C1 (PD 179) cells. Retinoblastoma protein (pRb) displayed partial hypophos-

phorylation in senescent C3 cells, apparently in a p53- and $p16^{INK4a}$-independent manner (Fig. 2*B*). Cyclin E and A levels were also decreased, but $p21^{cip1}$ levels were elevated in both presenescent and senescent C3 cells (Fig. 5*A*, which is published as supporting information on the PNAS web site). Cyclin D1, CDK4, and CDK2 protein levels (Fig. 5*A*) and $p14^{ARF}$ transcript levels (Fig. 5*B*) did not change.

Cancer cell senescence that we characterized here shared many features with normal cell replicative senescence (3), except that it was not accompanied with wild-type *p53* or *p16*^{INK4a} induction. However, *in vivo* relevance of the replicative senescence observed in cell culture is debated (6). Therefore, we compared *in vivo* replicative potentials of C3 (PD 59) and C1 (PD 119) cells in CD-1 *nude* mice. C3 cells did not form visible tumors, whereas C1 cells were fully tumorigenic in the same set of animals (Fig. 2*C*), like parental Huh7 cells (data not shown; ref. 24). C1 tumors collected at day 35 displayed scattered but low-rate SABG-positive staining, but remnant C3 cell masses collected from their injection sites were fully SABG-positive (Fig. 2*D Upper*). For confirmation, these remnants were removed from two different animals, passaged twice in cell culture for selection, and examined. Nearly all cells displayed senescence features including enlarged size, flattened shape, and highly positive SABG staining (Fig. 2*D Lower*). We concluded that loss of C3 tumorigenicity was due to replicative senescence *in vivo*.

Replicative senescence, also called telomere-dependent senescence is associated with progressive telomere shortening due to inefficient telomerase activity (3). When compared to parental Huh7 cells, presenescent C3 cells at PD 57 had telomeres that have already been shortened to ≈7 kbp from ≈12 kbp. These cells eroded their telomeres to <5 kbp at the onset of senescence. In contrast, immortal C1 clone (PD 179) telomeres did not shorten (Fig. 3*A*). These observations showed a perfect correlation with telomerase activity and *hTERT* expression. Immortal C1 cells displayed robust telomerase activity, whereas both presenescent and senescent C3 cells had no detectable telomerase activity (Fig. 3*B*). Accordingly, the expression of *hTERT* gene was high in C1, but barely detectable in C3 cells (Fig. 3*C*). Thus, senescence observed with C3 cells was characterized with the loss of *hTERT* expression and telomerase activity, associated with telomere shortening.

Mechanisms of *hTERT* expression are presently unclear, but several genes including *SIP1*, *hSIR2*, *c-myc*, *Mad1*, *Menin*, *Rak*, and *Brit1* have been implicated (14, 25). Therefore, we analyzed their expression in C1 and C3 clones. All tested genes, except *SIP1*, were expressed at similar levels in both C1 and C3 clones, independent of *hTERT* expression (Fig. 6, which is published as supporting information on the PNAS web site). SIP1 transcripts were undetectable in C1 cells, but elevated in C3 cells, moderately in presenescent, but strongly in senescent stages (Fig. 3*C*). We verified these findings with another Huh7-derived clone (G12) that displayed replicative senescence resulting in permanent cell proliferation arrest. Like C3, presenescent G12 cells that displayed low SABG staining with high BrdUrd index (98 ± 1%), became fully positive for SABG, and nearly negative for BrdUrd (3 ± 2%) at the onset of senescence (Fig. 7, which is published as supporting information on the PNAS web site). Presenescent G12 cells displayed only a weak *hTERT* repression associated with a slight increase in *SIP1* expression, whereas SIP1 was strongly elevated in hTERT-negative senescent cells (Fig. 3*D*). Thus, there was a close correlation between *SIP1* expression and *hTERT* repression in all Huh7 clones tested. The analysis of *SIP1* and *hTERT* expression in primary HCCs and their corresponding nontumor liver tissues confirmed this relationship. SIP1 transcript levels were high, but *hTERT* expression was low in nontumor liver tissues, whereas respective HCC tumors displayed diminished *SIP1* expression associated with up-regulated *hTERT* expression (Fig. 3*E*).

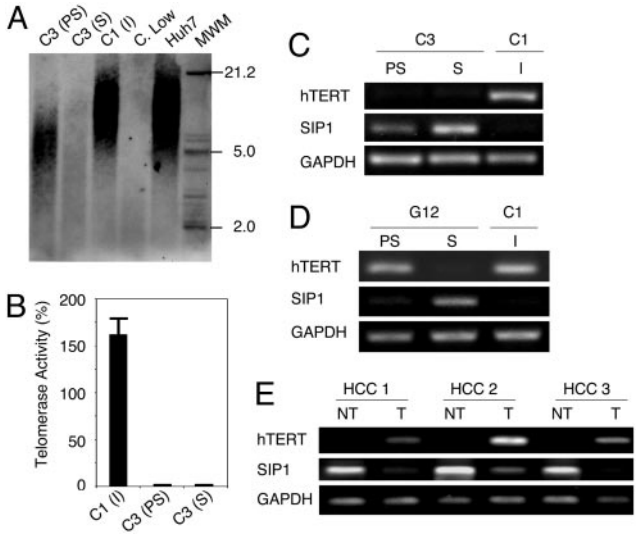

Fig. 3. C3 clonal cells undergo telomere-dependent replicative senescence associated with SIP1 expression and hTERT repression. SIP1 expression is lost, whereas hTERT is induced in primary HCC tumors. (*A*) Genomic DNAs from parental Huh7 and immortal C1 cells display long telomeres, whereas C3 telomeres are progressively shortened in presenescent and senescent stages, respectively. Equal amounts of genomic DNAs were blotted with a telomere repeat probe. C. Low, short telomere control DNA. (*B*) Presenescent and senescent C3 cells have lost telomerase activity, as measured by TRAP assay. Telomerase activity was shown as % value of test samples (± SD) compared to ''high positive'' control sample. (*C*) hTERT expression as tested by RT-PCR was high in immortal C1, but decreased to weakly detectable levels in C3 cells. Inversely, SIP1 expression tested by RT-PCR was undetectable in C1 cells, but showed a progressive increase in presenescent and senescent C3 cells. (*D*) Inverse relationship between SIP1 and hTERT expression was confirmed with another senescence-programmed Huh7 clone named G12 (for SABG and BrdUrd assays, see Fig. 7). hTERT expression in G12 showed a slight decrease in presenescent stage, followed by a loss at the onset of senescence. Inversely, the expression of SIP1 gene was weakly positive in presenescent G12, but highly positive in senescent G12 cells. C1 was used as control. PS, presenescent; S, senescent; I, immortal. (*E*) Negative correlation between hTERT and SIP1 expression in primary tumors (T) and nontumor liver tissues (NT).

The *SIP1* gene (Zinc finger homeobox 1B; *ZFHX1B*) encodes a transcriptional repressor protein that interacts with SMAD proteins of the TGF-β signaling pathway and CtBP corepressor (12, 13). This gene has recently been implicated in TGF-β-dependent regulation of *hTERT* expression in breast cancer cells (14). Our observations implicated *SIP1* gene as a candidate regulator of replicative senescence in HCC cells. To investigate whether *SIP1* expression constitutes a protective barrier against hTERT expression and senescence bypass, we constructed SIP1 short hairpin RNA (shRNA)-expressing plasmids, based on a reported effective SIP1 siRNA sequence (14). SIP1 shRNA was expressed by using either G-418-resistance plasmid pSuper.retro.neo+GFP or puromycin-resistance plasmid pSUPER.puro (see *shRNA* in *Methods*). Presenescent C3 cells at PD 75 were used for transfections, 3–4 weeks before expected senescence arrest stage. pSuper.retro.neo+GFP-based SIP1 shRNA suppressed the accumulation in SIP1 when expressed transiently (Fig. 4*A*, day 5). This resulted in a weak increase in *hTERT* expression. Transfected cells were maintained in culture in the presence of 500 μg/ml G-418 and observed for 30 days. At this period, C3 cells transfected with a control plasmid reached senescence-arrested stage with further up-regulation of *SIP1* expression (Fig. 4*A*, day 30) and resistance to BrdUrd incorporation after mitogenic stimuli (BrdUrd index = 3 ± 1%; Fig. 4*B Upper Left*). In sharp contrast, SIP1 shRNA-transfected cells lost

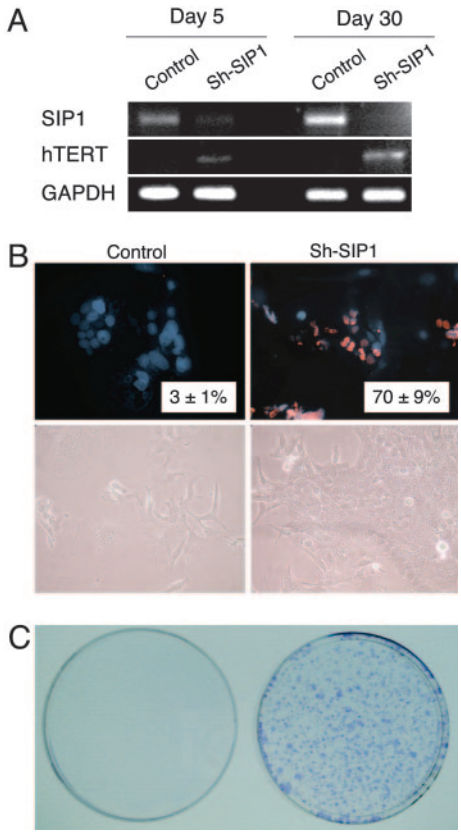

Fig. 4. ShRNA-mediated down-regulation of endogeneous SIP1 transcripts releases hTERT repression and rescues C3 cells from senescence arrest. (*A*) At day 5 after transfection, SIP1 shRNA-transfected cells (Sh-SIP1) show decreased expression of SIP1 and weak up-regulation of hTERT expression. At day 30, the expression of SIP1 is lost completely, and hTERT expression is stronger. (*B*) Cells transfected with empty vector (Control) are senescence-arrested as evidenced by resistance to BrdUrd incorporation (*Upper Left*) and morphological changes (*Lower Left*), but cells transfected with SIP1 shRNA vector (Sh-SIP1) escaped senescence arrest as indicated by high BrdUrd index (*Upper Right*) and proliferating cell clusters (*Lower Right*). (*C*) Colony-forming assay shows that C3 cells formed large number of colonies following puromycin selection after transfection with a puromycin-resistant SIP1-shRNA-expressing plasmid (*Right*), whereas cells transfected with empty vector did not survive (*Left*). SIP1 shRNA was expressed by using either G-418-resistance plasmid pSuper.retro.neo+GFP (*A* and *B*) or puromycin-resistance plasmid pSUPER. puro (*C*). Presenescent C3 cells at PD 75 were transfected with either SIP1 shRNA-expressing or empty plasmid vectors, maintained in culture in the presence of appropriate selection media and tested at days 5 (*A*) and 30 (*A–C*).

SIP1 expression and up-regulated *hTERT* transcripts (Fig. 4*A*, day 30). Furthermore, *SIP1*-inactivated cells escaped senescence, as evidenced with 70 ± 9% BrdUrd index (Fig. 4*B Upper Right*). Morphologically, SIP1 shRNA-transfected cells formed proliferating clusters, whereas cells transfected with control plasmid displayed hallmarks of senescence such as scattering, enlargement, and multiple nuclei (Fig. 4*B Lower*). Twelve independent clones were selected from SIP1 shRNA-transfected C3 cells. All but one of these clones have performed so far >15 PD beyond the expected senescence barrier (data not shown). As an additional confirmatory assay, C3 cells were transfected with the puromycin-selectable *pSUPER.puro-based* SIP1 shRNA vector and subjected to puromycin selection. SIP1 shRNA-transfected cells survived and formed large number of colonies after 30 days of puromycin selection. In contrast, no surviving colony was obtained from cells transfected with the control plasmid, as expected (Fig. 4*C*).

Discussion

Our observations provide experimental evidence for the generation of senescence-arrested clones from immortal HCC and breast cancer cell lines. Detailed analysis of clones from HCC-derived Huh7 cell line further indicates that what we observe is a replicative senescence, but not a stress-induced premature senescence-like arrest. Clonal C3 cells displayed telomerase repression, progressive telomere shortening, and permanent growth arrest after ≈80 PD with senescence-associated morphological changes and positive SABG staining. Similar changes have also been observed with G12, another independently derived clone. Thus, we demonstrate that immortal cancer cells have the intrinsic ability to reprogram the replicative senescence. As expected, this shift in cell fate results in a complete loss of tumorigenicity. The replicative senescence arrest that we identified with clonal C3 cells was not accompanied with the induction of the *p53*, $p16^{INK4a}$, $p14^{ARF}$, or $p21^{Cip1}$ gene. The nonparticipation of *p53* and $p16^{INK4a}$ to the senescence arrest described here was expected, in the light of published observations showing that Huh7 cells express a mutant p53 protein (20–22) and they are deficient in $p16^{INK4a}$ expression (23). Although the levels of $p21^{Cip1}$ protein displayed a slight increase in C3 cells, this was not related to senescence arrest, as early passage proliferating C3 cells also displayed this slight increase (Fig. 5). The early loss of *hTERT* expression in this clone could contribute to early $p21^{Cip1}$ up-regulation, because hTERT is known to down-regulate $p21^{Cip1}$ promoter activity (26). *p53*, $p16^{INK4a}$, $p14^{ARF}$, and $p21^{Cip1}$ form a group of replicative senescence-related cell cycle checkpoint genes. The lack of induction of these genes in senescence-arrested C3 cells clearly indicates that there are additional genes involved in senescence arrest in these tumor-derived cells.

The loss of *hTERT* expression in senescence programmed clones prompted us to analyze the expression of genes that have been implicated in *hTERT* regulation. Among seven candidate genes studied, only one, the *SIP1* gene, displayed a differential expression between immortal and senescence-programmed clones. This gene has been identified as a mediator of TGF-β-regulated repression of *hTERT* expression in a breast cancer cell line, although it was not effective in an osteosarcoma cell line (14). In our studies, SIP1 was not expressed in immortal hTERT-expressing C1 clone, but expressed in senescence-programmed hTERT-repressed C3 and G12 clones (Fig. 3 *B* and *C*). Furthermore, experimental depletion of SIP1 transcripts resulted in hTERT up-regulation in C3 clonal cells (Fig. 4*A*). This effect has been confirmed by using SKHep1, another HCC cell line (data not shown). Thus, we demonstrate that the *SIP1* gene acts as an hTERT repressor in HCC cells. More importantly, we also showed the bypass of senescence arrest after functional inactivation of SIP expression by shRNA in senescence-programmed C3 clonal cells. In contrast to C3 cells transfected with a control plasmid, SIP1 shRNA-treated cells displayed continued proliferation beyond PD ≈80 as evidenced by 70% BrdUrd incorporation index, and formation of large number of colonies. Selected shRNA-transfected clones from these experiments have already performed >15 PD beyond the senescence barrier. Thus, our findings indicate that the functional inactivation of *SIP1* in senescence-programmed cancer cells is sufficient to bypass senescent arrest.

SIP1 is a zinc finger and homeodomain containing transcription factor that exerts a repressive activity by binding to CACCT sequences in regulatory elements of target genes (12, 27). The *SIP1* gene is expressed at high levels in almost all human somatic tissues tested, including liver (28). Therefore, we also performed comparative analysis of hTERT and *SIP1* expression in nontumor liver and primary HCC tissues. *SIP1*

was strongly positive in nontumor liver samples, but its expression was significantly decreased in corresponding HCC samples. Inversely, *hTERT* expression was negative or low in nontumor liver samples, but highly positive in HCC tumors (Fig. 3*E*). We also detected complete loss of *SIP1* expression in 5 of 14 (36%) of HCC cell lines (data not shown). Taken together with *in vitro* studies, these observations strongly suggest that *SIP1* acts as a tumor suppressor gene in HCC. Although SIP1, as a repressor of *E-cadherin* promoter, has been suggested to be a promoter of invasion in malignant epithelial tumors (29), a tumor suppressive activity by the repression of *hTERT* and inhibition of senescence arrest is not precluded.

Hepatocellular carcinoma is one of the most common cancers worldwide. Liver cirrhosis is the major etiology of this tumor with limited therapeutic options (30, 31). Telomere shortening and senescence play a major role in liver cirrhosis, from which the neoplastic HCC cells emerge with high rates of telomerase reactivation (32). Furthermore, *p53* and $p16^{INK4a}$ are the most frequently inactivated genes in these tumors. This fact enhances the importance of our findings for potential therapeutic applications of replicative senescence programming in HCC.

Methods

Tissues, Cells, and Clones. Snap-frozen HCC and nontumor liver tissues were used. HCC and breast cancer cell lines T-47D (ATCC) and BT-474 (ATCC) were cultivated as described (33). hTERT-HME cells (Clontech) were cultivated in DMEM/Ham's F-12 (Biochrom) containing insulin (3.5 μg/ml), EGF (0.1 ng/ml), hydrocortison (0.5 μg/ml), and 10% FBS (Biochrom). Huh7- and Hep3B-derived isogenic clones were obtained by either G-418 selection after transfection with neomycin-resistance pcDNA3.1 (Invitrogen) or pEGFP-N2 (Clontech) plasmids, or by low-density cloning. Huh7-derived isogenic clones C1 and C3 were obtained with pCDNA3.1, and G12 with pEGFP-N2. Huh7-derived C11, and Hep3B-derived 3B-C6, 3B-C11 and 3B-C13 were obtained by low-density cloning. Cells transfected with calcium phosphate/DNA-precipitation method were cultivated in the presence of geneticin G-418 sulfate (500 μg/ml; GIBCO), and isolated single cell-derived colonies were picked up by using cloning cylinders and expanded in the presence of 200 μg/ml geneticin G-418 sulfate. For low-density cloning, cells were plated at 30 cells per cm^2 and single-cell derived colonies were expanded. Initial cell stocks were prepared when total number of cells became 1–3 $\times$ 10^7, and the number of accumulated population doubling (PD) at this stage was estimated to be 24, assuming that the progeny of the initial colony-forming cells performed at least 24 successive cell divisions until that step. Subsequent passages were performed every 4–7 days, and the number of additional PD was determined by using a described protocol (34).

Low-Density Clonogenic Assay. Cells (30–50 per cm^2) were plated in six-well plates and grown 1–3 weeks to obtain isolated colonies formed with 100–1,000 cells. The medium was changed every 4 days, and colonies were subjected to SABG staining (see below).

***In Vivo* Studies.** Cells were injected s.c. into CD-1 *nude* mice (Charles River Breeding Laboratory). Tumors and nontumorigenic cells at the injection sites were collected at day 35 and analyzed directly or after *in vitro* culture by SABG assay (see below). These experiments have been approved by the Bilkent University Animal Ethics Committee.

SABG Assay. SABG activity was detected by using a described protocol (15). After DAPI or eosin counterstaining, SABG-positive and negative cells were identified and counted.

BrdUrd Incorporation Assay. Subconfluent cells were labeled with BrdUrd for 24 h in freshly added culture medium and tested as described (33), using anti-BrdUrd antibody (Dako) followed by tetramethylrhodamine B isothiocyanate-labeled secondary antibody (Sigma). DAPI (Sigma) was used for counterstaining.

Immunoblotting. Antibodies against cyclin D1, CDK4, CDK2, $p21^{Cip1}$, pRb (all from Santa Cruz Biotechnology), cyclin E (Transduction), cyclin A (Abcam), $p16^{INK4a}$ (Abcam), p53 (clone 6B10; ref. 35), and calnexin (Sigma) were used for immunoblotting as described (33).

RT-PCR. RT-PCR expression analysis was performed as described (33), using primers listed in Table 1, which is published as supporting information on the PNAS web site.

TRAP and Telomere Length Assays. Telomerase activity and telomere length assays were performed by using Telo*TAGGG* Telomerase PCR $ELISA^{PLUS}$ and Telo*TAGGG* Telomere Length Assay (Roche Diagnostics), following kit instructions.

shRNA. SIP1-directed shRNA was designed according to a previously described effective siRNA sequence (14) using the pSUPER RNAi system instructions (Oligoengine) and cloned into pSuper.retro.neo+GFP and pSUPER.puro (Oligoengine), respectively. SIP1 shRNA-encoding sequence was inserted by using 5′-GATCCCCCTGCCATCTGATCCGCTCTTTCAAGAGAAGAGCGGATCAGATGGCAGTTTTTA-3′ (sense) and 5′-AGCTTAAAAACTGCCATCTGATCCGCTCTTCTCTTGAAAG AGCGGATCAG ATGGCAGGGG-3′ (antisense) oligonucleotides.

The integrity of the inserted shRNA-coding sequence has been confirmed by nucleic acid sequencing of recombinant plasmids. Clone C3 cells were transfected with calcium phosphate precipitation method, using either pSuper.retro.neo+GFP-based or pSUPER.puro-based SIP1 shRNA expression plasmid, and cells were maintained in the presence of 500 μg/ml geneticin G-418 sulfate and 2 μg/ml puromycin (Sigma), respectively. Empty vectors were used as control. Media changed every 3 days, and cells were tested at days 5 and 30.

We thank E. Galun, G. Hotamisligil, F. Saatcioglu, and A. Sancar for reading the manuscript and helpful suggestions. This work was supported by Grant SBAG-2774/104S045 from the Scientific and Technological Research Council of Turkey (TUBITAK) and funds from Bilkent University and Turkish Academy of Sciences (TUBA).

1. Nowell, P. C. (1976) *Science* **194,** 23–28.
2. Vogelstein, B. & Kinzler, K. W. (1993) *Trends. Genet.* **9,** 138–141.
3. Shay, J. W. & Wright, W. E. (2005) *Carcinogenesis* **26,** 867–874.
4. Campisi, J. (2005) *Cell* **120,** 513–522.
5. Dimri, G. P. (2005) *Cancer Cell* **7,** 505–512.
6. Ben-Porath, I. & Weinberg, R. A. (2004) *J. Clin. Invest.* **113,** 8–13.
7. Shay, J. W. & Bacchetti, S. (1997) *Eur. J. Cancer* **33,** 787–791.
8. Sherr, C. J. & McCormick, F. (2002) *Cancer Cell* **2,** 103–112.
9. Boehm, J. S. & Hahn, W. C. (2005) *Curr. Opin. Genet. Dev.* **15,** 13–17.
10. Roninson, I. B. (2003) *Cancer Res.* **63,** 2705–2715.
11. Shay, J. W. & Roninson, I. B. (2004) *Oncogene* **23,** 2919–2933.
12. Verschueren, K., Remacle, J. E., Collart, C., Kraft, H., Baker, B. S., Tylzanowski, P., Nelles, L., Wuytens, G., Su, M. T., Bodmer, R., *et al.* (1999) *J. Biol. Chem.* **274,** 20489–20498.
13. Postigo, A. A., Depp, J. L., Taylor, J. J. & Kroll, K. L. (2003) *EMBO J.* **22,** 2453–2462.
14. Lin, S. Y. & Elledge, S. J. (2003) *Cell* **113,** 881–889.
15. Dimri, G. P., Lee, X., Basile, G., Acosta, M., Scott, G., Roskelley, C., Medrano, E. E., Linskens, M., Rubelj, I., Pereira-Smith, O., *et al.* (1995) *Proc. Natl. Acad. Sci. USA* **92,** 9363–9367.
16. Lasfargues, E. Y., Coutinho, W. G. & Redfield, E. S. (1978) *J. Natl. Cancer Inst.* **61,** 967–978.

17. Keydar, I., Chen, L., Karby, S., Weiss, F. R., Delarea, J., Radu, M., Chaitcik, S. & Brenner, H. J. (1979) *Eur. J. Cancer* **15,** 659–670.
18. Nakabayashi, H., Taketa, K., Miyano, K., Yamane, T. & Sato, J. (1982) *Cancer Res.* **42,** 3858–3863.
19. Wei, W. & Sedivy, J. M. (1999) *Exp. Cell Res.* **253,** 519–522.
20. Bressac, B., Galvin, K. M., Liang, T. J., Isselbacher, K. J., Wands, J. R. & Ozturk, M. (1990) *Proc. Natl. Acad. Sci. USA* **87,** 1973–1977.
21. Volkmann, M., Hofmann, W. J., Muller, M., Rath, U., Otto, G., Zentgraf, H. & Galle, P. R. (1994) *Oncogene* **9,** 195–204.
22. Kubica, S., Trauwein, C., Niehof, M. & Manns, M. (1997) *Hepatology* **25,** 867–873.
23. Roncalli, M., Bianchi, P., Bruni, B., Laghi, L., Destro, A., Di Gioia, S., Gennari, L., Tommasini, M., Malesci, A. & Coggi, G. (2002) *Hepatology* **36,** 427–432.
24. Kaneko, S., Hallenbeck, P., Kotani, T., Nakabayashi, H., McGarrity, G., Tamaoki, T., Anderson, W. F. & Chiang, Y. L. (1995) *Cancer Res.* **55,** 5283–5287.
25. Wang, J., Xie, L. Y., Allan, S., Beach, D. & Hannon, G. J. (1998) *Genes Dev.* **12,** 1769–1774.
26. Young, J. I., Sedivy, J. M. & Smith, J. R. (2003) *J. Biol. Chem.* **278,** 19904–19908.
27. Remacle, J. E., Kraft, H., Lerchner, W., Wuytens, G., Collart, C., Verschueren, K., Smith, J. C. & Huylebroeck, D. (1999) *EMBO J.* **18,** 5073–5084.
28. Cacheux, V., Dastot-Le Moal, F., Kaariainen, H., Bondurand, N., Rintala, R., Boissier, B., Wilson, M., Mowat, D. & Goossens, M. (2001) *Hum. Mol. Genet.* **10,** 1503–1510.
29. Comijn, J., Berx, G., Vermassen, P., Verschueren, K., van Grunsven, L., Bruyneel, E., Mareel, M., Huylebroeck, D. & van Roy, F. (2001) *Mol. Cell* **7,** 1267–1278.
30. Thorgeirsson, S. S. & Grisham, J. W. (2002) *Nat. Genet.* **31,** 339–346.
31. Bruix, J., Boix, L., Sala, M. & Llovet, J. M. (2004) *Cancer Cell* **5,** 215–219.
32. Satyanarayana, A., Manns, M. P. & Rudolph, K. L. (2004) *Hepatology* **40,** 276–283.
33. Erdal, E., Ozturk, N., Cagatay, T., Eksioglu-Demiralp, E. & Ozturk, M. (2005) *Int. J. Cancer* **115,** 903–910.
34. Masutomi, K., Yu, E. Y., Khurts, S., Ben-Porath, I., Currier, J. L., Metz, G. B., Brooks, M. W., Kaneko, S., Murakami, S., DeCaprio, J. A., *et al.* (2003) *Cell* **114,** 241–253.
35. Yolcu, E., Sayan, B. S., Yagci, T., Cetin-Atalay, R., Soussi, T., Yurdusev, N. & Ozturk, M. (2001) *Oncogene* **15,** 1398–1401.